VSSR

Vehicle Safety Standards Report

DOTARS

DEPARTMENT OF TRANSPORT AND REGIONAL SERVICES

Vehicle Design and Operation for Pedestrian Protection

- Accident Simulations and Reconstructions

A Commissioned Report by
Road Accident Research Unit
Adelaide University

VSSR 1
2003

ISBN 0-642-50236-6

The Commonwealth Department of Transport and Regional Services commissioned the Road Accident Research Unit, University of Adelaide, Australia, to produce this report.

First Published 2003

Material referenced from this publication should bear the following citation:

Vehicle Safety Standards Report – Vehicle Design and Operation for Pedestrian Protection (VSSR 1), Commonwealth Department of Transport and Regional Services, Australia 2003.

Written by: Robert Anderson (University of Adelaide)
Luke Streeter (University of Adelaide)
Giulio Ponte (University of Adelaide)
Marleen Van de Griend (University of Adelaide)
Jack Mclean (University of Adelaide)
Electronic production: Commonwealth Department of Transport and Regional Services

DEPARTMENT OF TRANSPORT & REGIONAL SERVICES
VEHICLE SAFETY STANDARDS
DOCUMENT RETRIEVAL INFORMATION

Report No.	Date	Pages	ISBN
VSSR 1	2003	146	0-642-50236-6

Title and Subtitle

Vehicle Design and Operation for Pedestrian Protection
- Accident Simulations and Reconstructions

Author(s)

Robert Anderson, Luke Streeter, Giulio Ponte, Marleen Sommariva and Jack McLean

Performing Organisation

Road Accident Research Unit
Adelaide University

Available from	Price	Format
Vehicle Safety Standards Department of Transport and Regional Services GPO Box 594 CANBERRA 2601	No charge	CD

Abstract

This report details the reconstruction of impacts between pedestrians and cars. The principal aim of performing the reconstructions was to examine how injuries sustained by pedestrians in real life relate to the results of reconstruction tests that used the impactors designated by the European Enhanced Vehicle-safety Committee (EEVC) for assessing pedestrian protection.

The main finding was that the head impact test designated by the EEVC is a sound predictor for severe head injury in actual pedestrian collisions, as measured by the Abbreviated Injury Scale.

Keywords

Pedestrian protection, accident investigation, reconstructions, head impact test

Notes

(1) VSS research reports are disseminated in the interests of information exchange.
(2) The views expressed are those of the authors and do not necessarily represent those of the Commonwealth Government

Vehicle design and operation for pedestrian protection

Accident simulations and reconstructions

Robert Anderson, Luke Streeter, Giulio Ponte, Marleen Sommariva and Jack McLean

Road Accident Research Unit

Adelaide University

Executive Summary

This report details the reconstruction of impacts between pedestrians and cars. The principal aim of performing the reconstructions was to examine how injuries sustained by pedestrians in real life relate to the results of reconstruction tests that used the impactors designated by the European Enhanced Vehicle-safety Committee (EEVC) for assessing pedestrian protection.

The methodology of this study included accident investigation, computer simulation, and the physical reconstruction in a laboratory of impacts that occurred in the accident cases that were investigated. The accident investigation process provided the impact speed of the vehicles in each case, details of the contact between pedestrian and car, and the resulting injuries. This information was used to simulate the car-pedestrian collision in each case using the computer program, MADYMO. The simulation of the collision reproduced the kinematics of the pedestrian in the collision and provided estimates of the conditions of the impacts between the car and the pedestrian's leg, upper leg and head. Specifically, the simulation provided the relative angle and velocity of the head with respect to the car, just prior to impact. It also provided the relative angle, velocity and effective mass of the upper leg prior to impact. The striking speed of the vehicle was used as an estimate of the relative velocity of the lower leg on impact.

Ten pedestrian accidents were selected from a pool of 80 cases that had been previously investigated by the Road Accident Research Unit. The head impact from every case was reconstructed, and a total of 10 leg impacts were reconstructed in the manner described above. The results of each simulation were used to set the impact conditions of the EEVC subsystem impactors. A car of the same make, model and series as the car involved in the accident was used in the physical reconstruction of the impact, and the impact point on each vehicle was the same as the one identified on the case vehicle by the accident investigation. The results of the impact reconstructions were then compared to the severity of any injury caused by the associated impact in the accident.

The main findings were that the head impact test designated by the EEVC is a sound predictor for severe head injury in actual pedestrian collisions, as measured by the Abbreviated Injury Scale. Impacts that exceeded the acceptable limit of a HIC value of 1000 were positively associated with head injuries that were AIS3 or above ($p = 0.0238$, by Fisher's exact test).

The results of the leg impact reconstructions were more equivocal. The acceleration of the lower section of the EEVC WG10 Full Legform appears to be positively associated with the severity of any fractures of the tibia and fibula. However, the bending and shearing of the knee joint in the legform does not appear to relate to the presence of ligamentous damage to the knee. At this stage, too few Upper Legform tests have been used to reconstruct upper leg impacts, to make any firm conclusions regarding the accuracy of this test.

We recommend that consideration be given to further evaluation of the subsystem impactors and their associated test methods. This report contains results that support the use of the Headform test for the evaluation of pedestrian protection, but further research is needed to assess the appropriateness of the Full and Upper Legform tests.

Contents

Contents vii

Tables xi

Figures xiii

1 Introduction 1

2 Aims 2

3 Data and methods 2

3.1 Case selection 2

3.2 Accident investigation 3

3.3 Computer simulation 4

3.4 Physical reconstruction 9

4 Summary and discussion of the results 10

4.1 Simulation results 11

4.2 Head impact reconstructions 12

4.3 Leg impact reconstructions 14

5 Discussion and conclusions 20

6 References 23

7 Case PED011-99 25

7.1 Case description 25

7.2 Pedestrian injuries 25

7.3 Accident reconstruction 26

7.4 MADYMO simulation 26

7.5 Simulation results 28

7.6 Physical reconstruction 29

7.7 Summary of reconstruction results and injury diagnosis 33

8 Case PED018-99 35

8.1 Case description 35
8.2 Pedestrian injuries 35
8.3 Accident reconstruction 36
8.4 MADYMO simulation 36
8.5 Simulation results 39
8.6 Physical reconstruction 39
8.7 Summary of reconstruction results and injury diagnosis 45
9 Case PED035-99 47
9.1 Case description 47
9.2 Pedestrian injuries 47
9.3 Accident reconstruction 48
9.4 MADYMO simulation 48
9.5 Simulation results 51
9.6 Physical reconstruction 51
9.7 Summary of reconstruction results and injury diagnosis 55
10 Case PED043-99 57
10.1 Case description 57
10.2 Pedestrian injuries 57
10.3 Accident reconstruction 58
10.4 MADYMO simulation 58
10.5 Simulation results 59
10.6 Physical reconstruction 61
10.7 Summary of reconstruction results and injury diagnosis 66
11 Case PED049-99 67
11.1 Case description 67
11.2 Pedestrian injuries 67
11.3 Accident reconstruction 68
11.4 MADYMO simulation 68

11.5 Simulation results....70
11.6 Physical reconstruction....71
11.7 Summary of reconstruction results and injury diagnosis....75
12 Case PED056-99....77
12.1 Case description....77
12.2 Pedestrian injuries....77
12.3 Accident reconstruction....78
12.4 MADYMO simulation....78
12.5 Physical reconstruction....81
12.6 Summary of reconstruction results and injury diagnosis....85
13 Case PED057-99....87
13.1 Case description....87
13.2 Pedestrian injuries....87
13.3 Accident reconstruction....88
13.4 MADYMO simulation....88
13.5 Physical reconstruction....91
13.6 Summary of reconstruction results and injury diagnosis....97
14 Case PED061-99....99
14.1 Case description....99
14.2 Pedestrian injuries....99
14.3 Accident reconstruction....100
14.4 MADYMO simulation....100
14.5 Physical reconstruction....102
14.6 Summary of reconstruction results and injury diagnosis....105
15 Case PED064-00....107
15.1 Case description....107
15.2 Pedestrian injuries....107
15.3 Accident reconstruction....108

15.4 MADYMO simulation 108
15.5 Physical reconstruction 110
15.6 Summary of reconstruction results and injury diagnosis 114
16 Case PED076-00 115
16.1 Case description 115
16.2 Pedestrian injuries 115
16.3 Accident reconstruction 116
16.4 MADYMO simulation 116
16.5 Physical reconstruction 116
16.6 Summary of reconstruction results and injury diagnosis 126

Tables

Table 3-1 Cases selected for the study 3
Table 4-1 Summary of target Headform test conditions from the simulations 11
Table 4-2 Summary of target Full Legform test conditions from the simulations 12
Table 4-3 Summary of target Upper Legform test conditions from the simulations 12
Table 4-4 Results of the impact reconstructions and the MAIS of the head in each case 13
Table 4-5 Summary of the data on impact severity and the related level of injury 14
Table 4-6 Results of the leg impact reconstructions and the MAIS of the related body region in each case 16
Table 7-1 Case details for reconstruction 27
Table 7-2 Simulation results for PED011-99 29
Table 7-3 Physical reconstruction parameters and results (test no. 19060102) 29
Table 7-4 Physical reconstruction parameters and results (test no. 19060103). 31
Table 7-5 Physical reconstruction parameters and results (test no. 03080103). 32
Table 7-6 Summary of test results and relevant injuries 34
Table 8-1 Case details for reconstruction 36
Table 8-2 Simulation results for PED018-99 39
Table 8-3 Physical reconstruction parameters and results for the Headform test (test no. 05060100) 40
Table 8-4 Physical reconstruction parameters and results for the Legform test (test no.07060101) 41
Table 8-5 Physical reconstruction parameters and results for the Upper Legform test test no.05060101) 43
Table 8-6 Summary of test results and relevant injuries 45
Table 9-1 Case details for reconstruction 48
Table 9-2 Simulation results for PED035-99 51
Table 9-3 Physical reconstruction parameters and results for the Headform test (test no. 27070100) 52
Table 9-4 Physical reconstruction parameters and results for the Legform test (test no.30070100) 53
Table 9-5 Summary of test results and relevant injuries 55
Table 10-1 Case details for reconstruction 58
Table 10-2 Simulation results for PED043-99 60
Table 10-3 Physical reconstruction parameters and results for the Headform test (test no. 01060101) 61
Table 10-4 Physical reconstruction parameters and results for the Legform test (test no. 07060102) 63
Table 10-5 Physical reconstruction parameters and results for the Upper Legform test (test no.04060100) 64
Table 10-6 Summary of test results and relevant injuries 66
Table 11-1 Case details for reconstruction 68
Table 11-2 Simulation results for PED049-99 71
Table 11-3 Physical reconstruction parameters and results Headform test (test no. 19060101) 72
Table 11-4 Physical reconstruction parameters and results of the Legform test (test no. 14060102) 73
Table 11-5 Summary of reconstruction results and relevant injuries in PED 76

Table 12-1 Case details for reconstruction 78
Table 12-2 Simulation results for PED056-99 79
Table 12-3 Physical reconstruction parameters and results for the Headform test (test no.31070100) 81
Table 12-4 Physical reconstruction parameters and results for the Legform test (test no.30070101) 83
Table 12-5 Summary of test results and relevant injuries 85
Table 13-1 Case details for reconstruction 89
Table 13-2 Simulation results for PED057-99 91
Table 13-3 Physical reconstruction parameters and results for the Headform test (test no. 05060102; assuming a vehicle impact speed of 65 km/h) 92
Table 13-4 Physical reconstruction parameters and results for the Headform test (test no. 05060103; assuming a vehicle impact speed of 57 km/h) 92
Table 13-5 Physical reconstruction parameters and results for the Upper Legform test (test no. 07060100) 95
Table 13-6 Summary of test results and relevant injuries 97
Table 14-1 Case details for reconstruction 101
Table 14-2 Simulation results for PED061-99 102
Table 14-3 Physical reconstruction parameters and results (test no. 22060100) 103
Table 14-4 Summary of test results and relevant injuries 105
Table 15-1 Case details for reconstruction 108
Table 15-2 Simulation results for PED064-00 110
Table 15-3 Physical reconstruction parameters and results for the Headform test (test no. 21060100) 110
Table 15-4 Physical reconstruction parameters and results for the Legform test (test no.08060100) 112
Table 15-5 Summary of test results and relevant injuries 114
Table 16-1 Case details for reconstruction 116
Table 16-2 Simulation results for PED018-99 119
Table 16-3 Physical reconstruction parameters and results (test no. 18060100) 119
Table 16-4 Physical reconstruction parameters and results (test no. 19060100) 120
Table 16-5 Physical reconstruction parameters and results for the Legform test (test no. 12060101) 122
Table 16-6 Physical reconstruction parameters and results for the Legform test (test no. 14060101) 124
Table 16-7 Summary of test results and relevant injuries 126

Figures

Figure 3-1 Initial stance used in the validation test (shown with the profile of Car B) 4

Figure 3-2 Time history of the head velocity produced in the simulation of a collision between a Car A and a 50th percentile male PMHS, at 25 km/h. 5

Figure 3-3 Time history of the head velocity produced in the simulation of a collision between a Car A and a 50th percentile male PMHS, at 30 km/h. 5

Figure 3-4 Time history of the head velocity produced in the simulation of a collision between a Car A and a 50th percentile male PMHS, at 40 km/h. 5

Figure 3-5 Trajectories of body segments in the simulations with Car A in relation to corridors determined from PMHS tests. 5

Figure 3-6 Time history of the head velocity produced in the simulation of a collision between a Car B and a 50th percentile male PMHS, at 40 km/h. 5

Figure 3-7 Time history of the head velocity produced in the simulation of a collision between a Car B and a 50th percentile male PMHS, at 30 km/h. 5

Figure 3-8 Trajectories of body segments in the simulations with Car B in relation to corridors determined from PMHS tests. 6

Figure 3-9 Gait cycle variations used where the stance of the pedestrian was not known. 7

Figure 3-10 Geometry of a 1992 Ford Falcon, and the entities used to approximate its shape in MADYMO 8

Figure 4-1 Head injury severity in the cases studied, and the HIC values measured in the impact reconstructions. (A) The pedestrian in PED011-99 suffered an atlanto-occipital fracture (at the base of the skull), and if included increases the MAIS to 6. (B) The graph includes results of both tests for cases PED057-99 and PED076-99. 14

Figure 4-2 The deformation of the bonnet caused in the collision in Case PED057-99 (left). The deformation caused by the reconstruction tests was much less (right). The deformation created in the collision may have protected the head of the pedestrian by lifting the bonnet surface away from the under bonnet components of the car. 15

Figure 4-3 Lower leg injury severity in the cases studied, and the tibia acceleration measured in the impact reconstructions (* The likely severity of the impact in Cases PED018-99 and PED056-99 was probably greater than the reconstruction . ** The graph includes results of two tests for Case PED076-00 - see text) 17

Figure 4-4 Knee injury severity in the cases studied, and the knee bending angle measured in the impact reconstructions (** The graph includes results of two tests for Case PED076-00 - see text) 17

Figure 4-5 Knee injury severity in the cases studied, and the knee shear displacement measured in the Legform in the reconstructions (* The likely severity of the impact in Cases PED018-99 and PED056-99 was probably greater than the reconstruction .** The graph includes results of two tests for Case PED076-00 - see text) 18

Figure 4-6 Upper leg/pelvis injury severity in the cases studied, and the support forces measured in the Upper Legform in the reconstruction (* The likely severity of the impact in CasePED057-99 was probably greater than the reconstruction - see text) 18

Figure 4-7 Upper leg/pelvis injury severity in the cases studied, and bending moment in the Upper Legform in the reconstruction (* The likely severity of the impact in CasePED057-99 was probably greater than the reconstruction - see text) 19

Figure 7-1 Site diagram of the collision in Case PED011-99. 25

Figure 7-2 Collision damage to the Camira: (A) Pelvic/abdominal impact (B) Head impact 26

Figure 7-3 Geometry of the vehicle model involved in the collision (white lines). The approximation of this geometry for the simulation is shown by the shaded geometric entities. 27

Figure 7-4 Initial position of the pedestrian and vehicle in the simulations PED011-g1 through PED011-g6 (*left to right and top to bottom*). 28

Figure 7-5 The acceleration recorded in the physical reconstruction of case PED011-99 (test number 19060102)..... 30

Figure 7-6 Damage caused by impact with the pedestrian's head (left) and the damage produced in the reconstruction (right) of case PED011-99 (test 19060102). 30

Figure 7-7 The acceleration recorded in the physical reconstruction of case PED011-99 (test number 19060103)..... 31

Figure 7-8 Damage caused by impact with the pedestrian's head (left) and the damage produced in the second reconstruction (right) of case PED011-99 (test 19060103). 32

Figure 7-9 The acceleration recorded in the third reconstruction of case PED011-99 (test number 03080103). 33

Figure 7-10 Damage caused by impact with the pedestrian's head (left) and the damage produced in the third reconstruction (right) of case PED011-99 (test 03080103). 33

Figure 8-1 Site diagram of the collision in Case PED018-99 35

Figure 8-2 Geometry of the vehicle measured, shown in white. The approximation of this geometry for the simulation is shown by the shaded cylinders and planes. 37

Figure 8-3 Initial position of the pedestrian and vehicle in the simulations PED018-g1 through PED018-g6 (*left to right and top to bottom*). 38

Figure 8-4 A general view of the accident damage from the impact (left) and the damage produced in the physical reconstruction (right) of case PED018-99. 39

Figure 8-5 The acceleration recorded for the Headform test in the physical reconstruction of case PED018-99..... 40

Figure 8-6 A side view of the damage caused by impact with the pedestrian's head (left) and the damage produced in the reconstruction (right) of case PED018-99. 41

Figure 8-7 The tibia acceleration recorded in the physical reconstruction of case PED018-99. 42

Figure 8-8 Knee bending angle recorded for the physical reconstruction of case PED018-99..... 42

Figure 8-9 Knee shear displacement recorded for the physical reconstruction of case PED018-99..... 43

Figure 8-10 Upper leg force recorded in the physical reconstruction of case PED018-99..... 44

Figure 8-11 Bending moment recorded in the physical reconstruction of case PED018-99 44

Figure 8-12 A close up front view of the accident damage from impact with the pelvic area (left) and the damage from the reconstruction with the Upper Legform (right) of case PED018-99..... 45

Figure 9-1 Site diagram of the collision in Case PED035-99 47

Figure 9-2 Geometry of the vehicle (shown in white). The approximation of this geometry for the simulation is shown by the shaded geometric entities. 49

Figure 9-3 Initial position of the pedestrian and the vehicle in the simulations PED035-g1 through PED035-g3 *(top to bottom*)..... 50

Figure 9-4 A general view of the accident damage (left) and the damage produced by the reconstruction (right) of the head and leg impacts in case PED035-99. 51

Figure 9-5 Acceleration recorded in the physical reconstruction of the head impact in Case PED035-99..... 52

Figure 9-6 A front close up view of the vehicle involved, showing where the head impact occurred (left) and the damage as produced by the reconstruction (right) of case PED035-99..... 53

Figure 9-7 The tibia acceleration recorded in the physical reconstruction of case PED035-99. 54

Figure 9-8 Knee bending angle recorded for the physical reconstruction of case PED035-99..... 54

Figure 9-9 Knee shear displacement recorded for the physical reconstruction of case PED035-99..... 55

Figure 10-1 Site diagram of the collision in Case PED043-99. 57

Figure 10-2 Geometry of the vehicle (shown in white). The approximation of this geometry for the simulation is shown by the shaded geometric entities.....59
Figure 10-3 Initial position of the pedestrian and the vehicle in the simulations PED043-g1 to PED043-g2.....60
Figure 10-4 The acceleration recorded in the physical reconstruction of case PED043-99.....62
Figure 10-5 A side view of the vehicle involved in case PED043-99, showing where the head impact occurred (left) and the damage as produced by the reconstruction (right).....62
Figure 10-6 The tibia acceleration recorded in the physical reconstruction of case PED043-99.....63
Figure 10-7 Knee bending angle recorded for the physical reconstruction of case PED043-99.....64
Figure 10-8 Upper leg force recorded in the physical reconstruction of case PED043-99.....65
Figure 10-9 Bending moment recorded in the physical reconstruction of case PED043-99.....65
Figure 10-10 The accident damage caused by impact with the pelvic area (left) and the damage produced by the reconstruction with the Upper Legform impactor (right) of case PED043-99.....66
Figure 11-1 Site diagram of the collision in Case PED049-99.....67
Figure 11-2 Geometry of the vehicle measured, shown in white. The approximation of this geometry for the simulation is shown by the shaded geometric entities.....69
Figure 11-3 Initial position of the pedestrian and vehicle in the simulations PED049-g1 through PED049-g6 (*left to right and top to bottom*).....70
Figure 11-4 A general view of the accident damage(left) and the damage produced by the reconstruction (right) of case PED049-99.....71
Figure 11-5 The acceleration recorded in the physical reconstruction of case PED049-99.....72
Figure 11-6 The accident damage caused by the impact with the head of the pedestrian (*left*) and the physical reconstruction damage of the head impact (*right*) in case PED049-99.....73
Figure 11-7 The tibia acceleration recorded in the physical reconstruction of case PED049-99.....74
Figure 11-8 Knee bending angle recorded for the physical reconstruction of case PED049-99.....74
Figure 11-9 Knee shear displacement recorded for the physical reconstruction of case PED049-99.....75
Figure 11-10 The accident damage caused by the pedestrian's leg (left - negligible) compared with the physical reconstruction damage of the full leg impact (right) in case PED049-99.....75
Figure 12-1 Site diagram of the collision in Case PED056-99.....77
Figure 12-2 Geometry of the vehicle measured, shown in white. The approximation of this geometry for the simulation is shown by the shaded geometric entities.....79
Figure 12-3 Initial position of the pedestrian and vehicle in the simulations PED056-g1 through PED056-g6 (*left to right and top to bottom*), and the final posture based on head impact position and arm kinematics.....80
Figure 12-4 A general view of the accident damage(left) and the damage produced by the reconstruction (right) of case PED056-99.....81
Figure 12-5 The acceleration recorded in the physical reconstruction of case PED056-99.....82
Figure 12-6 The accident damage caused by the impact with the head of the pedestrian (*left*) and the physical reconstruction damage of the head impact (*right*) in case PED056-99.....82
Figure 12-7 The tibia acceleration recorded in the physical reconstruction of case PED056-99 83
Figure 12-8 Knee bending angle recorded for the physical reconstruction of case PED056-99.....84
Figure 12-9 Knee shear displacement recorded for the physical reconstruction of case PED056-99.....85
Figure 12-10 Close-up view of the vehicle involved in the actual pedestrian impact compared with the reconstruction of case PED056-99, very minor denting on the steel bumper bar in both cases.....85
Figure 13-1 Site diagram of the collision in Case PED057-99.....87

Figure 13-2 Geometry of the HQ Holden Kingswood. The approximation of this geometry for the simulation is shown by the shaded geometric entities. 89

Figure 13-3 Initial position of the pedestrian and vehicle in the simulations PED057-g1 through PED057-g6 (*left to right and top to bottom*). 90

Figure 13-4 The accident damage from the impact (left) and the damage produced in the physical reconstruction (right) of case PED057-99. 92

Figure 13-5 The acceleration recorded in the physical reconstruction of case PED057-99 for higher impact speed of the range. 93

Figure 13-6 The acceleration of the Headform recorded in the physical reconstruction of case PED057-99 for lower impact speed of the range. 94

Figure 13-7 Force recorded in the Upper Legform in the physical reconstruction of case PED057-99. 95

Figure 13-8 Bending moment recorded in the physical reconstruction of case PED057-99. 96

Figure 13-10 A close up front view of the accident damage from impact with the pelvic area (left) and the damage from the reconstruction with the Upper Legform (right) of case PED057-99. 96

Figure 13-11 Close up angle view after the physical reconstruction with the Upper Legform impactor of case PED057-99. 97

Figure 14-1 Site diagram of the collision in Case PED061-99. 99

Figure 14-2 Geometry of the Mitsubishi Magna. The approximation of this geometry for the simulation is shown by the shaded geometric entities. 101

Figure 14-3 Initial position of vehicle and pedestrian in the simulation of Case PED061-99 102

Figure 14-4 A general view of the vehicle involved in case PED061-99 (left) and the general view after the physical reconstruction (right) of case PED061-99. 103

Figure 14-5 The acceleration recorded in the physical reconstruction of case PED061-99. 104

Figure 14-6 Close-up of the damage caused by impact with the child pedestrian's head (left) and the damage produced in the reconstruction (right) of case PED061-99. 104

Figure 15-1 Site diagram of the collision in Case PED064-00. 107

Figure 15-2 Geometry of the Holden VP Commodore. The approximation of this geometry for the simulation is shown by the shaded geometric entities. 109

Figure 15-3 The initial position of the pedestrian and vehicle in the simulation of Case PED064-00. 109

Figure 15-4 The acceleration recorded in the physical reconstruction of case PED064-00. 111

Figure 15-5 Damage caused by impact with the pedestrian's head (left) and the damage produced in the reconstruction (right) of case PED064–00. 111

Figure 15-6 The acceleration recorded in the physical reconstruction of case PED064-00. 113

Figure 15-7 Knee bending angle recorded for the physical reconstruction of case PED064-00. 113

Figure 15-8 Knee shear displacement recorded for the physical reconstruction of case PED064-00. 113

Figure 15-9 Close up front view showing the accident damage to the bumper (left) and the damage produced by the reconstruction (right) with the Legform of case PED064–00. 114

Figure 16-1 Site diagram of the collision in Case PED076-00. 115

Figure 16-2 The approximation of the vehicle geometry for the simulation is shown by planes and ellipsoids illustrated. 117

Figure 16-3 Initial position of the pedestrian and vehicle in the simulations PED076-g1 through PED076-g6 (*left to right and top to bottom*). 118

Figure 16-4 The acceleration recorded in the physical reconstruction of case PED076-00 for the lower speed range. 120

Figure 16-5 The acceleration recorded in the physical reconstruction of case PED076-00 for the higher speed range.....121
Figure 16-6 The accident damage (left) from impact with the pedestrians head compared to the damage produced by the reconstruction of case PED076-00 (test # 18060100).....121
Figure 16-7 The acceleration recorded in the physical reconstruction of case PED076-00 for lower impact speed of the range. 122
Figure 16-8 Knee bending angle recorded for the physical reconstruction of case PED076-00 for lower impact speed of the range. 123
Figure 16-9 Knee shear displacement recorded for the physical reconstruction of case PED076-00 for lower impact speed of the range. 123
Figure 16-10 The acceleration recorded in the physical reconstruction of case PED76-00 for higher impact speed of the range. 124
Figure 16-11 Knee bending angle recorded for the physical reconstruction of case PED076-00 for higher impact speed of the range. 125
Figure 16-12 Knee shear displacement recorded for the physical reconstruction of case PED076-00 for higher impact speed of the range. 125
Figure 16-13 Close-up view of impact points of test # 12060101 (left) and test # 14060101 (right) there was no evidence of damage in either test. 126

1 Introduction

Pedestrian fatalities account for approximately 16 percent of Australia's road toll (ATSB, 2001). The numbers of pedestrians killed in Australia is declining, with a fatality rate per 100,000 population similar to other industrialised countries (ATSB, 2000). Pedestrian fatalities as a proportion of road fatalities is much higher worldwide, with some estimates as high as 40-50 percent of the world's annual road toll (Mohan and Tiwari, 2000).

One strategy being pursued to further reduce the numbers of pedestrians killed and injured is the introduction of specific test methods to measure the levels of protection afforded to pedestrians by a vehicle in the event of a collision.

The European Experimental Vehicles Committee (now known as the European Enhanced Vehicle-safety Committee) was one of the first groups to examine the possibility of developing a test procedure to evaluate the degree of pedestrian friendliness of the front of vehicles. Working Group 7 of the EEVC examined injury patterns and sources of injury among pedestrian casualties and fatalities in Europe. The data collected indicated that the most commonly injured regions of the body were the head, lower limbs, the arms the thorax and pelvis. When only severe injuries were examined, the head and lower limbs were most frequently involved (Working Group 10 of the EEVC, 1994). Working Group 10 of the EEVC was formed as a result of the report of an ad hoc group of the EEVC that examined further research findings that followed the final report of Working Group 7. Working Group 10 was given the mandate to determine test methods and acceptance levels for assessing the protection afforded to pedestrians by the fronts of cars in an accident. They devised a set of impact tests to measure the risk of injury to the head of adults and children using free flight Headforms, the risk of injury to the upper leg of an adult using a guided impactor, and the risk of injury to the knee and tibia of an adult using a free flight leg impactor (Working Group 10 of the EEVC, 1994). WG10 was superseded by WG17 in 1997 which further refined the tests and test devices. Their report was released in 1998 (Working Group 17 of the EEVC, 1998).

The tests devised by the EEVC are now used in the New Car Assessment Programs in Europe (EuroNCAP) and in Australia (ANCAP). There are also efforts to make the procedures part of a safety standard for cars sold in Europe. It is pertinent to examine how these tests may or may not predict the occurrence of real-world pedestrian injuries. That is the subject of this report.

The subsystem tests cannot replicate exactly the impacts that would be produced in a real-world pedestrian accident. For example, the nature of a subsystem test does not allow for the direct inclusion of the inertial effects created by forces that act through the neck on the head. Instead, the 'effective mass' of the head in a real-world collision (the impact force divided by the acceleration of the head), must be incorporated into the mass of the subsystem Headform. The mass of the subsystem Headform is fixed whereas the effective mass of the head may vary throughout the duration of the impact in a real-world pedestrian collision. Similarly, the effective mass of the upper leg of the pedestrian may vary throughout an impact with the leading edge of the car, and may also rotate throughout the duration of the impact. The Upper Legform, which is designed to represent this contact, is constrained not to rotate, and is a fixed mass (although this can be varied between tests). As with the Headform test, the angle and mass of the Upper Legform is an approximate representation of the upper leg in such an impact.

Nevertheless, to be useful, the results of the subsystem tests should reflect injury outcomes in the real world. Where a test is used to represent an impact that occurred in a real-world pedestrian accident, the results of the test should relate to the injuries sustained from that impact. In this report we have attempted to reconstruct real-world impacts from pedestrian collisions with the corresponding subsystem tests. This has enabled us to assess the extent to which the subsystem tests reflect the actual injuries sustained as a result of real-world impacts, and to explore the limitations of the subsystem tests for representing such impacts.

2 Aims

The aims of this study are:

- To reconstruct impacts involved in real-world pedestrian collisions, through a combination of accident investigation, computer simulation and physical reconstructions using the EEVC subsystem impactors, and
- To examine the ability of the results of such tests to consistently explain the injuries sustained in such real-world pedestrian collisions

3 Data and methods

3.1 CASE SELECTION

The cases used for this study were selected from the pedestrian accidents investigated by the Road Accident Research Unit for the Australian Commonwealth Department of Transport and Regional Services (Anderson et al., 2000a). The report on those accidents contained the details of eighty collisions, covering a range of severities. The ten cases selected for simulation and reconstruction were chosen based on the level of certainty about the dynamics of the accident, and on the basis that the injuries sustained by the pedestrian were known and could be related to impacts with the vehicle. This discounted cases, for example, where the pedestrian was crushed under a vehicle or cases where the impact speed of the car relied on information that could not be substantiated by the evidence left at the scene of the accident. The selection criteria were also designed to encapsulate a range of impacts that are covered by the EEVC-type subsystem tests: the Upper Legform test, the Full Legform test and the Adult and Child Headform tests.

The list of cases is presented in Table 3-1. This table also summarises the impacts that were reconstructed from each case. In two cases, it was appropriate to examine all three subsystem tests, as the car involved in the case came into substantial contact with those parts of the body of the pedestrian that are covered by each test. In Case PED061-99, the child Headform test was used as the fatally injured pedestrian was a ten year old female. In this case, and in Case PED011-99 (which involved a 13 year old female), it was not appropriate to undertake a Full Legform test, as the Full Legform is not designed to measure the risk of injury for pedestrians of such a small stature.

Table 3-1 Cases selected for the study

Case number	Pedestrian age and sex	Relevant injuries	Car year, Make and model	Physical reconstructions		
				Head	Upper leg	Full leg
PED011	13 year old female	Fatal head and neck injuries	1988 Holden Camira	●		
PED018	79 year old female	Fatal head injuries. Pelvic fractures, tibia and fibula fractures	1982 Nissan Bluebird	●	●	●
PED035	83 year old female	Ankle fracture	1991 Ford Falcon	●		●
PED043	52 year old male	Fatal head injuries, laceration of right hip	1992 Ford Fairmont	●	●	●
PED049	15 year old female	Head injuries, knee contusions	1997 Ford Falcon	●		●
PED056	35 year old male	Open fracture of tibia and fibula	1983 Holden VK Commodore	●		●
PED057	15 year old female	Brief loss of consciousness and concussion, open knee wound, fracture of pelvis	1973 Holden HQ Kingswood	●	●	
PED061	10 year old female	Fatal head injuries	1997 Mitsubishi Magna	● [1]		
PED064	19 year old female	Deep bruising of knee	1993 Holden VP Commodore	●		●
PED076	79 year old female	Brief loss of consciousness, tibia fractures	1996 Ford Falcon	●		●

1. Child Headform

3.2 ACCIDENT INVESTIGATION

The accident investigation typically began with notification from the South Australian Ambulance Service that they were to attend the scene of a pedestrian accident. In fatal cases, the investigation often began with a member of the research team attending the autopsy at the mortuary of the South Australian Coroner. The scene of the accident was surveyed and the lengths of any skid-marks left by the vehicle were measured, along with the location of the impact point and final position of the pedestrian, scuff marks on the road, debris, and any other feature of relevance. If the pedestrian was fatally injured, their injuries were recorded at the autopsy, along with their height, weight and the dimensions of various body segments. In non-fatal cases, the pedestrian was interviewed to determine the nature and severity of their injuries, and the circumstances of the collision. Consent was sought for access to hospital medical records, from which information on their injuries was collected. The South Australian Trauma Registry was also consulted in cases where data on the pedestrian's injuries were not complete.

The vehicle involved in the accident was inspected, at the scene of the accident, or if the accident was fatal, at the vehicle compound of the South Australian Police. The vehicle was inspected for signs of contact with the pedestrian, such as dents, scratches and scuffs in the body of the vehicle. The location of the head contact could be identified not only by a dent in a panel or crack in the windscreen, but also often by the presence of hair on the contact area. The location of each contact

location was also measured, so that the fidelity of the motion of the computer simulation could be verified, and for identifying the test point on the test vehicle.

3.3 COMPUTER SIMULATION

3.3.1 The pedestrian model

The model that was used for the simulation part of this study was developed specifically to simulate pedestrians in car-pedestrian collisions (Anderson et al., 2000a). The model has been presented previously (Garrett, 1998; Garrett, 1996), and used for accident simulation purposes (Anderson et al., 2000b; Anderson et al., 2000c). The model consists of 17 rigid segments linked by kinematic joints that are largely based on the model proposed by Ishikawa et al., (1993) although some joints have been added, while others have been modified (see Garrett, 1996). Recently the neck has been redesigned to better reflect the findings of human volunteer tests (Thunnissen et al., 1995; Wismans et al., 1986). The model has been implemented in the dynamic simulation program MADYMO (TNO, Delft, the Netherlands).

3.3.2 Model validation

Before the simulations could be made, the model was checked to see that it satisfied validation corridors that were constructed based on post-mortem human subject (PMHS) tests carried out in Hanover (Ishikawa et al., 1993). These corridors specify the trajectory of different body components, as well as the time history of the head velocity. The fidelity of the model was tested using two car profiles used in the PMHS experiments. 'Car A' was simulated with the pedestrian model at three speeds, while 'Car B' was simulated at two speeds. The initial stance of the model was chosen to match the general stance of the PMHS in the experiments (Figure 3-1). The results of the validation runs are shown in Figure 3-2 to Figure 3-8.

The model's behaviour is generally in accordance with the corridors drawn from the PMHS tests. The results of the simulation of the collision between the PMHS and Car B are particularly close. The characteristics of the model in a collision with the profile of Car A still produces results that mostly fit the corridors of the tests, but the behaviour seems to diverge from experimental results in some parts of the simulation. The profile of Car A has a higher leading edge than Car B. The results of pedestrian collision models appear to become more variable with higher leading edges (Anderson, 2001).

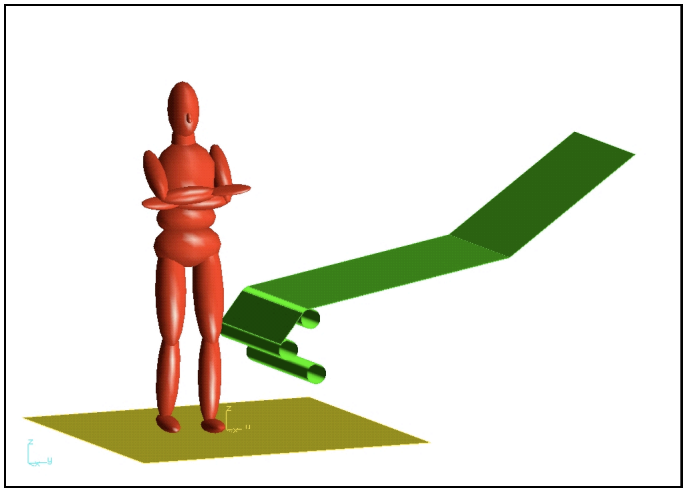

Figure 3-1 Initial stance used in the validation test (shown with the profile of Car B)

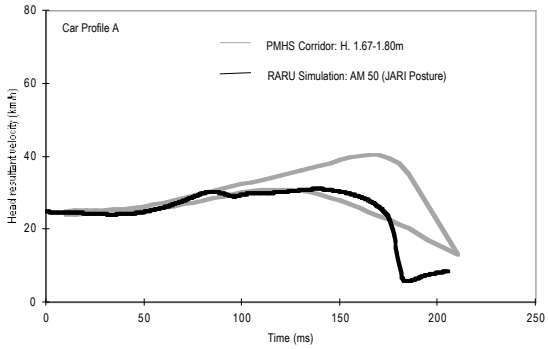

Figure 3-2 Time history of the head velocity produced in the simulation of a collision between a Car A and a 50th percentile male PMHS, at 25 km/h

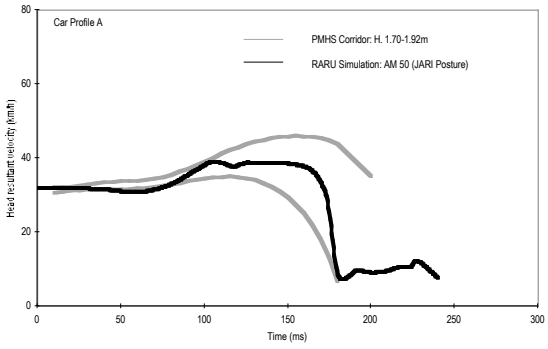

Figure 3-3 Time history of the head velocity produced in the simulation of a collision between a Car A and a 50th percentile male PMHS, at 30 km/h.

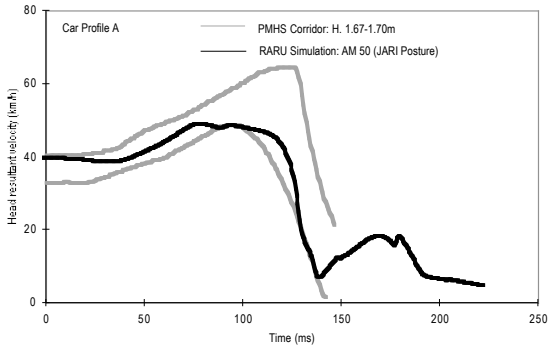

Figure 3-4 Time history of the head velocity produced in the simulation of a collision between a Car A and a 50th percentile male PMHS, at 40 km/h

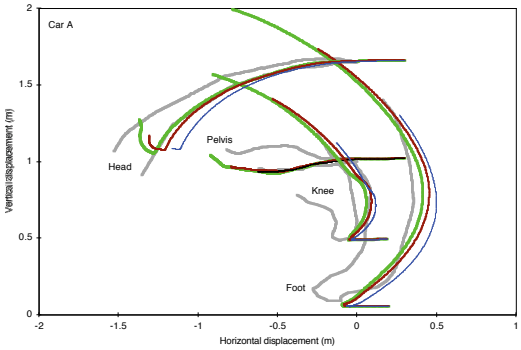

Figure 3-5 Trajectories of body segments in the simulations with Car A in relation to corridors determined from PMHS tests.

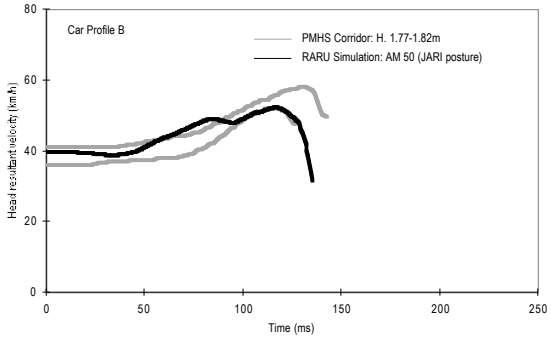

Figure 3-6 Time history of the head velocity produced in the simulation of a collision between a Car B and a 50th percentile male PMHS, at 40 km/h.

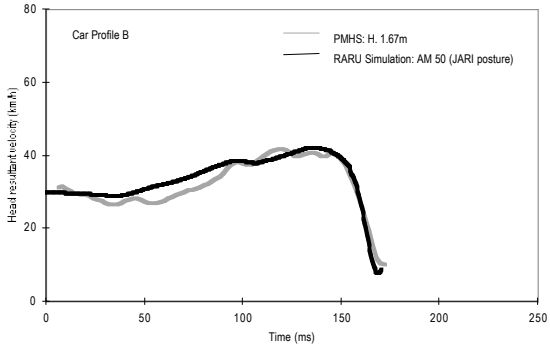

Figure 3-7 Time history of the head velocity produced in the simulation of a collision between a Car B and a 50th percentile male PMHS, at 30 km/h.

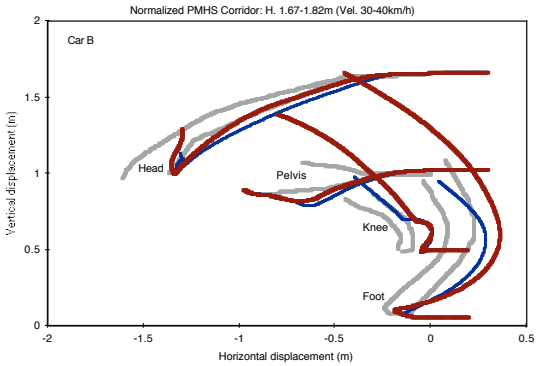

Figure 3-8 Trajectories of body segments in the simulations with Car B in relation to corridors determined from PMHS tests.

3.3.3 Implementation of the model in the simulation of the accidents

The cases that were modelled in this study involved pedestrians of varying ages and statures. The model was based on and validated against, the behaviour of a fiftieth percentile adult male. Therefore, the model had to be scaled appropriately for the simulation of each case. The anthropometric data for each pedestrian (segment dimensions, masses and moments of inertia) were derived from GEBOD (Baughman, 1983), a program which generates anthropometric segment data using regression equations derived from a database of human body measurements. In several cases, the resulting dimensions could be checked against body dimensions of the actual pedestrians, measured by a member of the research team, either during interview, or at autopsy for fatal cases. In cases where the dimensions could be cross-referenced, the dimensions corresponded closely.

The next step in the simulation process was to determine the posture of the pedestrian prior to impact. It was assumed that both the walking velocity and the velocity of the limbs during locomotion could be ignored. The orientation of the pedestrian relative to the car was known in each of these cases, either from the pedestrian themselves or from drivers, witnesses and/or marks on the body. In some cases, the posture of the body of the pedestrian could be similarly determined. The impression of the bumper or other component often indicated the orientation of the pedestrian, and the alignment of marks often indicated the position of limbs and torso as they were struck. However, in many cases it was not possible to determine the exact position or posture of the pedestrian. In these cases, body postures representative of the human gait cycle were used to generate separate simulations. Further, the presence of ankle fractures thought to have occurred due to inversion/eversion type deformations of the ankle were used to determine the weight bearing leg at the time of impact. This reduced the number of simulations required in some cases.

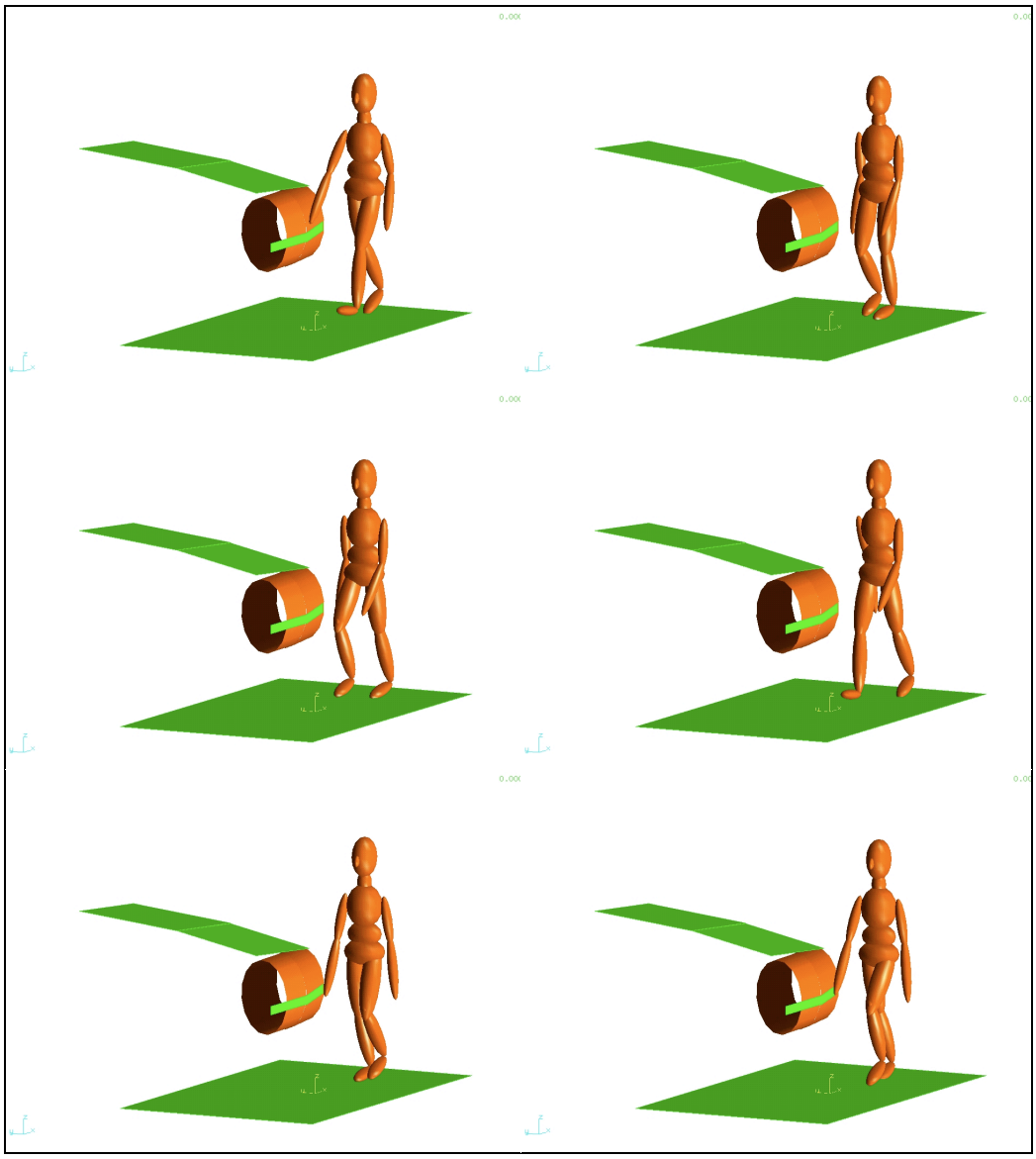

Figure 3-9 Gait cycle variations used where the stance of the pedestrian was not known

3.3.4 Vehicle modelling

Vehicles that corresponded to the make, model and series of those involved in the cases were obtained for the physical reconstruction process. The cars also provided the geometry of the cars for the simulation exercise. A Geodimeter (usually used in surveying) was used to measure the main geometrical features of the car. A prism was held at various feature points and the Geodimeter recorded the position of the prism in Cartesian coordinates. These were linked by lines and used as a basis of the geometry created in MADYMO. The geometry was imported into Easi-CrashMAD (a MADYMO pre-processor) in IGES format. The vehicle geometry was then approximated by the definition of planes, elliptical cylinders and ellipsoids. An example of this is shown in Figure 3-10. Where the vehicle in the case braked heavily, the front of the vehicle was lowered by 100 mm and then rotated by 3 – 5˚, to take account of the dip in cars produced by braking.

This method of approximating the geometry has the advantage of simplifying the contact definitions between the pedestrian and the car. The disadvantage is that more than one shape may

contact the same body region in what should be considered one contact. For example, the upper leg of the pedestrian may strike simultaneously a cylinder, which represents the leading edge of the vehicle, and a plane, which represents the bonnet. These two contacts will produce two separate contact forces on the upper leg, which would be summed, artificially stiffening the contact. This was overcome by using the EVALUATION keyword, which instructs MADYMO to use only the largest of any contact forces in a list of contact interactions.

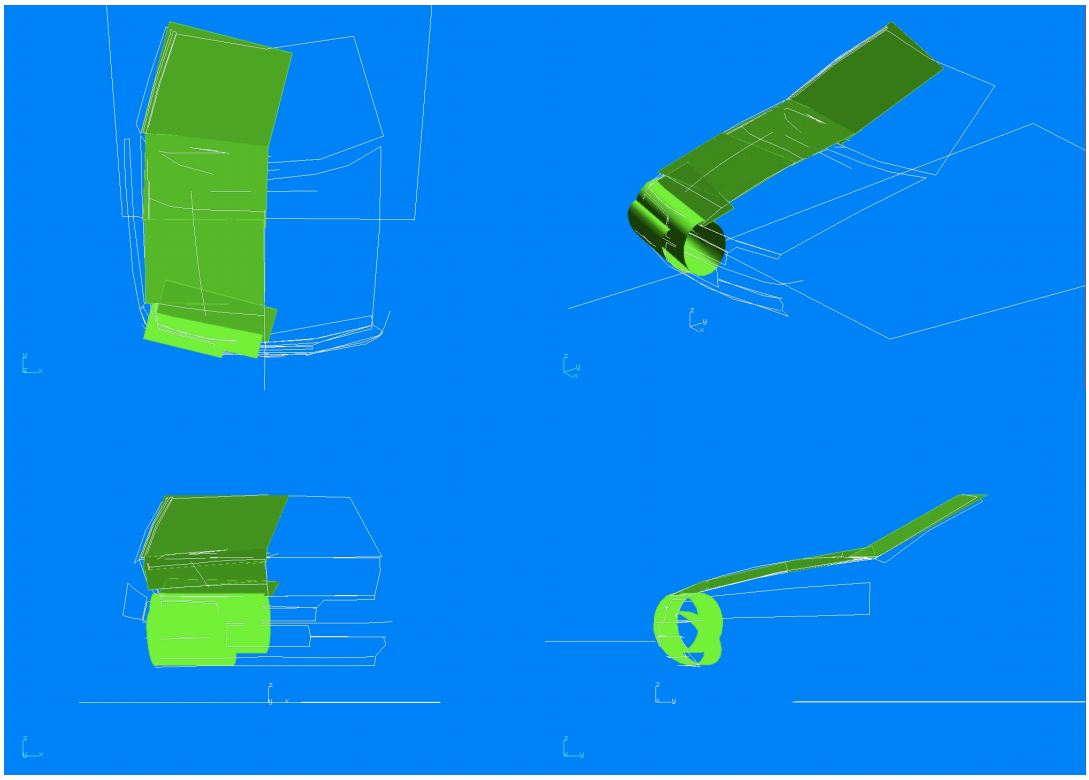

Figure 3-10 Geometry of a 1992 Ford Falcon, and the entities used to approximate its shape in MADYMO

3.3.5 Effective mass and velocity calculations

The EEVC WG10 Upper Legform test procedure is intended to reproduce the angle, velocity and inertia of an impact with the upper leg of a pedestrian. The Upper Legform is constrained to one degree of freedom, in the direction normal and posterior to the femur section of the Legform. In a pedestrian collision, the upper leg of the pedestrian is not constrained in this way, and the angle and effective mass of the upper leg varies throughout the impact. The set up of the test is, therefore, an approximation of reality.

The test conditions in these reconstructions were determined in the same way that the test conditions have been established in the EEVC WG10 and WG17 test procedures. In the EEVC test procedures, a collision speed of 40 km/h is assumed, and the vehicle geometry is then used to determine the mass, angle and speed of the impactor in the test. The relationship between the vehicle geometry and the test conditions is encapsulated in a series of charts that are used to look up the test conditions.

In these reconstructions, the impact speeds were obviously not the standard 40 km/h as is assumed in the EEVC test procedures. Consequently, the charts used to determine the test conditions could not be used. Instead, the simulations were analysed using the same methods that were used to

generate the charts used in the EEVC test procedure. The methods for determining test conditions are described in Janssen and Nieboer, (1990) and reviewed in Konosu et al. (1998).

In this study, each simulation was analysed using post-processing software specifically written for the task. The upper leg velocity, the penetration of the upper leg ellipsoid/leading edge, and the forces associated with this interaction were extracted from the simulation. MADYMO does not resolve contact forces into Cartesian components, and so these were extracted from the DEBUG file generated by MADYMO. For the purposes of determining the test angle, the kinetics of the upper leg/leading edge interaction were examined in the interval where the impact force was greater than 40 percent of the peak impact force. This restricted the examination of the kinetics to the main part of the impact. The components of the impact force in the vertical direction and the longitudinal direction of the car were used to calculate the angle at which the impact force was acting over the interval of the contact. The DEBUG file does not separate the elastic, friction and damping forces. Consequently, the angle was adjusted by the arc tan of the coefficient of friction, effectively removing the friction force from the calculation of the impact angle. The average of this adjusted angle over the contact interval was calculated and used as the angle of impact in the physical reconstruction.

The effective mass of the upper leg in the simulation was calculated by examining the peak elastic energy stored during the impact. The elastic contact force (F) was integrated with respect to the penetration (p) from the beginning of the contact to the peak penetration (p_{max}). The speed of the upper leg relative to the vehicle just prior to its contact with the leading edge (v) was then used to determine the effective mass of the upper leg at peak penetration. The effective mass, m_{eff} was calculated as follows:

$$m_{eff} = \frac{2}{v^2} \int_{p=0}^{p_{\max}} F dp$$

The minimum mass of the Upper Legform is 8.75 kg, and so where the calculated effective mass of the upper leg was less than this, the velocity of the Legform was adjusted to maintain the energy of the impact, as follows:

$$v_{adjusted} = \sqrt{\frac{m_{eff}}{8.75} v^2}$$

The velocity of the head was determined by taking the velocity of the head relative to the car at the time step prior to initial contact with the vehicle surface. Similarly, the Full Legform velocity was taken from the impact speed of the vehicle.

3.4 PHYSICAL RECONSTRUCTION

The final step in the study of each case was the reconstruction of the head and leg impacts associated with each colission. The matrix of tests is shown in Table 3-1 on Page 3. The car used to reconstruct impacts from each case was a vehicle of the same make, model and series as that involved in the actual accident. Where possible, a vehicle of the same year of manufacture was obtained. Otherwise, a vehicle with a construction date that was close to that of the case vehicle was obtained.

The results of the simulation of each accident were used to determine the initial conditions. The exceptions to this procedure were the following cases:

• In Case PED057-99, the test speed in the Upper Legform test was lowered as it was thought that the impact would be severe enough to damage the test equipment. It was decided that if the test at the lower speed did not fail, the test would be repeated at a higher speed.

• In another case, PED011-99, the head impact reconstruction produced much less damage than expected. In this case, the test was repeated until the damage from the accident was replicated. (In all other cases, the damage produced by the reconstruction was similar to that seen in the actual accident).

• The head impact velocity estimated in the simulation of Case PED076-00 was relatively low, and the design of the launcher is such that it is not possible to fire the Headform at such a low speed, at the angle specified. This is because gravity would cause the Headform to interfere with the launcher before it exits. The only feasible alternative in this case was to launch the Headform vertically downward.

The acceleration of the Headform was measured throughout the duration of the impact, and this was used to calculate the HIC value. The HIC is the criterion most commonly used for head injury risk assessment. It is calculated according to the formula

$$HIC = (t_2 - t_1)\left[\frac{\int_{t_1}^{t_2} a\,dt}{t_2 - t_1}\right]^{2.5}$$

where t is measured in milliseconds and a is the acceleration measured in units of g (the acceleration due to gravity). The values of t_2 and t_1 are chosen so that the function is maximised. Impacts that produce HIC values of more than 1000 are considered unacceptably severe, and the EEVC criterion is that the HIC value of the test should not exceed this value.

The Upper Legform consists of a tubular steel “femur” section that is simply supported at its ends. Force transducers at each end of the “femur” record the loads on the supports of the femur, and three strain gauges measure the bending moment across the “femur”. The EEVC WG10 criteria are that the sum of the support forces should not exceed 4 kN and the bending moment should not exceed 220 Nm.

The Full Legform consists of a femur and tibia section, connected by a frangible knee. The Legform measures the risk of ligamentous injury to the knee and the risk of a fracture to the tibia. The EEVC WG10 criteria are that the tibia acceleration should not exceed 150 g, and the knee rotation should be less than 15˚ while the knee shear displacements should be less than 6 mm.

4 Summary and discussion of the results

Detailed results of the reconstruction of each case are given in Sections 7 to 16. This section summarises the results of the simulation and the results of the physical reconstructions, comparing the results of the reconstruction to the injuries caused by the impacts.

4.1 SIMULATION RESULTS

The results of the simulations were used to choose initial conditions for the impact reconstructions (with the exceptions described in Section 3.4). In two cases, a single impact speed of the vehicle could not be determined from the evidence. In these cases, the simulations were run at the upper and lower limits of the estimate of the impact speed of the vehicle.

The results of the simulations are summarised in Table 4-1 to Table 4-3. The simulation results given in each table are those that defined the set-up of the impact reconstruction (refer to Section 3.4). The tables below also describe how the test conditions were determined for each test, and the actual test conditions measured during the test. The MADYMO simulation provided the impact speed for the Headform and Upper Legform, while the vehicle's impact speed (from the collision reconstruction) was used to determine the speed of the Legform test

Table 4-1 Summary of target Headform test conditions from the simulations

Case Number	Simulation results		Target test conditions	Actual set up	
	Speed (m/s)	Angle (deg.)		Speed (m/s)	Angle (deg.)
PED011	8.5	42	Based on simulation (first attempt)	8.47	42
			Based on simulation (second attempt)	8.42	42
			Based on damage to bonnet	12.67	42
PED018	11.6	65	Based on simulation	11.48	64
PED035	8.2	52	Based on simulation	8.1	52
PED043	9.9	47	Based on simulation	9.76	47
PED049	10.6	46	Based on simulation	10.37	46
PED056	15.5	45	Based on simulation	15.32	45
PED057	13.8	54	Based on simulation (high speed of range)	13.65	54
	12.3	55	Based on simulation (low speed of range)	12.21	55
PED061	6.4	39	Based on simulation	6.45	39
PED064	6.5	47	Based on simulation	6.51	47
PED076	4.4	61	Based on simulation (high speed of range)	4.41	90
	2.9	70	Based on simulation (low speed of range)	2.89	90

Table 4-2 Summary of target Full Legform test conditions from the simulations

Case Number	Impact speed from collision analysis (m/s)	Target test conditions	Measured test speed (m/s)
PED018	13.6	Reduced impact speed to reduce damage to test tool	10.85
PED035	9.4	Based on impact speed	9.24
PED043	9.7	Based on impact speed	9.74
PED049	11.9	Based on impact speed	11.55
PED056	16.7	Reduced impact speed to reduce damage to test tool	11.80
PED064	10.0	Based on impact speed	10.00
PED076	6.1 / 8.1	Based on impact speed (low / high)	6.08 / 7.72

Table 4-3 Summary of target Upper Legform test conditions from the simulations

Case Number	Simulation results			Target test conditions	Actual set up	
	Speed (m/s)	Angle (deg.)	Upper leg Mass (kg)		Speed (m/s)	Angle (deg.)
PED018	10.5	47	8.75	Based on simulation	10.4	47
PED043	6.8	60	8.75	Based on simulation	6.6	50
PED057	17.6 / 15.5	38 / 30	8.8 / 9.5	Simulation results too severe, therefore a lower impact speed was chosen	12.1	30

4.2 HEAD IMPACT RECONSTRUCTIONS

A summary of results of the head impact reconstructions is given in Table 4-4. This table also lists the injuries associated with the impact in the related case. These injuries have been categorised by the maximum score assigned to the head according to the Abbreviated Injury Scale (1990 edition). In the case of PED011-99, the pedestrian suffered a fracture-dislocation of the atlanto-occipital joint. This was probably due to tensile loads placed on the neck (Winkelstein and Myers, 1998), but the shear loads placed on this joint during the impact with the head would also have been significant, possibly contributing to the fracture-dislocation. The atlanto-occipital injury has been included in Table 4-4 because of the possible significance of the head impact in its production.

The relationship between the results of the head impact reconstructions and the head injuries sustained by the pedestrians in the study is presented in Figure 4-1. The figure plots the values of the Head Injury Criterion for each test against the severity of the head injury in the associated head impact. There appears to be a positive association between the value of the HIC and the severity of the injury. The exception appears to be the reconstruction of Case PED057-99. This case was unusual in that the pedestrian was not as severely injured as we might have expected, given the high speed at which she was struck.

On closer inspection of Case PED057-99, it appears that the extent of the deformation created in the car may have prevented a worse outcome than might have otherwise occurred. The deformation in the car involved in the collision is shown in Figure 4-2. This figure also shows the car used in the reconstruction of this case, after the impact reconstructions. The bonnet of the car involved in the collision was pushed upward some distance by the initial impact at the front of the bonnet. We hypothesise that this increased the clearance between the bonnet and the car structure beneath. This increased clearance may have softened the impact considerably. Increasing the clearance between the bonnet of a car and the components of the car beneath the bonnet has been shown to be a very effective way of reducing the severity of the impact in pedestrian accidents (Fredricksson and Håland, 2001). If this is the case, the head impact may have been far less severe in the accident than predicted by the reconstruction.

Nevertheless, there is a statistically significant positive association between the severity of the head injury in the case and the severity of the impact assessed by the EEVC criteria. Table 4-5 summarises the severity of the injuries in the cases by the impact severity, estimated by the reconstruction process. Fisher's exact test applied to this data supports the hypothesis that head injuries MAIS 3 or greater are associated with HIC values greater than 1000 ($p = 0.0238$).

Table 4-4 Results of the impact reconstructions and the MAIS of the head in each case

Case Number	Test results		Case data	
	HIC	Peak acceleration (g)	Head Injury	MAIS of head (and cervical spine where relevant)
PED011-99	2953	232	Head injury (Fatal neck injury)	3 (6)
PED018-99	3765	281	Fatal head injury	4
PED035-99	491	97	Mild confusion, no head injury diagnosed	2
PED043-99	1177	126	Fatal head injury	5
PED049-99	1678	193	Closed basal fracture of the skull and secondary brain injury (a complication of the skull fracture)	3
PED056-99	524	168	None diagnosed	1
PED057-99	3558 / 4109	326 / 319	Brief loss of consciousness & concussion	2
PED061-99	1718	229	Fatal head and brain injuries	5
PED064-99	136	96	None diagnosed	0
PED076-99	28 / 128	46 / 47	Brief loss of consciousness	2

Table 4-5 Summary of the data on impact severity and the related level of injury

		Head injury severity		
		MAIS≤2	MAIS>3	Total
Result of reconstruction	HIC<1000	4	0	4
	HIC≥1000	1	5	6
	Total	5	5	10

p = 0.0238 by Fisher's exact test

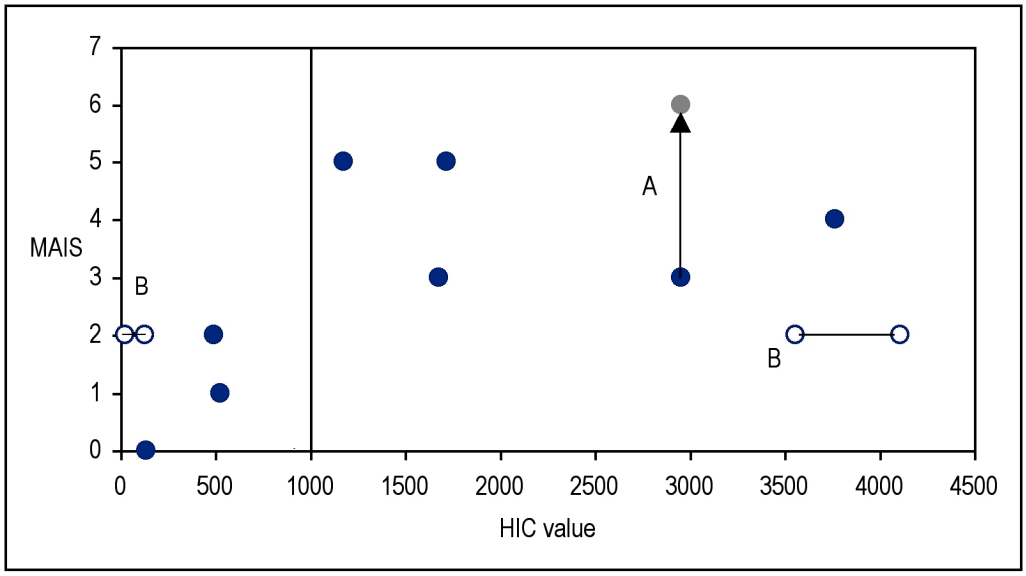

Figure 4-1 Head injury severities in the cases studied, and the HIC values measured in the impact reconstructions. (A) The pedestrian in PED011-99 suffered an atlanto-occipital fracture (at the base of the skull), and if included increases the MAIS to 6. (B) The graph includes results of both tests for cases PED057-99 and PED076-99.

4.3 LEG IMPACT RECONSTRUCTIONS

The results of the leg impact reconstructions and the relevant injuries associated with the impact in each case are tabulated in Table 4-6 in a similar fashion to the results of the head impact reconstructions in Table 4-4. The results of the Full Legform tests and the Upper Legform tests have been combined in the Table 4-6 because of the small numbers of Upper Legform impact reconstructions.

The results shown in Table 4-6 are presented graphically in Figures 4-3 to 4-7. The results of the reconstruction show the severity of injury below the knee appears to be positively associated with higher tibia accelerations in the tests. However, all tests in this study failed the EEVC criteria, based on the tibia acceleration, including two tests that were associated with no injury in the actual case. It should be noted that two tests were made using less severe test set-up conditions than those recommended by the simulations. This was done to protect the test tool from potentially damaging loads. The result of testing at a higher energy would have been to move the associated test result to

higher levels. If the acceleration levels associated with these reconstructions were increased, the data points in Figure 4-3 would be moved to the right. The resulting trend in the data would more strongly indicate that the EEVC WG10 limit is too low.

Figure 4-2 The deformation of the bonnet caused in the collision in Case PED057-99 (left). The deformation caused by the reconstruction tests was much less (right). The deformation created in the collision may have protected the head of the pedestrian by lifting the bonnet surface away from the under bonnet components of the car.

There seems to be little association between knee injury severity and the parameters that describe the kinematics of the knee in the test (Figure 4-4 and Figure 4-5). This may be because the test is specifically designed to measure lateral loading to the knee, and the loads applied to the knee in real life collisions are rarely purely lateral. Even if the leg is orientated so that the load is initially applied in a lateral direction, the impact may produce rotation of the leg during the impact, decreasing the lateral loads.

The final two graphs (Figure 4-6 and 4-7) show the relationship between the reconstruction of the upper leg impact in each case for which a reconstruction was performed, and the injuries produced by the associated impact in each case. Although the AIS 2 injuries were associated with impacts that failed the EEVC criteria, the number of reconstructions is too few to make any conclusions about the relationship between the results of the tests and real life injury. In Case PED057-99, the test was conducted at a lower speed than that suggested by the simulation. This was done because of the stiffness of the structure being struck and the associated risk of damaging the test device. Therefore, the result of this test should be considered a low estimate of the actual impact severity. We predict that had the test conditions been set to those suggested by the simulation, a much more severe impact would have resulted.

Table 4-6 Results of the leg impact reconstructions and the MAIS of the related body region in each case

Case Number	Test results			Case data	
	Test tool	Measurement	Result	Injury	MAIS
PED011	n.a.				
PED018-99	Full leg	Tibia acceleration	169.2 g (min)[1]	Compound fracture of tibia and fibula	2
		Knee bending	32.3˚(min)	No knee injury diagnosed	0
		Knee shear	4.1 mm (min)		
	Upper leg	Support forces	5 kN	Pelvic fracture	2
		Maximum bending moment	423 Nm		
PED035-99	Full leg	Tibia acceleration	289.6 g	Ankle fracture	2
		Knee bending	29.1˚		0
		Knee shear	7.9 mm		
PED043-99	Full leg	Tibia acceleration	293.4 g	No fractures identified. Bruising	1
		Knee bending	32.2˚	No knee injuries identified.	0
		Knee shear	n.a.		
	Upper leg	Support forces	4 kN	Laceration. No skeletal injuries identified on autopsy.	1
		Maximum bending moment	344 Nm		
		Tibia acceleration	165.8 g		
PED049-99	Full leg	Tibia acceleration	165.8 g	No fractures	0
		Knee bending	32.5˚	Knee contusions	1
		Knee shear	3.9 mm		
PED056-99	Full leg	Tibia acceleration	283.7 g (min) [1]	Tibia and fibula fractures	3
		Knee bending	33.1˚ (min)	No knee injury diagnosed	0
		Knee shear	7.5 mm (min)		
PED057-99	Upper leg	Support forces	8 kN (min) [1]	Pelvic acetabular fracture	2
		Maximum bending moment	605 Nm (min)		
PED061-99	n.a.				
PED064-00	Full leg	Tibia acceleration	199.4 g	No fracture	0
		Knee bending angle	29.9˚	Deep bruising of the knee	1
		Knee shear displacement	2.8 mm		
PED076-00	Full leg	Tibia acceleration	233.7/338.0 g	Tibia fracture	3
		Knee bending angle	15.9/21.7˚	No knee injuries diagnosed	0
		Knee shear displacement	3.4/3.7 mm		

1. Underestimate of impact severity – reduced impact conditions

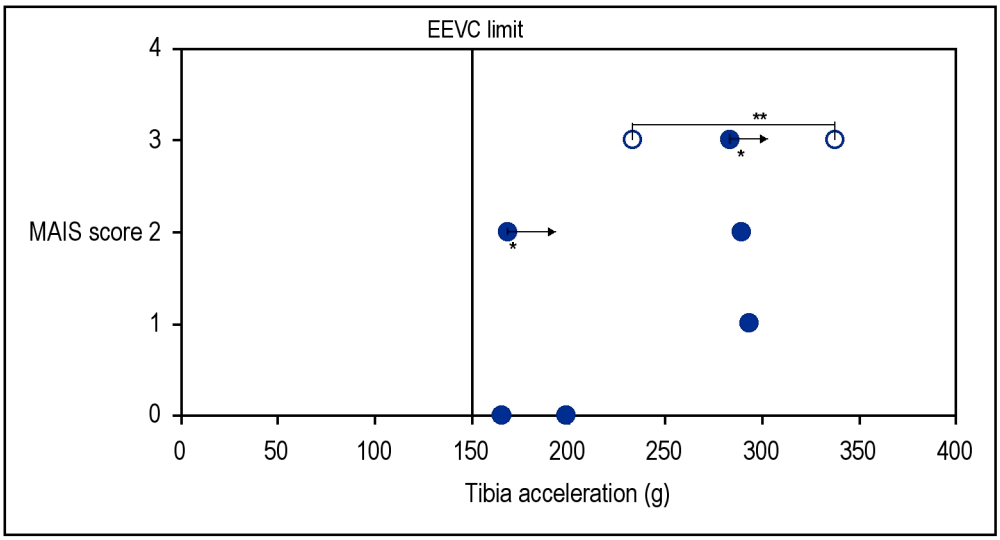

Figure 4-3 Lower leg injury severity in the cases studied, and the tibia acceleration measured in the impact reconstructions (* The likely severity of the impact in Cases PED018-99 and PED056-99 was probably greater than the reconstruction. ** The graph includes results of two tests for Case PED076-00 - see text)

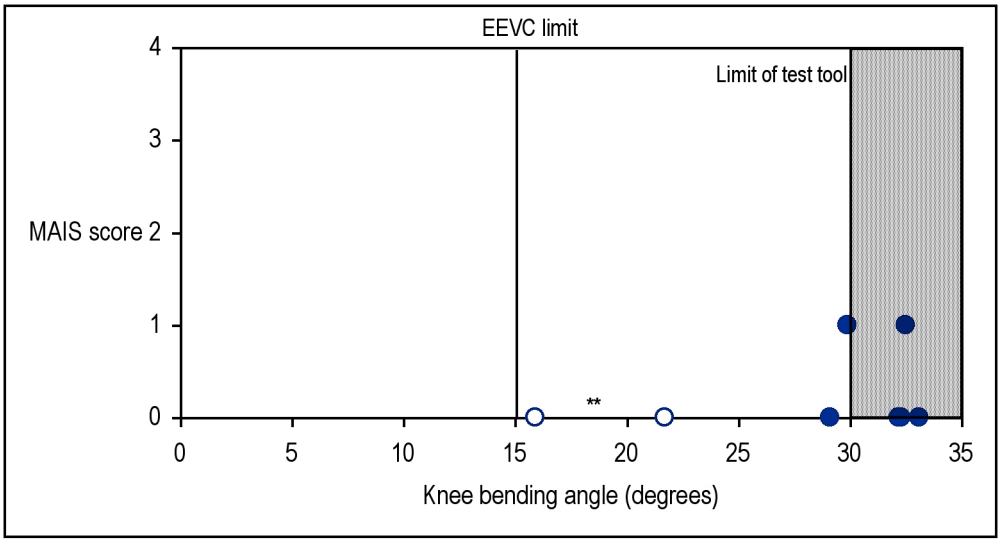

Figure 4-4 Knee injury severity in the cases studied, and the knee bending angle measured in the impact reconstructions (The graph includes results of two tests for Case PED076-00 - see text)**

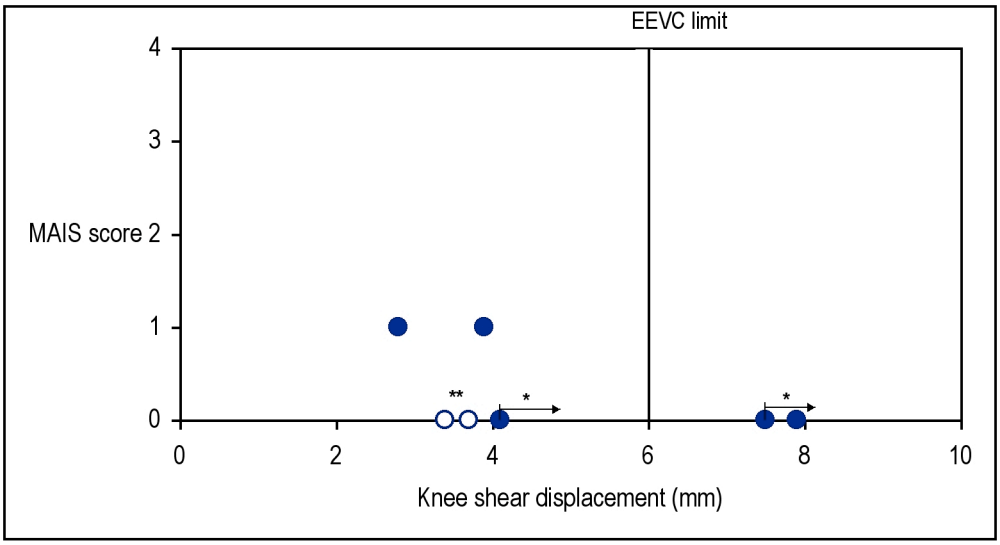

Figure 4-5 Knee injury severity in the cases studied, and the knee shear displacement measured in the Legform in the reconstructions (* The likely severity of the impact in Cases PED018-99 and PED056-99 was probably greater than the reconstruction. ** The graph includes results of two tests for Case PED076-00 - see text)

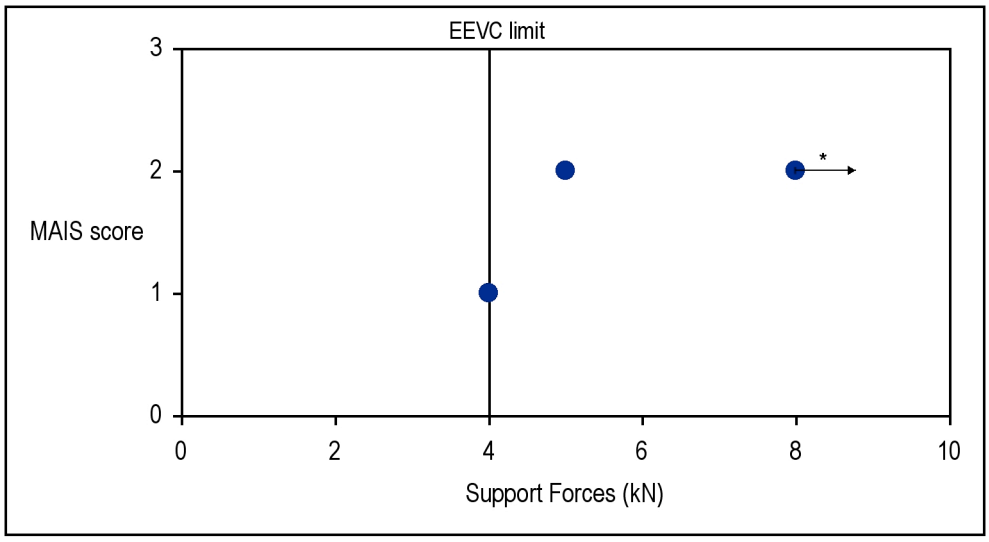

Figure 4-6 Upper leg/pelvis injury severity in the cases studied, and the support forces measured in the Upper Legform in the reconstruction (* The likely severity of the impact in Case PED057-99 was probably greater than the reconstruction - see text)

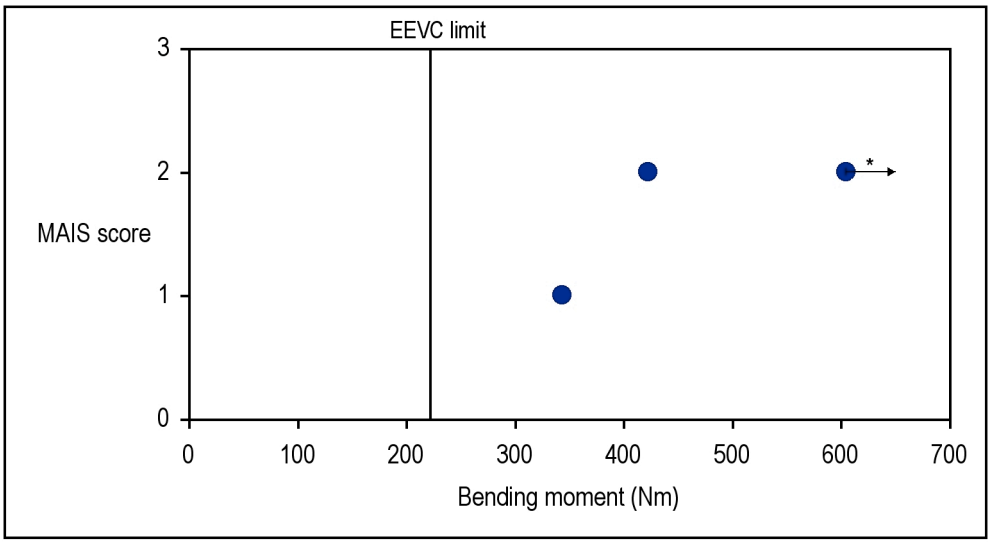

Figure 4-7 Upper leg/pelvis injury severity in the cases studied, and bending moment in the Upper Legform in the reconstruction (* The likely severity of the impact in Case PED057-99 was probably greater than the reconstruction - see text)

5 Discussion and conclusions

Pedestrian injuries and fatalities remain a significant problem in motorised countries. There is a very real need for the development of technology to protect pedestrians in the event of a collision with a vehicle. The data reported here show that vehicle design measures can be taken to protect pedestrians in a collision.

Test procedures such as those developed by the EEVC provide a means of assessing the performance of technology that is introduced to protect pedestrians in collisions. However, the EEVC tests are based on available data on human tolerance to impact. The aim of the research reported here has been to assess the validity of these tests with reference to the levels that have been assumed for impact tolerance. We have been able to demonstrate that the EEVC WG10 Headform impact test, when used to reconstruct a real-world impact, does relate to the severity of the injury. While the number of cases was small, there was a positive and statistically significant relationship between the results of the reconstruction tests using the EEVC WG10 Headforms, as measured by the Head Injury Criterion, and the severity of the injury in the cases, as measured by the Abbreviated Injury Scale.

The ability of the Full Legform to predict below-the-knee leg fractures appears promising, although more tests are required before this can be shown statistically. The results from the Full Legform that pertain to the kinematics of the knee appear more problematic, as there is no apparent relationship between the kinematics of the knee in the reconstruction test, and the injuries observed in the cases. The knee of the Legform is designed to replicate the behaviour of the human knee in lateral bending. It could be argued that the test is not appropriate in the reconstruction of impacts where the knee was not loaded in a purely lateral fashion.

Nevertheless, even when knee bending was more than double the EEVC WG10 pass criterion, no ligamentous damage was caused in the real collision. A recent study argued that the criterion for knee bending and shear should be increased, to take into to account the effect of bending in the lower leg (Tanahashi et al., 2001). The lower section of the Full Legform is rigid, whereas the human lower leg has some flexibility. An impact of a given force will tend to bend the bones in the leg, as well as generating bending and shearing in the knee joint. The bending of the bones will reduce the amount of knee bend and shear. However, the rigid tibia section in the Full Legform means that the energy in an equivalent impact is expressed only in knee bending and shearing, and these kinematics are amplified. Tanahashi et al., (2001) argue that this effectively means that the limit for knee bending should be increased to 20˚, and the shear limit to 23 mm (a displacement not possible with the current design). They argue that it would be more appropriate to redesign the lower section of the Legform to allow some bending.

A further problem of compensating for the behaviour in the knee by increasing the acceptable limit is that it is difficult to decouple the tibia acceleration from the knee kinematics. The stiffness of the knee will affect the acceleration of the tibia section. Specifically, stiffening the knee would be likely to reduce the acceleration of the tibia during the impact, as would the introduction of a frangible tibia element.

As mentioned above, this study appears to confirm that the reconstructed level of the tibia acceleration is associated with the severity of injuries to the tibia and fibula, as defined by AIS90. It may be observed, however, that the tolerance level that has been set by the EEVC WG10 appears

too low. As we have said, certain modifications of the legform would be likely to reduce the acceleration of the tibia during the impact. Therefore, for a given injury severity, such modifications would probably reduce the associated tibia acceleration. It is possible, therefore, that it is not the criterion that is too low, but that the Full Legform may be producing accelerations that are too high, by the nature of the knee and/or the tibia section. Clearly, further evaluation of the Full Legform is warranted.

We recommend that consideration be given to further evaluation of the subsystem impactors and their associated test methods. This report contains results that support the use of the Headform test for the evaluation of pedestrian protection. But further research is needed to assess the appropriateness of the Full and Upper Legform tests.

6 References

Anderson, R.W.G., Dar, L.H., Lindsay, V.L., Van de Griend, M., Ponte, G., Wundersitz, L.N., Baldock, M.R.J. and McLean, A.J. 2000a, 'Vehicle Design and Operation for Pedestrian Protection: Accident Investigation Reports', Department of Transport and Regional Services, Canberra.

Anderson, R.W.G., Gibson, T. and Benetatos, A. 2000b, 'Computer and physical reconstruction of pedestrian accidents involving children', Roads and Transport Authority of New South Wales, Sydney.

Anderson, R.W.G., Streeter, L.D. and McLean, A.J. 2000c, 'Estimation of impact severity in pedestrian accidents using accident investigation, computer simulation and physical reconstruction', *Road Safety Research, Policing and Education Conference Proceedings*, 26-28 November 2000, Brisbane, Australia. Brisbane: Carrs-Q, pp.285-290

Anderson R.W.G., McLean A.J. 2001, 'Vehicle design and speed and pedestrian injury: Australia's involvement in the International Harmonised Research Activities Pedestrian Expert Group' in *Road Safety Research, Policing and Education Conference Proceedings*, 18-20 November 2001, Melbourne, Victoria, Australia, vol. I. Melbourne: Monash University, pp. 1-7.

ATSB 2000, 'Australia's international pedestrian safety performance 1990 to 1997', Australian Transport Safety Bureau, Canberra.

ATSB 2001, 'ATSB Monthly bulletin: Road fatalities Australia', Australian Transport Safety Bureau, Canberra.

Baughman, L. 1983, 'Development of an interactive program to produce body description data', Report no. AFAMRL-TR-83-058, US Air Force Aerospace Medical Research Laboratory.

Fredricksson, R. and Håland, Y. 2001, 'Evaluation of a new pedestrian head injury protection system with a sensor in the bumper and lifting of the bonnet's rear part', *17th International Technical Conference on the Enhanced Safety of Vehicles, Amsterdam,* Paper 131-O, National Highway Traffic Safety Administration, USA.

Garrett, M. 1996, 'Head impact modelling using computer accident simulation based on cadaver records', *24th International workshop on human subjects for biomechanical research, Albuquerque, New Mexico, November 3, 1996*, US Department of Transportation. National Highways Traffic Safety Administration, pp. 81-92.

Garrett, M. 1998, 'Head impact modelling using MADYMO simulations of documented pedestrian accidents', *Conference on Pedestrian Safety, Melbourne, Victoria, 29 & 30 June 1998*, VicRoads, RACV, Federal Office of Road Safety, Australian Hotels Association, pp. 158-168.

Ishikawa, H., Kajzer, J. and Schroeder, G. 1993, 'Computer simulation of impact response of the human body in car-pedestrian accidents', *37th Stapp Car Crash Conference,* Paper 933129, Society of Automotive Engineers (SAE), Warrendale PA, pp. 235-248.

Janssen, E.G. and Nieboer, J.J. 1990, 'Protection of vulnerable road users in the event of a collision with a passenger car: Part 1 - Computer simulations', Report no. 754050002/I, TNO Road-Vehicles Institute, Delft.

Konosu, A., Ishikawa, H. and Sasaki, A. 1998, 'A study on pedestrian impact test procedure by computer simulation: the Upper Legform to bonnet leading edge test', *16th International Technical Conference on the Enhanced Safety of Vehicles, Windsor, Ontario,* Paper paper no. 98-S10-W-19.

Mohan, D. and Tiwari, G. 2000, 'Road safety in less motorized countries – relevance of international vehicle and highway standards', *International Conference on Vehicle Safety, London, 2000 7-9 June 2000*, IMechE, London, pp. 155-166.

Tanahashi, M., Konosu, A. and Ishikawa, H. 2001, 'Reconsideration of injury criteria for pedestrian subsystem legform test - problem of RIGID legform impactor', *17th International Technical Conference on the Enhanced Safety of Vehicles, Amsterdam,* Paper ID 263-O.

Thunnissen, J., Wismans, J., Ewing, C.L. and Thomas, D.J. 1995, 'Human volunteer head-neck response in frontal flexion: a new analysis', *39th Stapp Car Crash Conference, Coronado, California, November 8-10, 1995*, Paper 952721, Society of Automotive Engineers, Inc. (SAE), Warrendale PA.

Winkelstein, B.A. and Myers, B.S. 1998, In *Frontiers in Head and Neck Trauma* (Eds, N. Yoganandan, F. Pintar, S. Larson and A. Sances) IOS Press, Netherlands, pp. 266-298.

Wismans, J., Oorschot, H. and Woltring, H.J. 1986, 'Omni-directional human head-neck response', *30th Stapp Car Crash Conference,* Society of Automotive Engineers, Inc. (SAE), Warrendale PA., pp. 313-331.

Working Group 10 of the EEVC 1994, 'Proposals for methods to evaluate pedestrian protection for passenger cars', EEVC/CEVE.

Working Group 17 of the EEVC 1998, 'Improved test methods to evaluate pedestrian protection afforded by passenger cars', European Enhanced Vehicle-safety Committee.

7 Case PED011-99

7.1 CASE DESCRIPTION

A vehicle was travelling north in the right-hand lane of an arterial road. Two adolescent pedestrians were standing on the lane marking that divided the two traffic lanes. The collision occurred when one pedestrian stepped into the path of the vehicle, in an attempt to cross the lane. This pedestrian died as a result of her injuries.

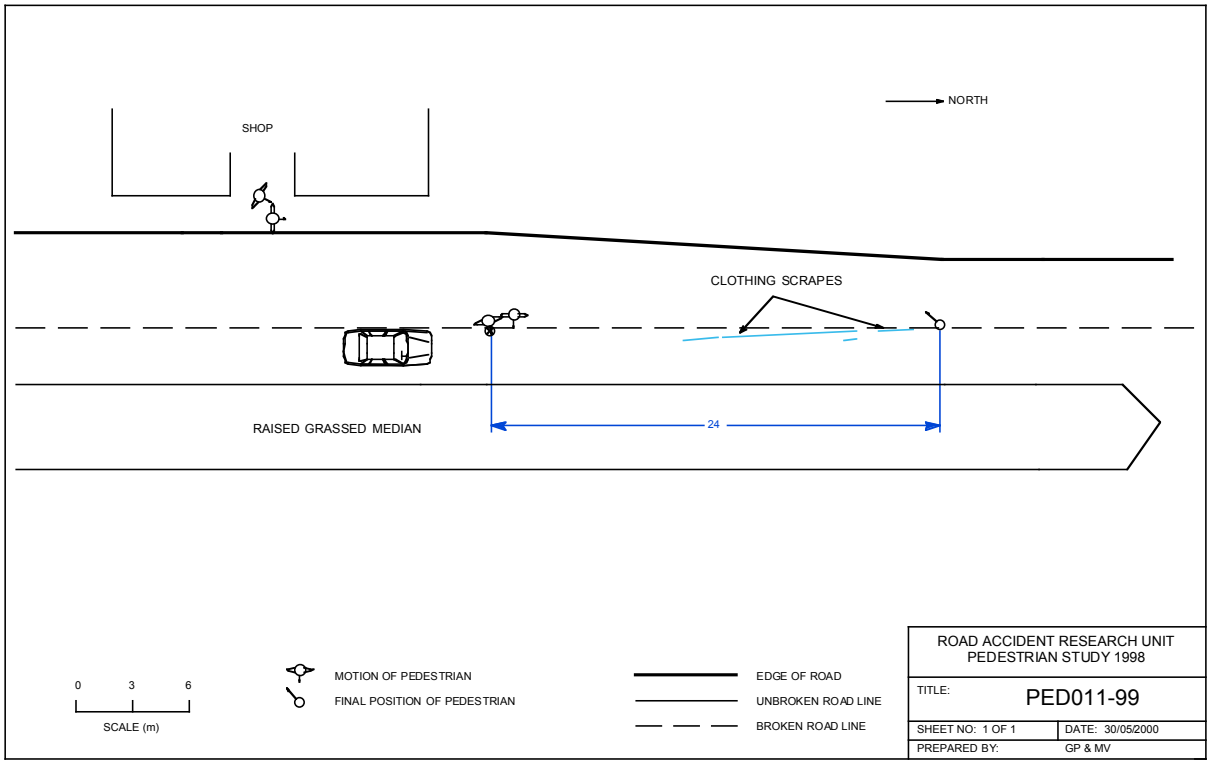

Figure 7-1 Site diagram of the collision in Case PED011-99

7.2 PEDESTRIAN INJURIES

The pedestrian experienced loss of consciousness and circulatory compromise as a result of the accident. She was transported by ambulance to hospital. Full cardiopulmonary resuscitation was commenced en route to hospital and continued on admission. Resuscitation was unsuccessful and she was pronounced dead one hour following the accident. The cause of death was determined to be complications resulting from a fracture/dislocation of the atlanto-occipital joint. Her other significant injuries were:

Soft tissue haemorrhage surrounding the fracture/dislocation of the atlanto-occipital joint;

Diffuse subarachnoid haemorrhage;

Laceration of the right side of the scalp measuring 80 mm;

Congestion and intra-alveolar haemorrhage of lungs;

Minor retroperitoneal haemorrhage and a lacerated liver.

7.3 ACCIDENT RECONSTRUCTION

The companion of the fatally injured pedestrian located the point of the collision on the roadway for the police. Other witnesses also verified the point. The pedestrian was thrown 24 m down the roadway. The pedestrian slid along the road for approximately half of this distance, as evidenced by scuffmarks on the roadway. There was no evidence of pre-impact or post-impact braking, so the travel speed and impact speed of the vehicle was calculated to be 52-61 km/h (using projection distance methods), with the mean of 56 km/h being used for reconstruction purposes. This speed is also consistent with witness and driver estimates of how fast the car was travelling.

Bruising to the upper thigh and liver laceration was associated with the dent on the leading edge of the bonnet and the damage to the left hand headlight/front corner of the mudguard (marked as location A in Figure 7-2). There was also a significant dent on the seam of the bonnet and left hand mudguard panel (marked as B), which was the source of the head impact resulting in scalp laceration, brain injuries and dislocation of the atlanto-occipital joint.

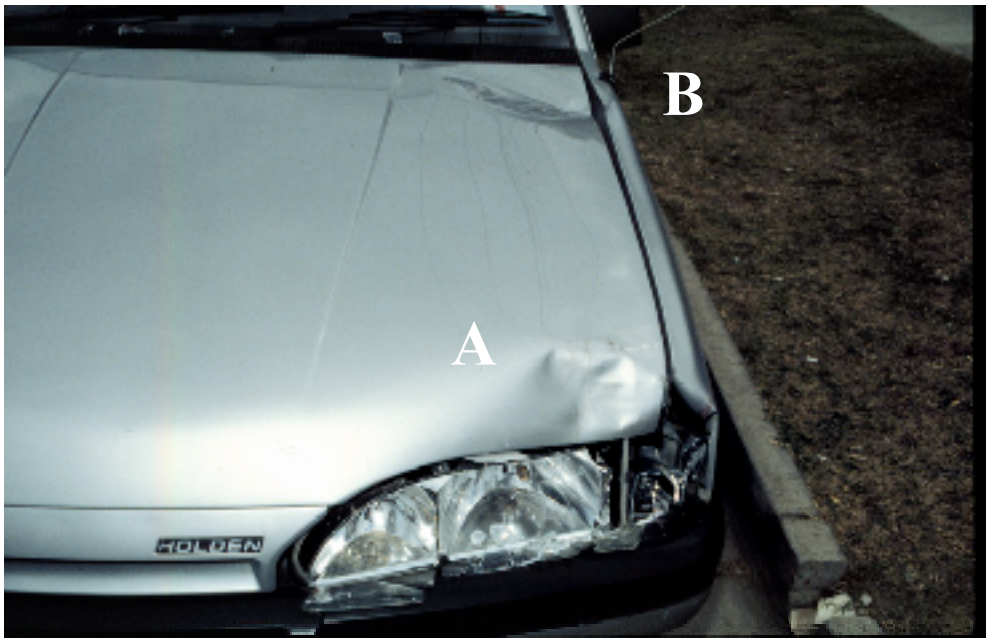

Figure 7-2 Collision damage to the Camira: (A) Pelvic/abdominal impact (B) Head impact

7.4 MADYMO SIMULATION

The details of the case that were used in the simulation are summarised in Table 7-1. The geometry of a 1988 Holden Camira was measured using a Geodimeter, as described in Section 3.3.4. The parts of the car that struck the pedestrian were approximated with planes and elliptical cylinders as

shown in Figure 7-3. The companion of the struck pedestrian described how the struck pedestrian walked into the path of the vehicle. Beyond this statement, her stance on impact could not be firmly established. Six stances, representing a gait cycle, were modelled and the resulting range of kinematics was examined. The initial positions of these models are illustrated in Figure 7-4. The simulations are numbered PED011-g1 through PED011-g6.

Table 7-1 Case details for reconstruction

Pedestrian details		
	Age, sex and height	13 year old female, 145 cm
	Orientation	Struck on right side
Vehicle details		
	Year, Make and model	1988 Holden Camira
	Impact speed	56 km/h (determined from pedestrian projection distance)

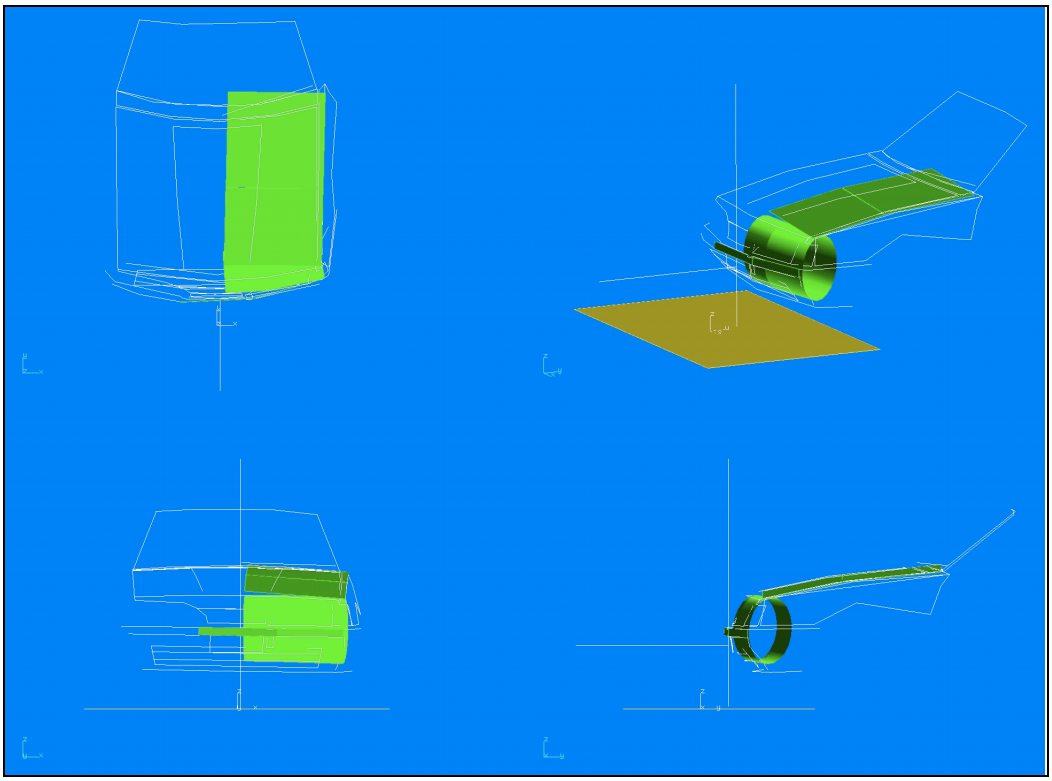

Figure 7-3 Geometry of the vehicle model involved in the collision (white lines). The approximation of this geometry for the simulation is shown by the shaded geometric entities.

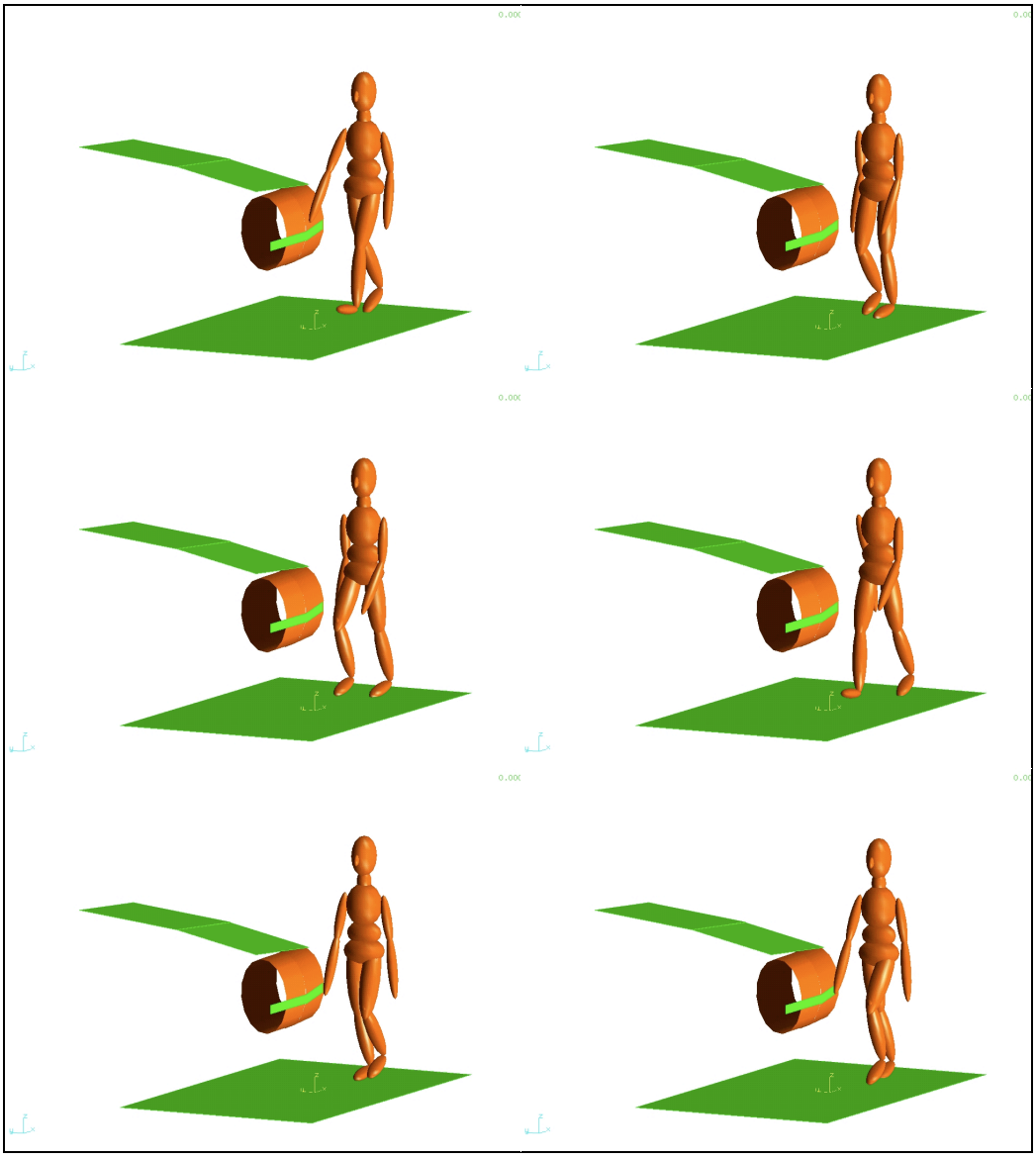

Figure 7-4 Initial position of the pedestrian and vehicle in the simulations PED011-g1 through PED011-g6 (*left to right and top to bottom*).

7.5 SIMULATION RESULTS

The results of the simulations of the accident are listed in Table 7-2. The range of head impact speeds predicted by the model was 7.7 m/s to 9.4 m/s, which is significantly less than the striking speed of the vehicle (15.5 m/s). The head speed is relatively low because of the kinematics that are produced when the leading edge of the vehicle is high relative to the height of the pedestrian.

In cases such as these, the body is struck near its centre of gravity. This causes a more rapid acceleration of the pedestrian than that which occurs in cases where the leading edge is lower with respect to the pedestrian's centre of gravity. Because the pedestrian is accelerated toward the speed of the striking vehicle, the horizontal component of the *relative* velocity of the head to the car drops quickly. Although the vertical component of this relative velocity increases as the head approaches the surface of the vehicle, the overall effect is that the velocity of the head relative to the car is lower than would have been the case if the leading edge of the car were lower.

The average result of the velocity of the head on impact was used for the physical reconstruction of the head impact in this case (Table 7-3).

Table 7-2 Simulation results for PED011-99

Simulation number	Head Velocity	Impact angle
	(m/s)	(deg.)
ped011-g1	8.70	39.32
ped011-g2	8.95	45.90
ped011-g3	9.35	44.36
ped011-g4	8.70	40.88
ped011-g5	7.80	44.60
ped011-g6	7.73	37.63
Average	**8.54**	**42.12**

7.6 PHYSICAL RECONSTRUCTION

7.6.1 Head impact reconstruction

The EEVC Working Group 10 sub-system impactors were used to simulate the impact between the different parts of the pedestrian and the vehicle, as described in Section 3.4. The location of the head impact was the centre point between the left hand bonnet edge and the left hand mudguard, measured at a wrap around distance of 1360 mm from the ground and a perpendicular distance of 680 mm from the centre of the bonnet. This location corresponded to the head impact measured on the original crash-involved vehicle. The test set up conditions are shown in Table 7-3.

Three impact tests were performed to try and reconstruct the head impact. The damage left after the first test (19060102) indicated that the target point was too near the wing panel of the car. A comparison between the damage left by the test, and the damage caused in the collision, shows that the test location should have been more toward the centre of the bonnet (Figure 7-6). The acceleration of the Headform in this test is shown in Figure 7-5 and the peak acceleration and HIC value are given in Table 7-3.

Table 7-3 Physical reconstruction parameters and results (test no. 19060102)

	Parameter	Value
Test set-up	Launch Angle	42°
	Measured velocity	8.47 m/s
Results	Peak acceleration	158 g
	HIC value (interval)	1298 (5.6 ms)

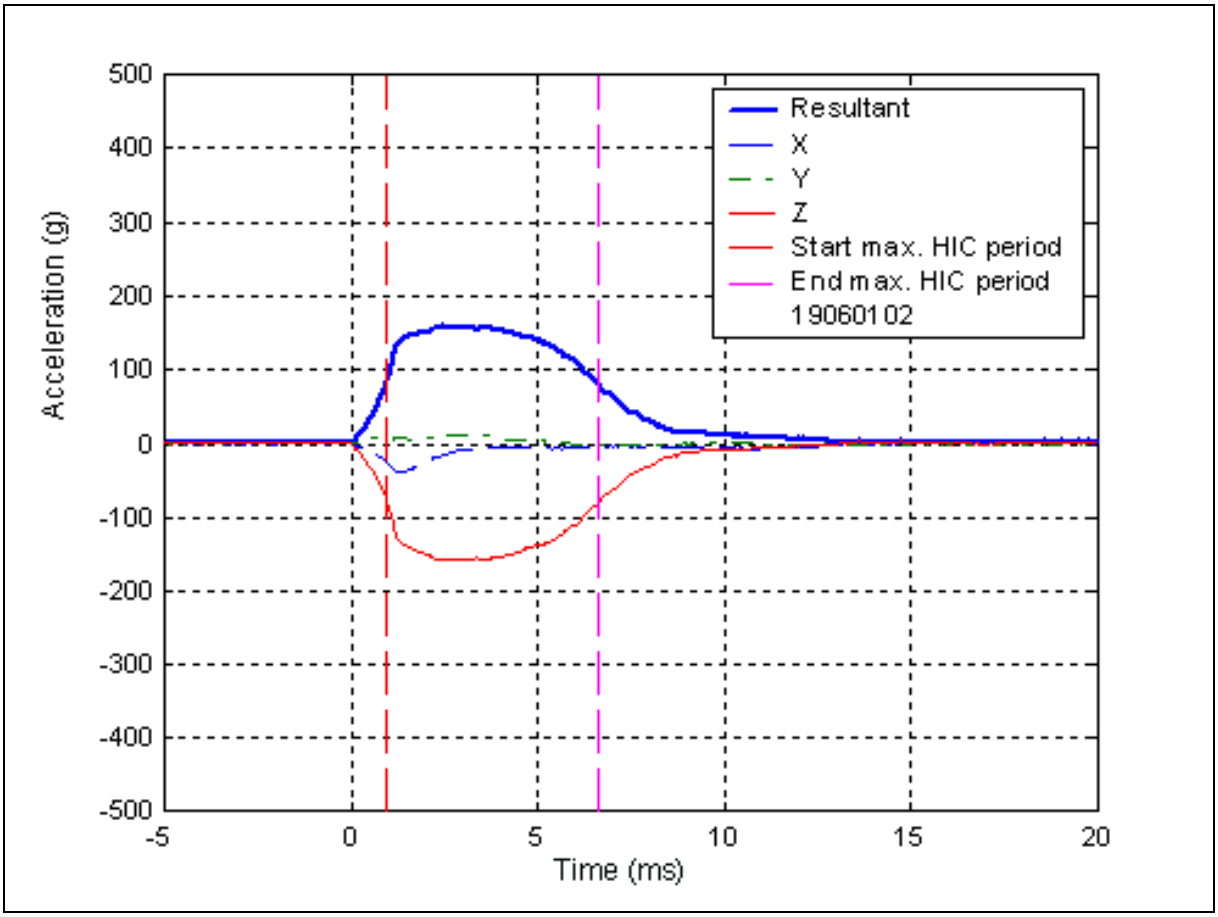

Figure 7-5 The acceleration recorded in the physical reconstruction of case PED011-99 (test number 19060102).

Figure 7-6 Damage caused by impact with the pedestrian's head (left) and the damage produced in the reconstruction (right) of case PED011-99 (test 19060102).

The point chosen for the second head impact test (19060103 p) was 145 mm closer to the front of the car than the first, and measured 650 mm from the centreline. The results of this test are shown

in Figure 7-7 and in Table 7-4, and the damage caused by the impact is shown in Figure 7-8. The pattern of damage between the bonnet and the wing was a better reflection of the damage on the case car. However, it is clear that the reconstruction test caused significantly less damage than did the head impact in the collision. This suggests that the estimate of the head impact speed from the simulation is too low.

Table 7-4 Physical reconstruction parameters and results (test no. 19060103).

	Parameter	Value
Test set-up	Launch Angle	42˚
	Measured velocity	8.42 m/s
Results	Peak acceleration	159 g
	HIC value (interval)	792 (4.8 ms)

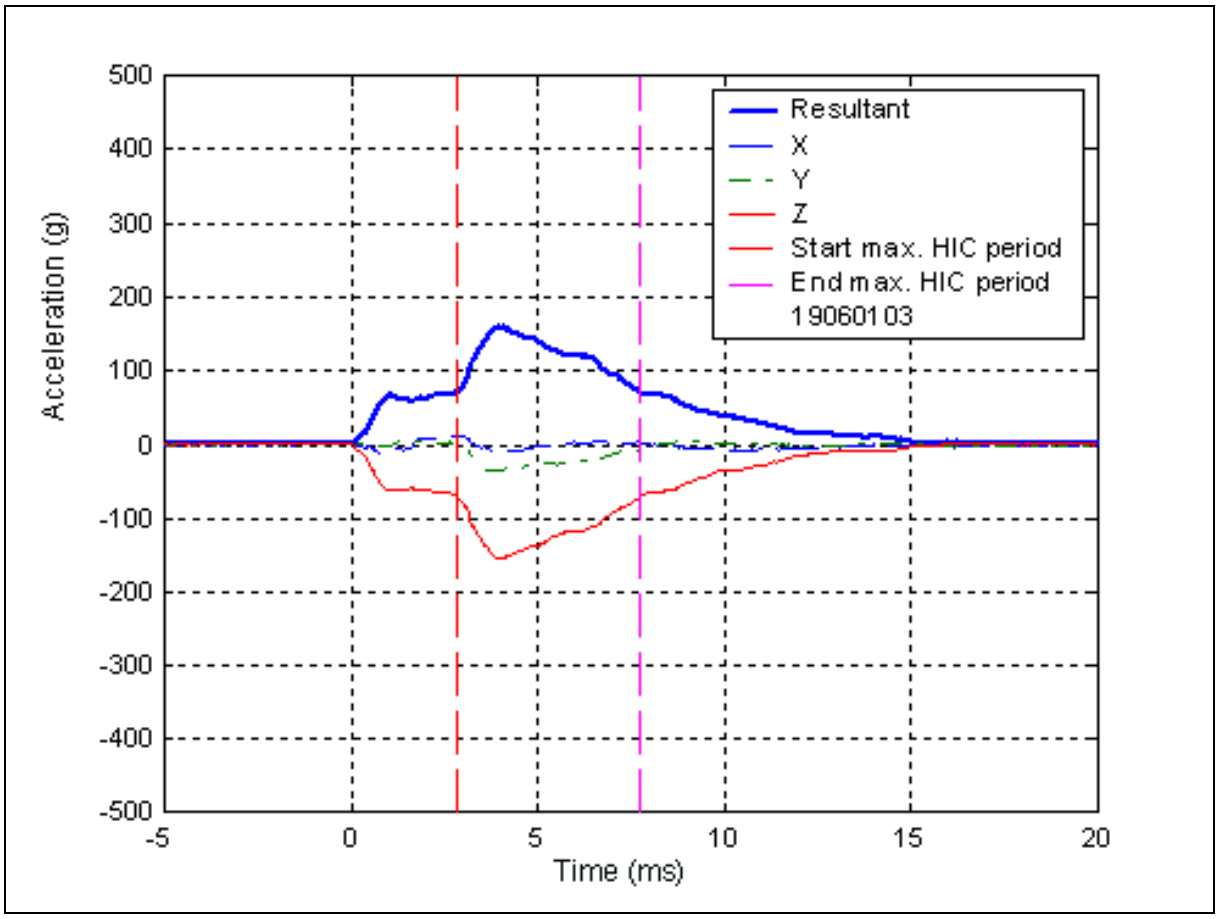

Figure 7-7 The acceleration recorded in the physical reconstruction of case PED011-99 (test number 19060103).

Figure 7-8 Damage caused by impact with the pedestrian's head (left) and the damage produced in the second reconstruction (right) of case PED011-99 (test 19060103).

A third test was performed to try and estimate more accurately the head impact severity in the collision. The simulation was re-examined to see if any specific assumptions that had been made had unduly lowered the head impact speed. Five degrees of braking dip was introduced into the model of the vehicle, on the assumption that the vehicle may have been braking in the accident. This lowered the leading edge by approximately 100 mm, but had little effect on the prediction of the head impact velocity.

A likely source of the underestimate of the head impact speed was the impact speed of the vehicle. This was based on the distance that the pedestrian was thrown after the initial impact. The pedestrian's companion identified the location of the impact point. It is possible that this location is not accurate. No other estimate of impact speed could be made, as the throw distance was the only piece of evidence available to make the estimate.

The aim of the third test was to show what impact severity was required to produce damage similar to that seen on the case vehicle. This entailed repeating the test, increasing the impact speed of the Headform until a pattern of damage was produced consistent with the damage produced in the accident. The set-up and result of this test is given in Table 7-5, and the acceleration of Headform is shown in Figure 7-9.

Table 7-5 Physical reconstruction parameters and results (test no. 03080103).

	Parameter	Value
Test set-up	Launch Angle	42˚
	Measured velocity	12.67 m/s
Results	Peak acceleration	232 g
	HIC value (interval)	2953 (5.4 ms)

A comparison of the damage caused in the accident and that caused in the third reconstruction may be made by inspecting the photographs in Figure 7-10. The amount of damage created by the reconstruction appears to be consistent with that observed in the case vehicle. The result of this test is the closest representation, of the three reconstruction tests reported here, of the head impact severity in the case.

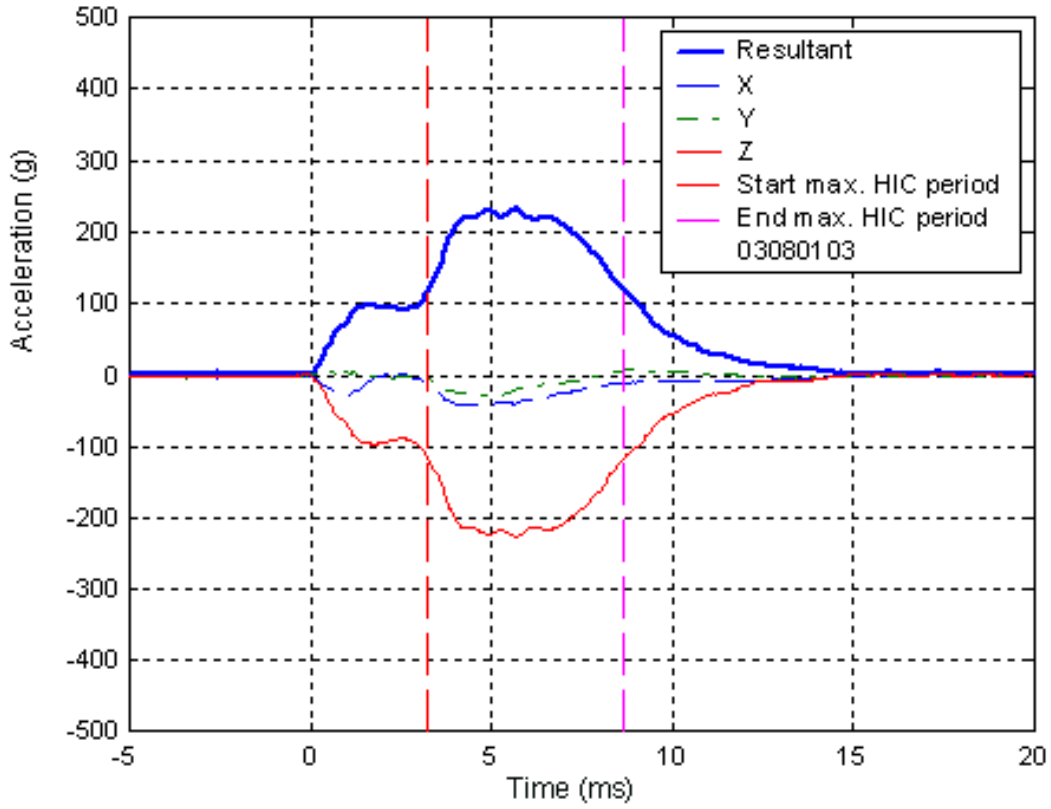

Figure 7-9 The acceleration recorded in the third reconstruction of case PED011-99 (test number 03080103).

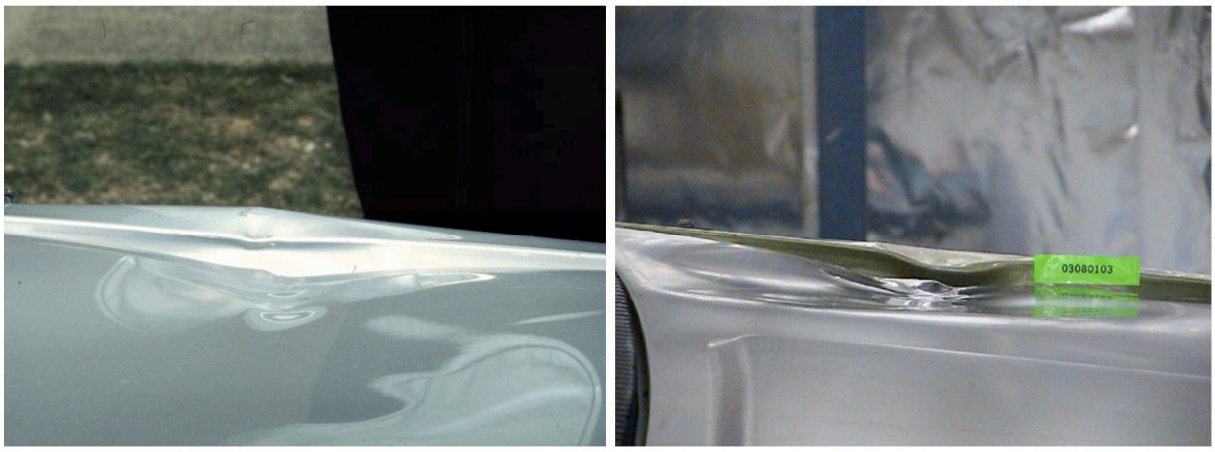

Figure 7-10 Damage caused by impact with the pedestrian's head (left) and the damage produced in the third reconstruction (right) of case PED011-99 (test 03080103).

7.7 SUMMARY OF RECONSTRUCTION RESULTS AND INJURY DIAGNOSIS

A summary of the test results and the corresponding injuries identified in the case are given in Table 7-6. Because the energy of the initial reconstruction impact appears to have been significantly less than that of the impact in the case itself, it is difficult to make firm comparisons.

It is clear, however, that a test result that better reflects the impact damage in this case had a significantly higher HIC value associated with it.

Table 7-6 Summary of test results and relevant injuries

Test	Measure	Result	Relevant Injury
Head	HIC	Test 1: 1298	Fatal head/neck injury
		Test 2: 792	
		Test3: 2953 (best estimate)	

Indicates a result which exceeds a safe limit according to EEVC WG10

8 Case PED018-99

8.1 CASE DESCRIPTION

The vehicle was travelling north on an arterial road initially in the right-hand lane, but changed to the left-hand lane to overtake a 4WD which was slowing down. Two pedestrians (an elderly lady and a male child pedestrian) were crossing from east to west at a Koala crossing, which was not activated at the time. The driver applied and locked the vehicle's brakes, but could not avoid the collision with the pedestrians. The vehicle came to stop at the end of the skid marks and the pedestrians landed about 5 m in front of the vehicle. The elderly female died as a result of the collision and the child pedestrian suffered minor injuries.

The reconstruction of this case involves only the female pedestrian.

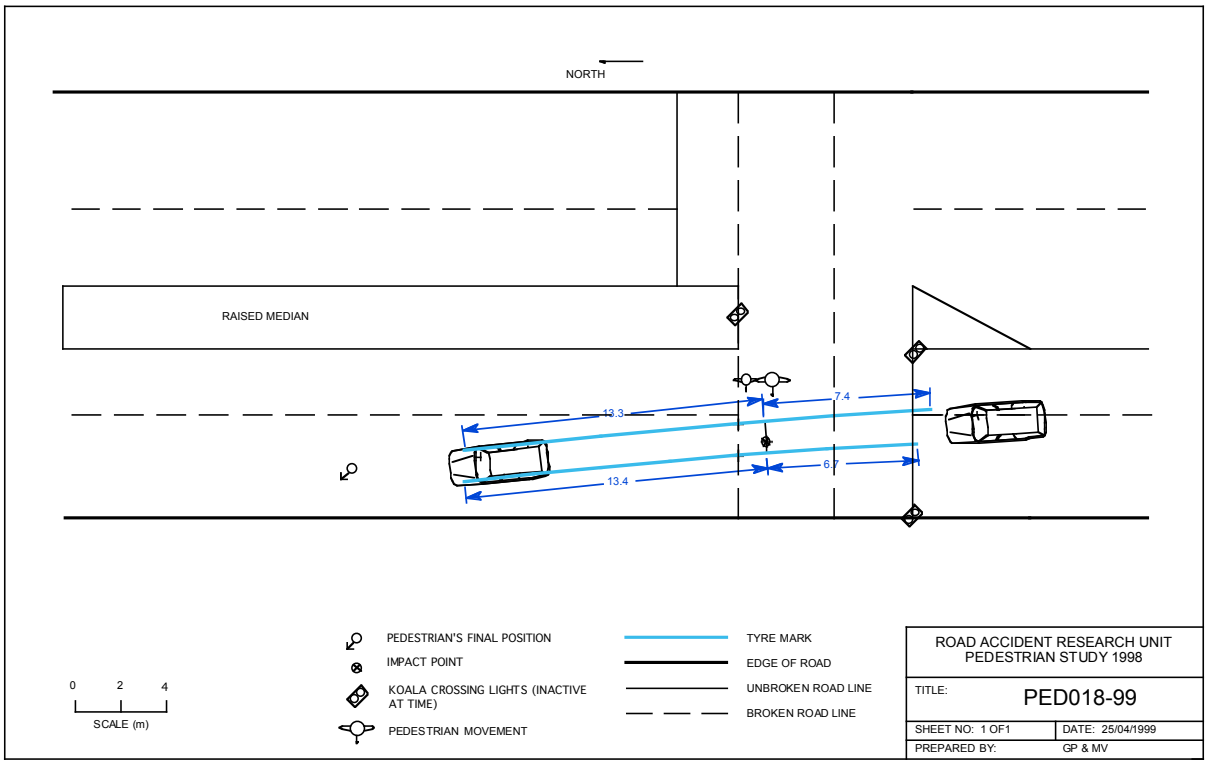

Figure 8-1 Site diagram of the collision in Case PED018-99

8.2 PEDESTRIAN INJURIES

The pedestrian was attended at the scene by St. John ambulance. On arrival of the ambulance service the pedestrian was unconscious with a Glasgow Coma Score of 3/15. Cardiopulmonary resuscitation was commenced but the pedestrian was pronounced dead at the scene. The cause of death was determined as closed head injury with significant frontal and left temporal skull fractures. Other injuries resulting from the accident included:

Other fractures to the skull

Brain injuries

Rib fractures to the anterolateral aspects of left and right rib cage

Fractured left pubis of pelvis

Compound fracture to the left tibia and fibula (proximal) and closed fractures to right tibia and fibula (proximal)

Fracture/dislocation of thoracic spine

Various cuts and abrasions.

8.3 ACCIDENT RECONSTRUCTION

The location of the collision in the crossing, and the skid marks left by the vehicle, make the striking speed of the vehicle reasonably certain. The skid marks indicate that the striking speed of the vehicle was 49 km/h, a speed entirely consistent with the distance the pedestrian was thrown along the roadway. A witness in a vehicle who had slowed to allow the pedestrians passage recalls that the adult woman was walking on the near side of the pedestrian crossing, her left side to the oncoming traffic, with her younger male companion on her right. The large laceration on the lateral aspect of her left calf was associated with blood found on the bumper of the vehicle, and this blood indicated the point of contact between her leg and the bumper of the vehicle. In line with this mark was denting of the bonnet, which indicated subsequent contact between the female pedestrian and the bonnet of the vehicle. There was a dent in the plenum cover of the vehicle, which was identified as the contact point between the vehicle and the head of the female pedestrian.

Table 8-1 Case details for reconstruction

Pedestrian details		
	Age, sex and height	79 year old female, 155 cm
	Orientation	Struck on left side
Vehicle details		
	Year, Make and model	1982 Nissan Bluebird
	Impact speed	49 km/h (determined from skid mark analysis and pedestrian throw distance)

8.4 MADYMO SIMULATION

A 1982 Nissan Bluebird was measured to obtain the geometry of the vehicle for the simulation. The procedure used to do this is described in Section 3.3.4. The geometry was represented by a series of planes and elliptical cylinders, as illustrated in Figure 8-2.

The evidence of first contact between the vehicle and the pedestrian was a blood mark around 240 mm left of the centre-line (indicated by the arrow in Figure 8-12) of the vehicle. Measurements at

autopsy showed that the 79 year old female pedestrian was 155 cm tall and weighed 53 kg. GEBOD was used to generate a MADYMO model, using the weight and height of the pedestrian as input. The resulting tabulation of body dimensions was inspected and checked against segment lengths taken at autopsy. The length of the lower leg segment, defined by patellar height corresponded to that measured at autopsy. Similarly, the height of the pedestrian's iliac crest from the heel corresponded to that generated by GEBOD.

The initial position of the pedestrian was not clear from the evidence on her body, nor was it clear from evidence on the car. The compound fracture to the left tibia and fibula may indicate that the left leg was the load bearing leg at the moment of impact, but such fractures may have also occurred had the right leg been the load bearing leg, given the high impact speed.

As the stance could not be firmly established beyond the orientation at the moment of impact, the modelling of the accident was performed using six representative postures, through a normal gait cycle.

The initial positions generated for these models are illustrated in Figure 8-3.

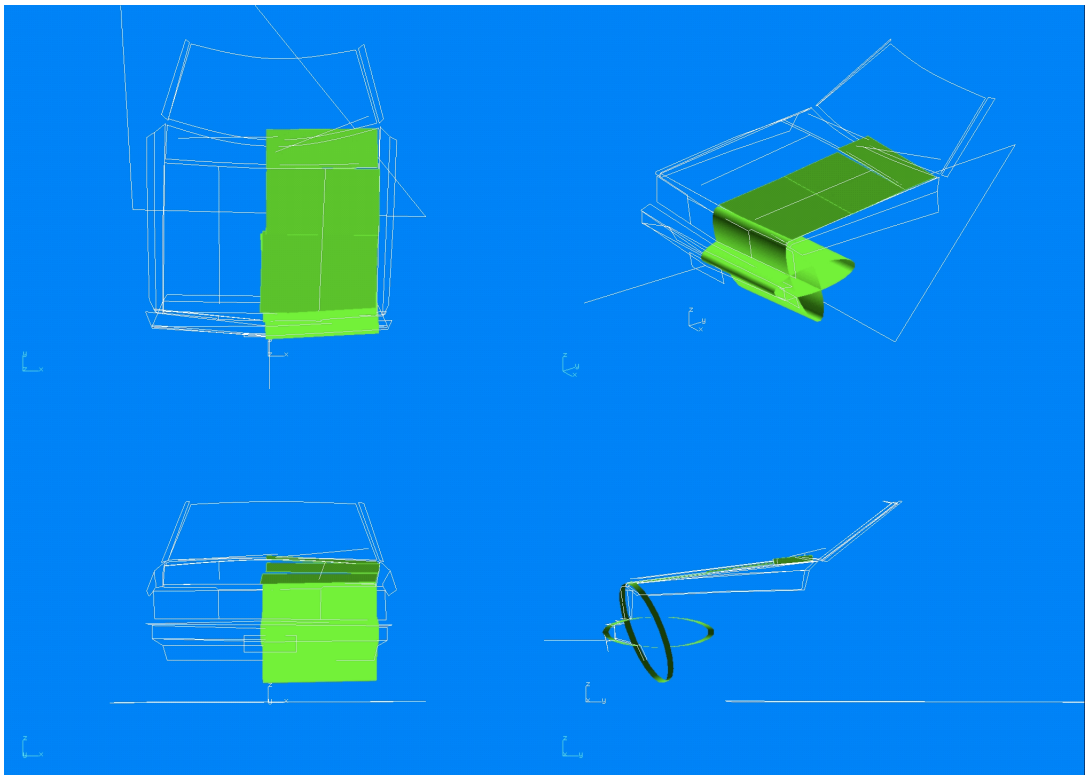

Figure 8-2 Geometry of the vehicle measured, shown in white. The approximation of this geometry for the simulation is shown by the shaded cylinders and planes.

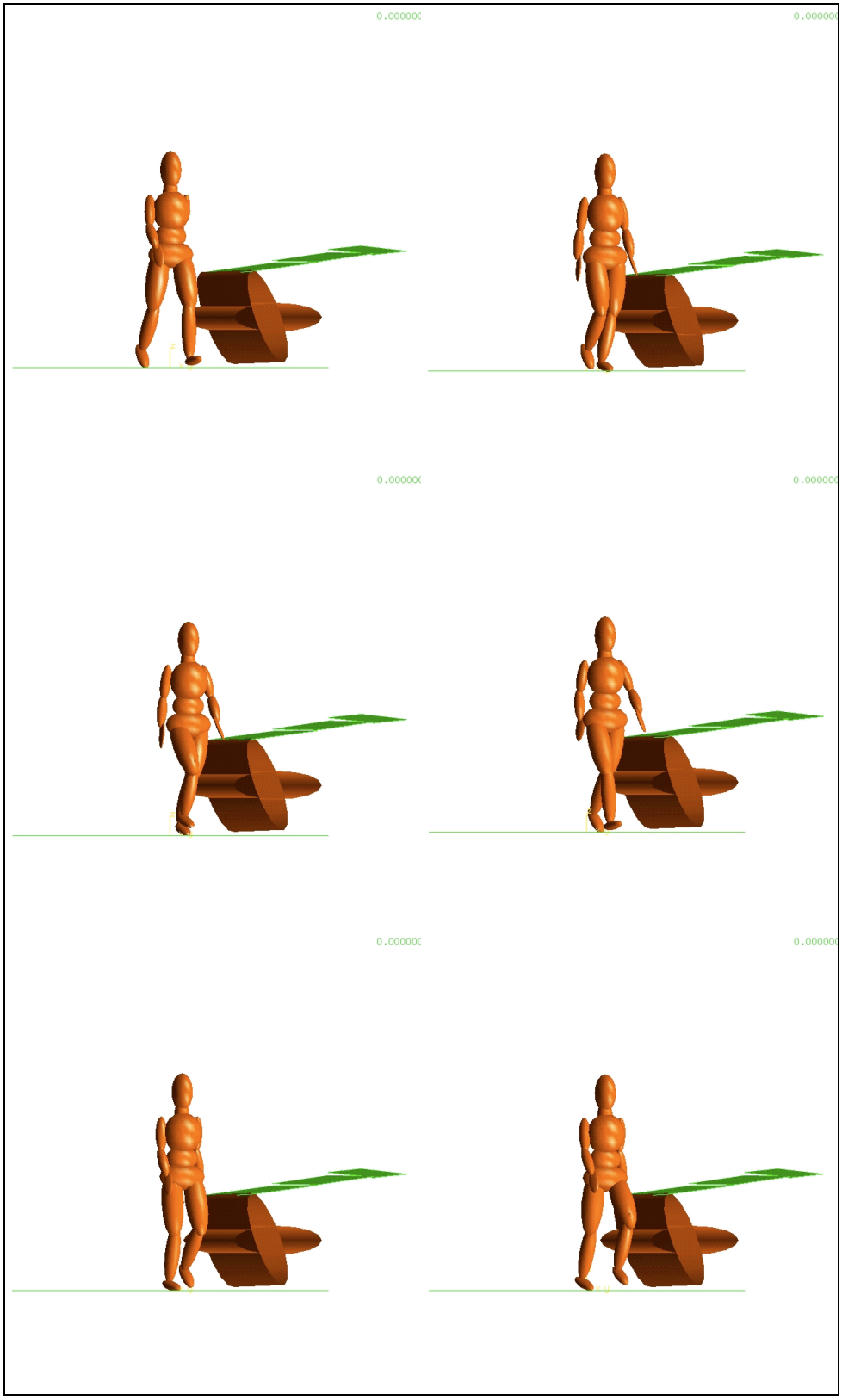

Figure 8-3 Initial position of the pedestrian and vehicle in the simulations PED018-g1 through PED018-g6 (*left to right and top to bottom*).

8.5 SIMULATION RESULTS

The results of the simulations of the accident are listed in Table 8-2. The upper leg test conditions were calculated as described in Section 3.3.5. The effective mass in all simulations was less than the minimum that could be used in the laboratory, and consequently, the velocity was adjusted to maintain the elastic energy calculated in the simulation.

Table 8-2 Simulation results for PED018-99

Simulation number	Upper leg velocity	Upper leg impact angle	Elastic energy	Upper leg effective mass	Corrected mass for test	Adjusted velocity for test	Head Velocity	Impact angle
	(m/s)	(deg.)	(J)	(kg)	(kg)	(m/s)	(m/s)	(deg.)
PED018_g1	13.73	42.89	400.65	4.25	8.75	9.57	13.09	60.12
PED018_g2	13.85	41.71	634.45	6.62	8.75	12.04	10.92	58.03
PED018_g3	14.02	42.96	472.02	4.80	8.75	10.39	10.48	60.46
PED018_g4	14.04	45.70	351.82	3.57	8.75	8.97	10.77	61.93
PED018_g5	14.11	41.97	580.34	5.83	8.75	11.52	11.74	59.35
PED018_g6	13.95	44.49	566.30	5.82	8.75	11.38	12.69	63.06
Average	**13.95**	**47.29**	**500.93**	**5.15**	**8.75**	**10.50**	**11.62**	**64.49**

8.6 PHYSICAL RECONSTRUCTION

The EEVC Working Group 10 sub-system impactors were used to simulate the impact between the different body segments of the pedestrian and the vehicle, as described in Section 3.4. The following tables and graphs show the results of the tests.

Figure 8-4 A general view of the accident damage from the impact (left) and the damage produced in the physical reconstruction (right) of case PED018-99.

8.6.1 Head impact reconstruction

Table 8-3 Physical reconstruction parameters and results for the Headform test (test no. 05060100)

	Parameter	Value
Test set-up	Launch Angle	64˚
	Measured velocity	11.48 m/s
Results	Peak acceleration	281 g
	HIC value (interval)	3765 (5.4 ms)

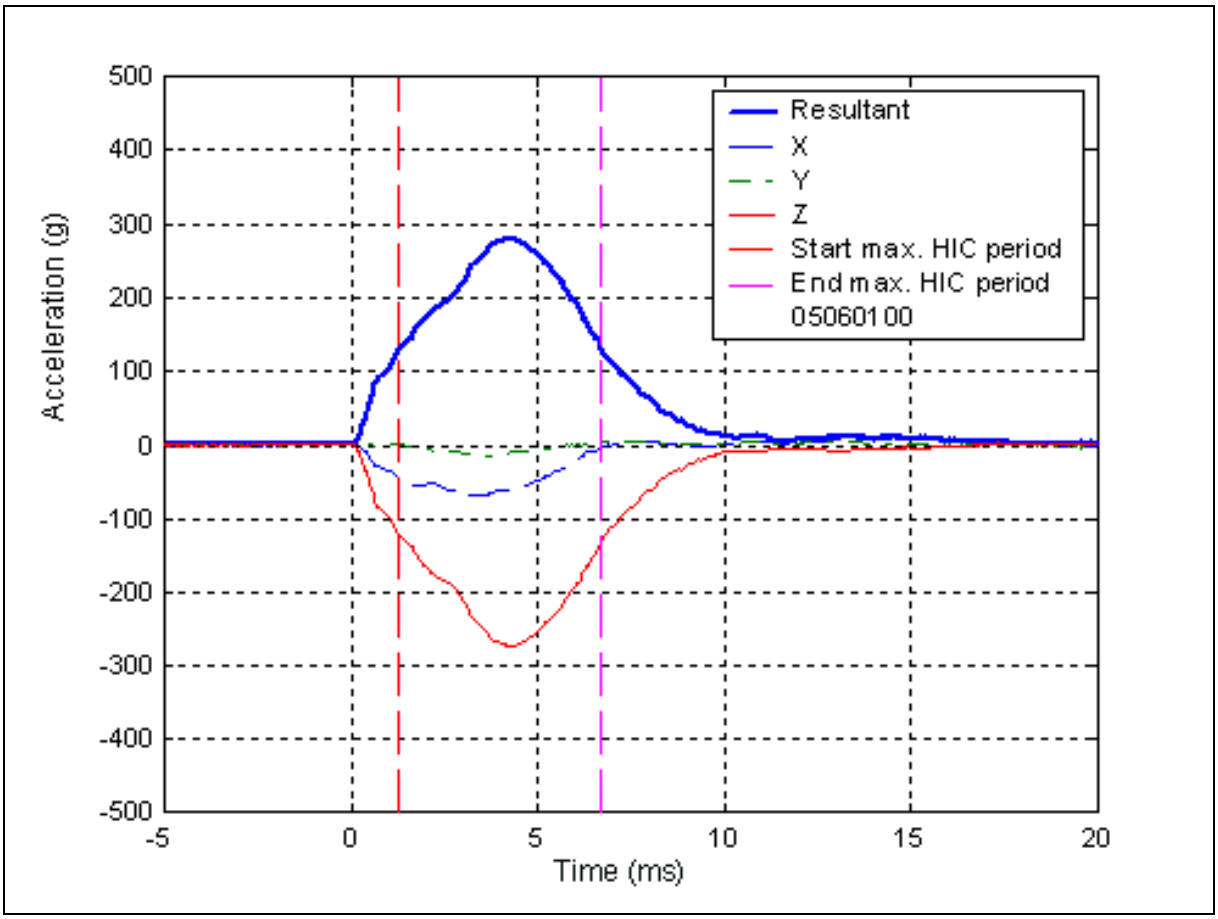

Figure 8-5 The acceleration recorded for the Headform test in the physical reconstruction of case PED018-99.

Figure 8-6 A side view of the damage caused by impact with the pedestrian's head (left) and the damage produced in the reconstruction (right) of case PED018-99.

8.6.2 Leg impact reconstruction

The analysis of the collision indicated that the appropriate reconstruction speed for the Legform was 13.6 m/s. We anticipated that the bumper of the vehicle, being steel, would cause a severe impact, and a more conservative speed was chosen, knowing that the impact severity would be lower than had the test been conducted at 13.6 m/s. The measurements made during the test are shown in Table 8-4. The results of the reconstruction are shown in Figures 8-7 to 8-9.

Table 8-4 Physical reconstruction parameters and results for the Legform test (test no.07060101)

	Parameter	Value
Test set-up	Measured velocity	10.85 m/s
Results	Tibia acceleration	169.2 g
	Knee bending angle	32.2˚
	Knee shear displacement	4.1 mm

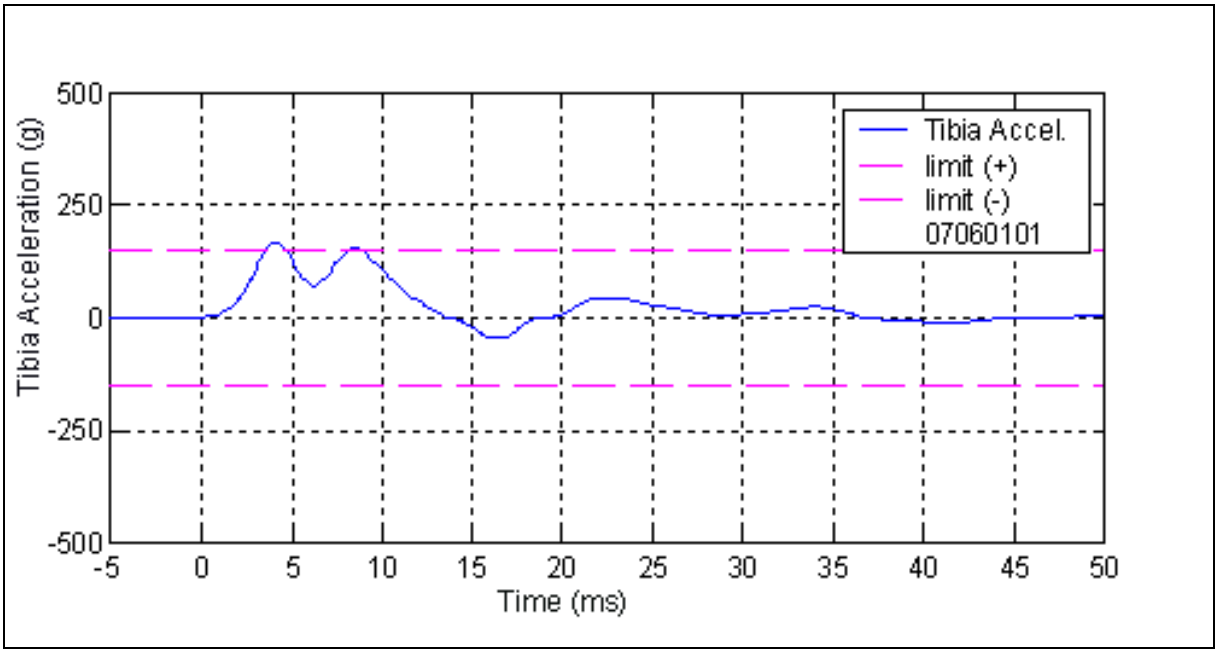

Figure 8-7 The tibia acceleration recorded in the physical reconstruction of case PED018-99.

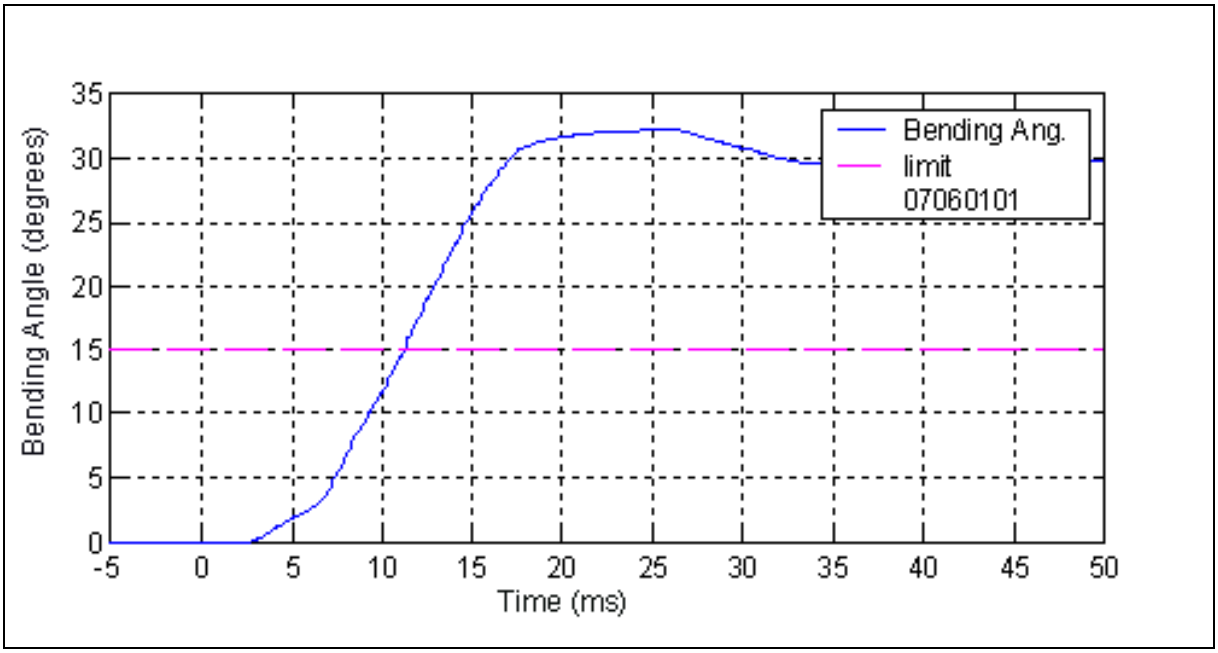

Figure 8-8 Knee bending angle recorded for the physical reconstruction of case PED018-99.

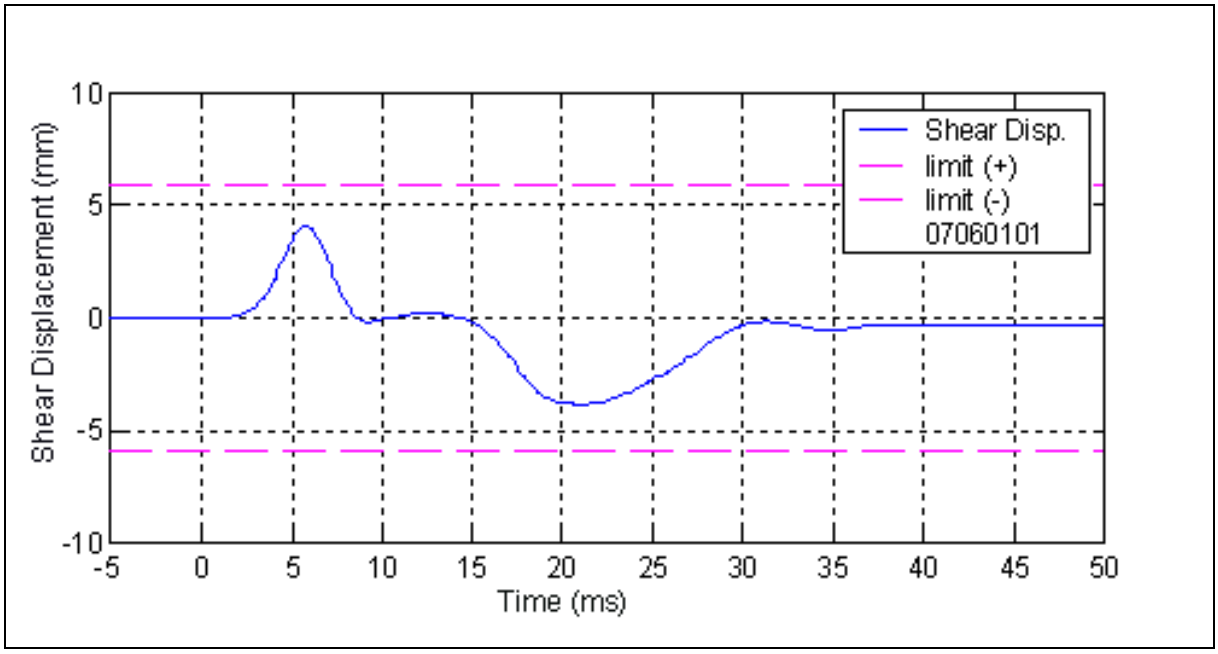

Figure 8-9 Knee shear displacement recorded for the physical reconstruction of case PED018-99.

8.6.3 Upper leg impact reconstruction

An Upper Legform reconstruction was undertaken on the basis of the MADYMO simulation. As the effective mass was lower than that achievable, the velocity was adjusted to maintain the impact energy predicted by the simulation. The measurements made from the reconstruction are given in Table 8-5, and the instrumentation traces are shown in Figures 8-10 and 8-11. A comparison of the accident damage and the deformation caused in the reconstruction is made in Figure 8-12.

Table 8-5 Physical reconstruction parameters and results for the Upper Legform (test no.05060101)

	Parameter	Value
Test set-up	Launch Angle	47˚
	Impactor mass	8.75 kg
	Target velocity	10.5 m/s
	Actual velocity	10.4 m/s
Results	Maximum force	5 kN
	Bending Moment	423 Nm

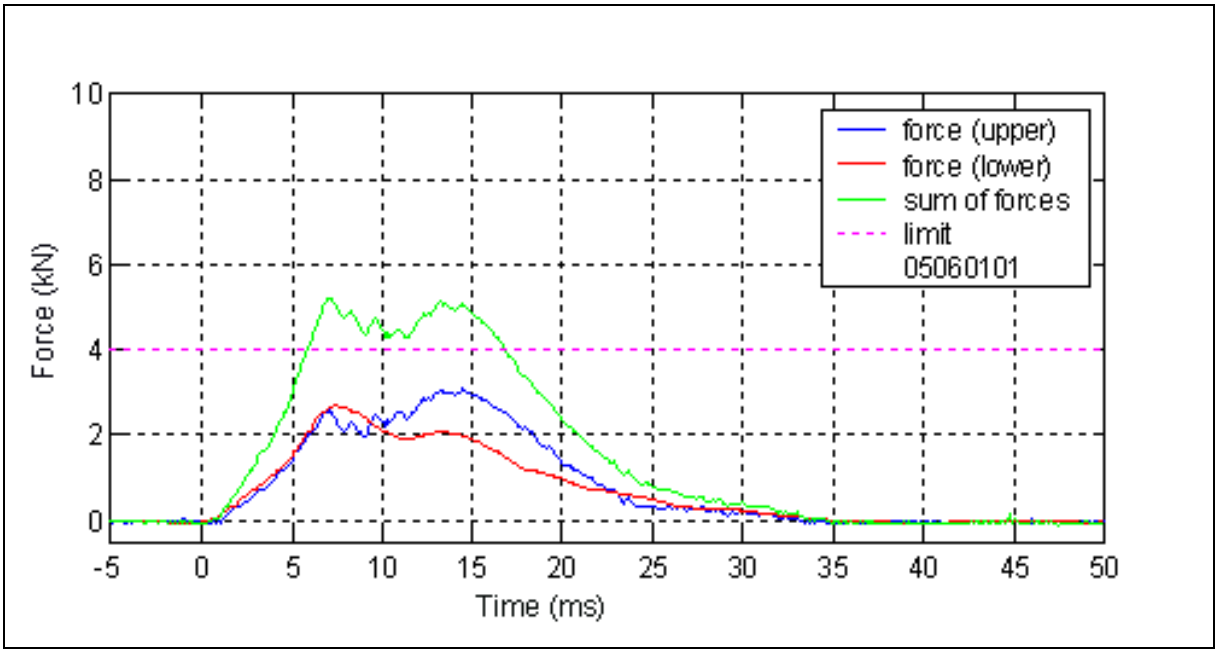

Figure 8-10 Upper leg force recorded in the physical reconstruction of case PED018-99.

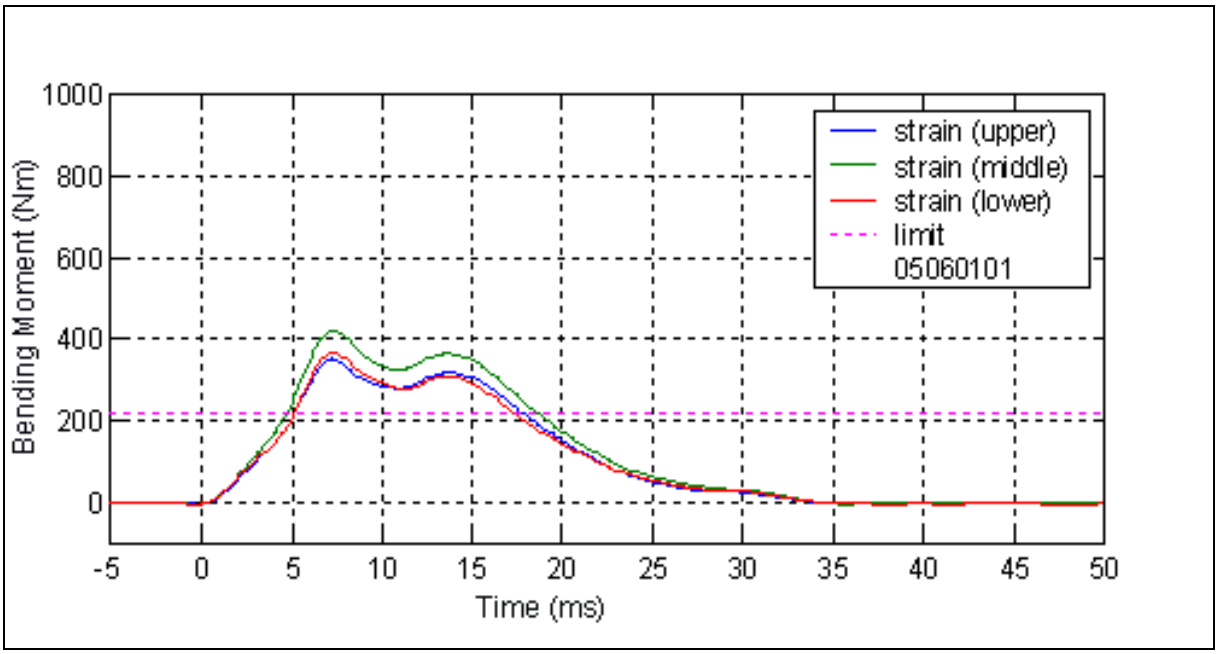

Figure 8-11 Bending moment recorded in the physical reconstruction of case PED018-99

Figure 8-12 A close up front view of the accident damage from impact with the pelvic area (left) and the damage from the reconstruction with the Upper Legform (right) of case PED018-99.

8.7 SUMMARY OF RECONSTRUCTION RESULTS AND INJURY DIAGNOSIS

A summary of the test results and the corresponding injuries identified in the case are given in Table 8-6. A qualitative comparison between the damage present on the case vehicle and the damage caused to the test vehicle would suggest that the energy of the respective impacts (case and reconstruction) were similar. The evidence available for the accident investigation was clear and unambiguous, which gives some credibility to the reconstruction.

Given that this case provided relatively clear impact speeds and the physical test produced somewhat similar vehicle damage, one may assume that the results of the tests are a fair representation of sub-system tests that are equivalent to impacts in the actual case.

Table 8-6 Summary of test results and relevant injuries

Test	Measure	Result	Relevant Injury
Full leg	Tibia acceleration	169.2 g	Compound fracture of tibia and fibula, no knee injury diagnosed
	Knee bending	32.2°	
	Knee shear	4.1 mm	
Upper leg	Support forces	5 kN	Pelvic fracture
	Maximum bending moment	423 Nm	
Head	HIC	3765	Fatal head injury

Indicates a result which exceeds a safe limit according to EEVC WG10

9 Case PED035-99

9.1 CASE DESCRIPTION

A female pedestrian attempted to cross a two-lane road from the west to the east side. She was struck by a car in the right-hand lane. Her head then struck the windscreen and she was thrown to the side of the car onto the road.

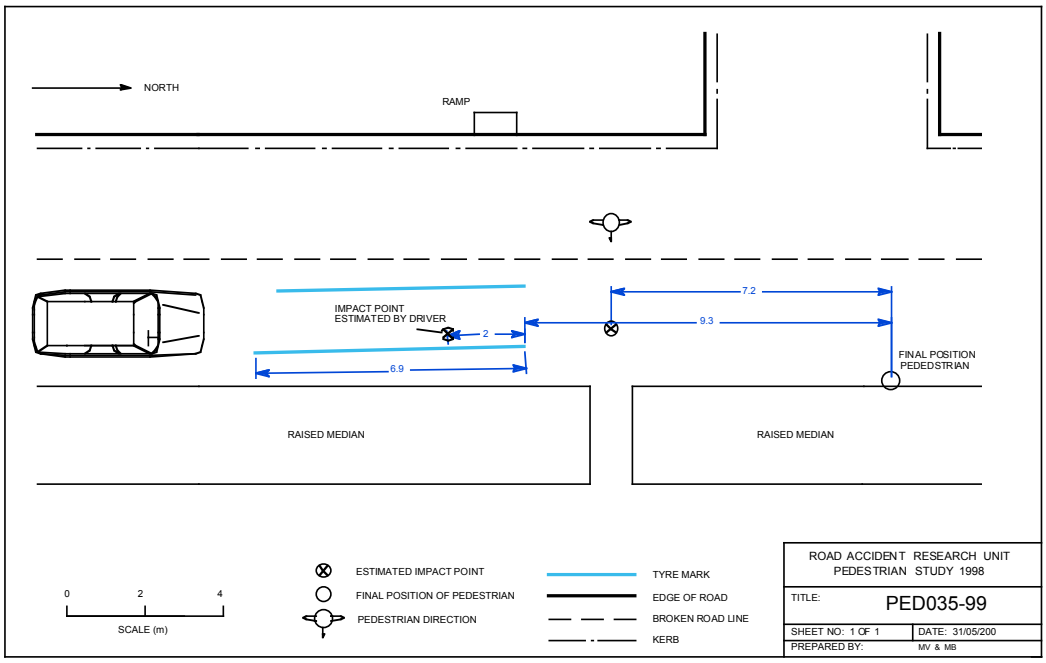

Figure 9-1 Site diagram of the collision in Case PED035-99

9.2 PEDESTRIAN INJURIES

The pedestrian was transported by ambulance and admitted to hospital. She was conscious following the accident but was confused for several hours following admission. Her other significant injuries were:

A fracture of the right ankle,

A blistered area on her right inner calf, cause unknown,

A right shoulder injury with no conclusive diagnosis. On last contact with her (3 months following accident) she continued to have a diminished range of motion in her shoulder.

9.3 ACCIDENT RECONSTRUCTION

The driver observed the pedestrian from 50 to 60 m away. Although the driver did not indicate it, it is possible that the driver was slowing down, but at the last moment when the driver realised he was not slowing rapidly enough, he braked hard (and locked the wheels of the vehicle). The impact point marked on the roadway was based on information received from the driver. If it assumed that the car came to rest at end of the skid marks, the speed of the vehicle at wheel lock-up would have been in the range of 35-39 km/h (the driver said he was travelling around 55 km/h) and the impact speed would have been 19 km/h. However, this would mean that distance the pedestrian was thrown was 11.3 m. This throw distance would imply an impact speed in the range of 37-49 km/h, which is not consistent with the other evidence.

The pedestrian had parked her vehicle in the side street and specifically states that she was walking straight across the road (and not at an angle), toward the break in the raised median. She made this journey weekly. If the impact point was aligned with the break in the median, and not at the point nominated by the driver, the driver must have locked his wheels and then released them again prior to striking the pedestrian. In this scenario, the pedestrian would have been thrown 7.2 m, implying an impact speed of 34 km/h. If the driver had been travelling at 55 km/h, and locked his brakes for 6.9 m (losing 20.5 km/h by braking), his speed would have been 34.5 km/h immediately before impact. On the evidence, this scenario seems more plausible.

The fracture to the pedestrian's right ankle could have been produced by a mechanism associated with the impact between the vehicle's bumper and the pedestrian's leg, her foot being 'trapped' on the road. This would imply that the right foot was the load-bearing foot at the instant of the collision. The injury to the pedestrian's right shoulder may have come from impact with the vehicle's bonnet/right mudguard. The delayed concussion suffered by the pedestrian was probably caused by the head impact with the lower right hand section of the windscreen.

9.4 MADYMO SIMULATION

A 1991 Ford Falcon was measured to obtain the geometry of the vehicle for the simulation. The procedure used to do this is described in Section 3.3.4. The geometry was represented by a series of planes and elliptical cylinders, as illustrated in Figure 9-2.

Based on the presence of a right-ankle fracture, the simulations examined three positions in the gait cycle where the right foot is grounded (Figure 9-3). In each of the simulations the head struck the vehicle surface in the correct location, when the pedestrian was placed 410 mm from the centre-line of the vehicle.

Table 9-1 Case details for reconstruction

Pedestrian details		
	Age, sex and height	83 year old female, 164 cm
	Orientation	Struck on the right side, right foot load bearing
Vehicle details		
	Year, Make and model	1991 EA Ford Falcon
	Impact speed	34 km/h

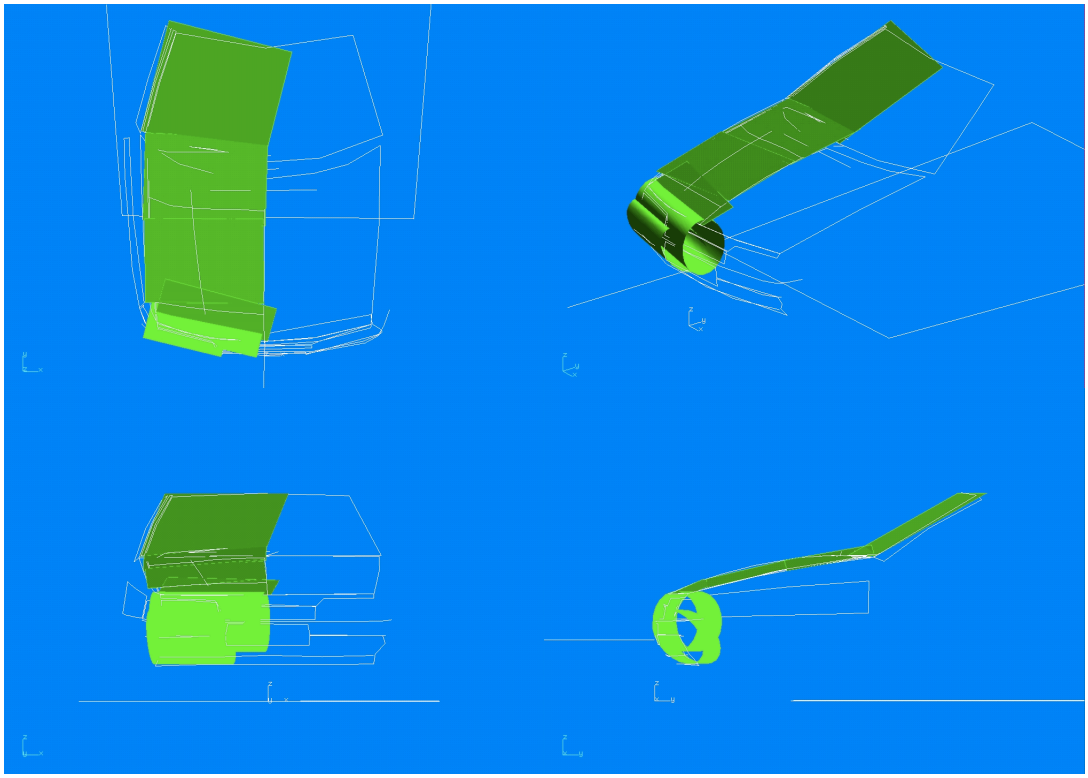

Figure 9-2 Geometry of the vehicle (shown in white). The approximation of this geometry for the simulation is shown by the shaded geometric entities.

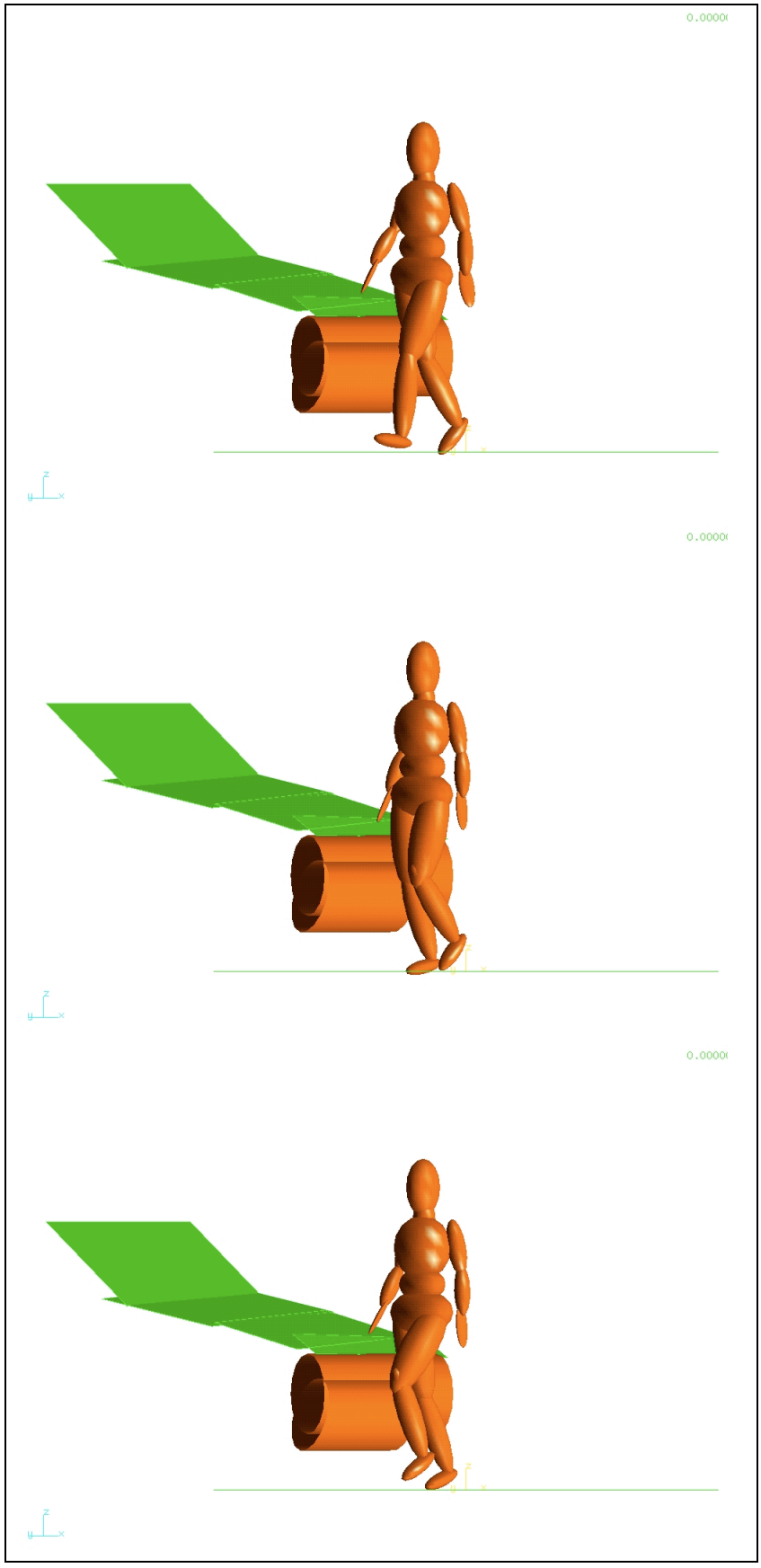

Figure 9-3 Initial position of the pedestrian and the vehicle in the simulations PED035-g1 through PED035-g3 *(top to bottom)*.

9.5 SIMULATION RESULTS

The results of the simulations of the accident are listed in Table 9-2. In each simulation the kinematics of the model caused the head to strike the base of the windscreen. The head impact velocity was insensitive to the stance of the pedestrian. Hence, the mean value of the head velocity was used in the physical reconstruction of the head impact.

Table 9-2 Simulation results for PED035-99

Simulation number	Head Velocity	Impact angle
	(m/s)	(deg.)
ped035_g1	8.27	51.59
ped035_g5	8.16	52.83
ped035_g6	8.27	50.06
Average	**8.23**	**51.49**

9.6 PHYSICAL RECONSTRUCTION

The head impact was reconstructed by firing the Adult Headform at a point on the windscreen, measuring 2120 mm (wrap-around-distance) from the ground and in the lower corner of the windscreen, on the driver's side. The Legform was fired at a point measuring 410 mm from the centre-line of the vehicle. Although there was no physical evidence to indicate the leg impact point on the case vehicle, the simulation suggested that the leg of the pedestrian must have struck the bumper in this vicinity for the head of the pedestrian to strike the car where it did.

The EEVC Working Group 10 sub-system impactors were used to simulate the impact between the full leg of the pedestrian and the head of the pedestrian, as described in Section 3.4.

Figure 9-4 A general view of the accident damage (left) and the damage produced by the reconstruction (right) of the head and leg impacts in case PED035-99.

9.6.1 Head impact reconstruction

Table 9-3 lists the test set-up parameters, and the results of the test. The Headform acceleration is plotted in Figure 9-5. The damage caused by the Headform may be compared to the damage caused

to the vehicle by the head of the pedestrian. It can be seen that the Headform closely reproduced the damage caused to the vehicle by the collision.

Table 9-3 Physical reconstruction parameters and results for the Headform test (test no. 27070100)

	Parameter	Value
Test set-up	Launch Angle	52˚
	Measured velocity	8.1 m/s
Results	Peak acceleration	97 g
	HIC value (interval)	491 (10.2 ms)

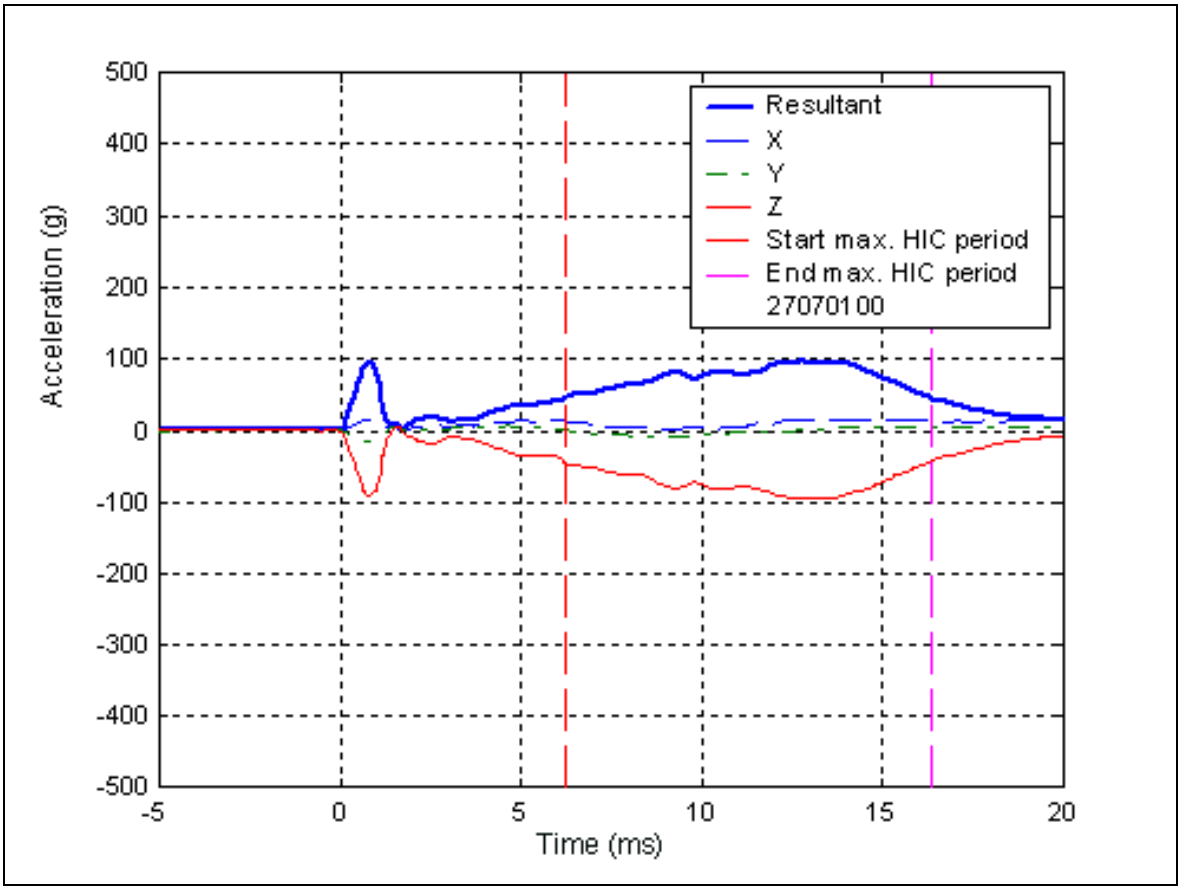

Figure 9-5 Acceleration recorded in the physical reconstruction of the head impact in Case PED035-99

Figure 9-6 A front close up view of the vehicle involved, showing where the head impact occurred (left) and the damage as produced by the reconstruction (right) of case PED035-99.

9.6.2 Leg impact reconstruction

The Legform was fired at a point measuring 410 mm from the centre-line of the vehicle. The other test set-up parameters are given in Table 9-4, along with the results of the test. Figure 9-7 to Figure 9-9 contain the time-histories of the tibia acceleration, the bending angle of the knee and the knee shear displacement. All measures of leg impact severity fail the limits of the EEVC WG10 procedures.

Table 9-4 Physical reconstruction parameters and results for the Legform test (test no.30070100)

	Parameter	Value
Test set-up	Measured velocity	9.24 m/s
Results	Tibia acceleration	289.6 g
	Knee bending angle	29.1˚
	Knee shear displacement	7.9 mm

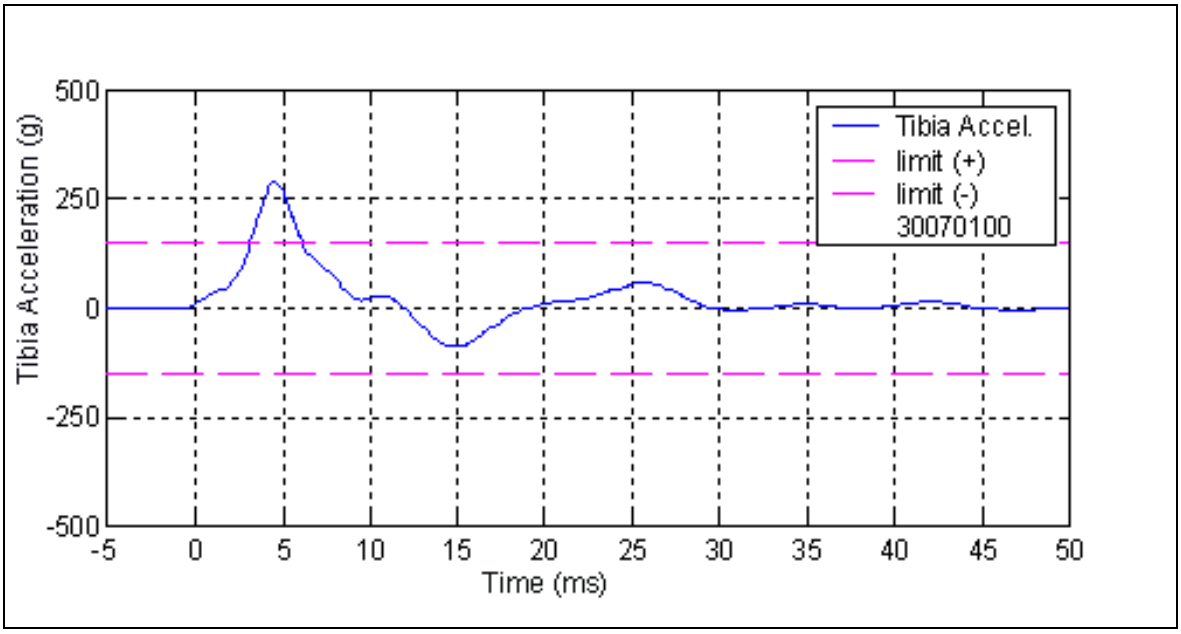

Figure 9-7 The tibia acceleration recorded in the physical reconstruction of case PED035-99.

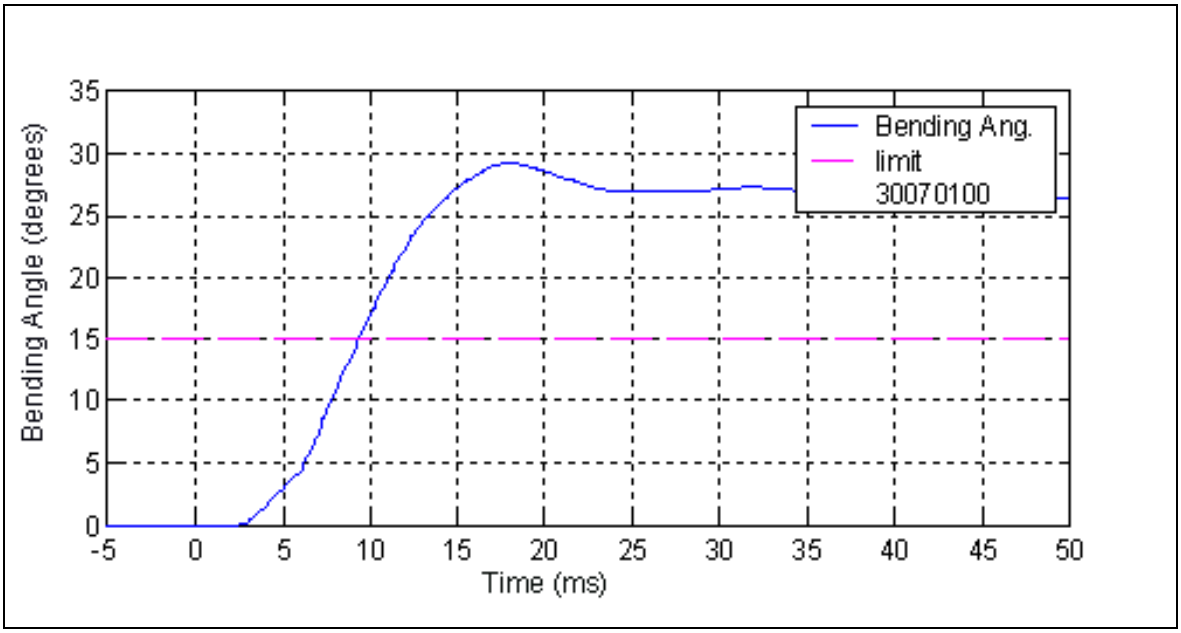

Figure 9-8 Knee bending angle recorded for the physical reconstruction of case PED035-99.

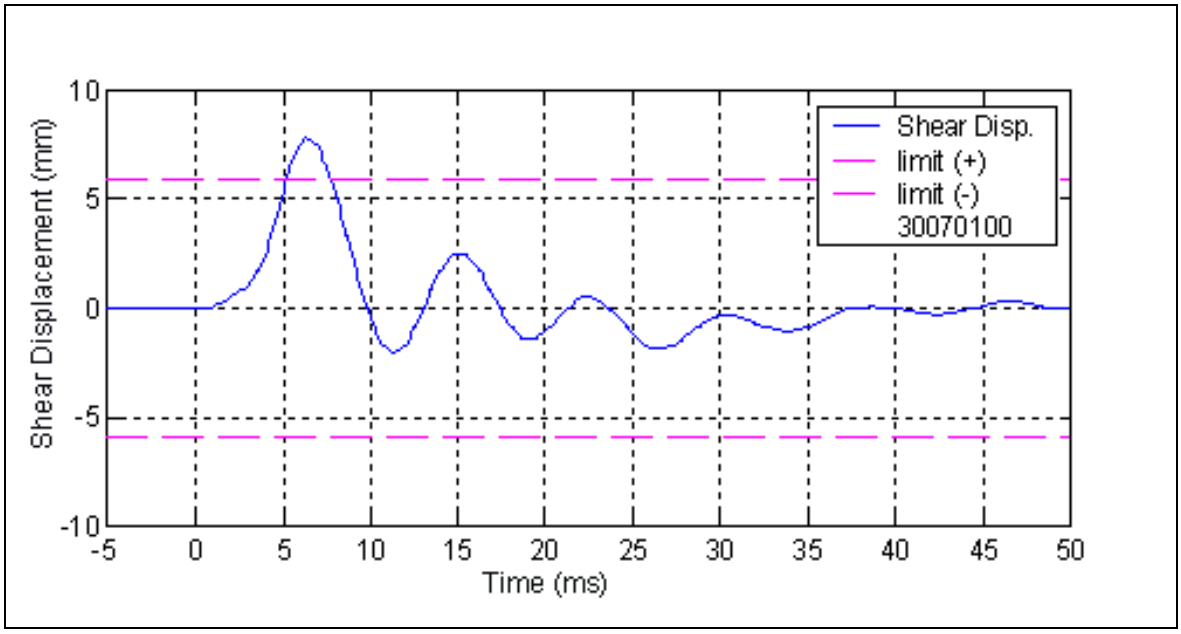

Figure 9-9 Knee shear displacement recorded for the physical reconstruction of case PED035-99.

9.7 SUMMARY OF RECONSTRUCTION RESULTS AND INJURY DIAGNOSIS

A summary of the test results and the corresponding injuries identified in the case are given in Table 9-5. A qualitative comparison between the damage to the windscreen of the case vehicle and the damage caused to the head impact reconstruction would suggest that the energy of the respective impacts (case and reconstruction) was similar. It is not possible to say the same for the leg impact reconstruction, as no damage was caused to the case vehicle from the impact with the pedestrian's leg, and nor was any damage caused in the reconstruction. However, given that the head impact seems to have been reproduced faithfully in this case, the estimate of the vehicle's impact speed, and hence the speed of the Legform test, appears to have been acceptably accurate.

The result of the head impact reconstruction reflects the fact that no head injuries were caused by the accident. The result of the leg impact reconstruction, however, would indicate that more severe injuries should have been seen in this case. Although the pedestrian's ankle was fractured, it is questionable whether the mechanism of such a fracture is measurable by the leg impact test.

Table 9-5 Summary of test results and relevant injuries

Test	Measure	Result	Relevant Injury
Full leg	Tibia acceleration	289.6 g	Ankle fracture
	Knee bending	29.1°	No knee injury diagnosed
	Knee shear	7.9 mm	
Head	HIC	491	Mild confusion, no head injury diagnosed

Indicates a result which exceeds a safe limit according to EEVC WG10

10 Case PED043-99

10.1 CASE DESCRIPTION

A male pedestrian wearing dark clothing was crossing the road at night. He was near the centre line when he stepped backwards into the path of a vehicle travelling north in the right-hand lane. The pedestrian was struck by the front right-hand side of the vehicle and was thrown off the vehicle to the right-hand side.

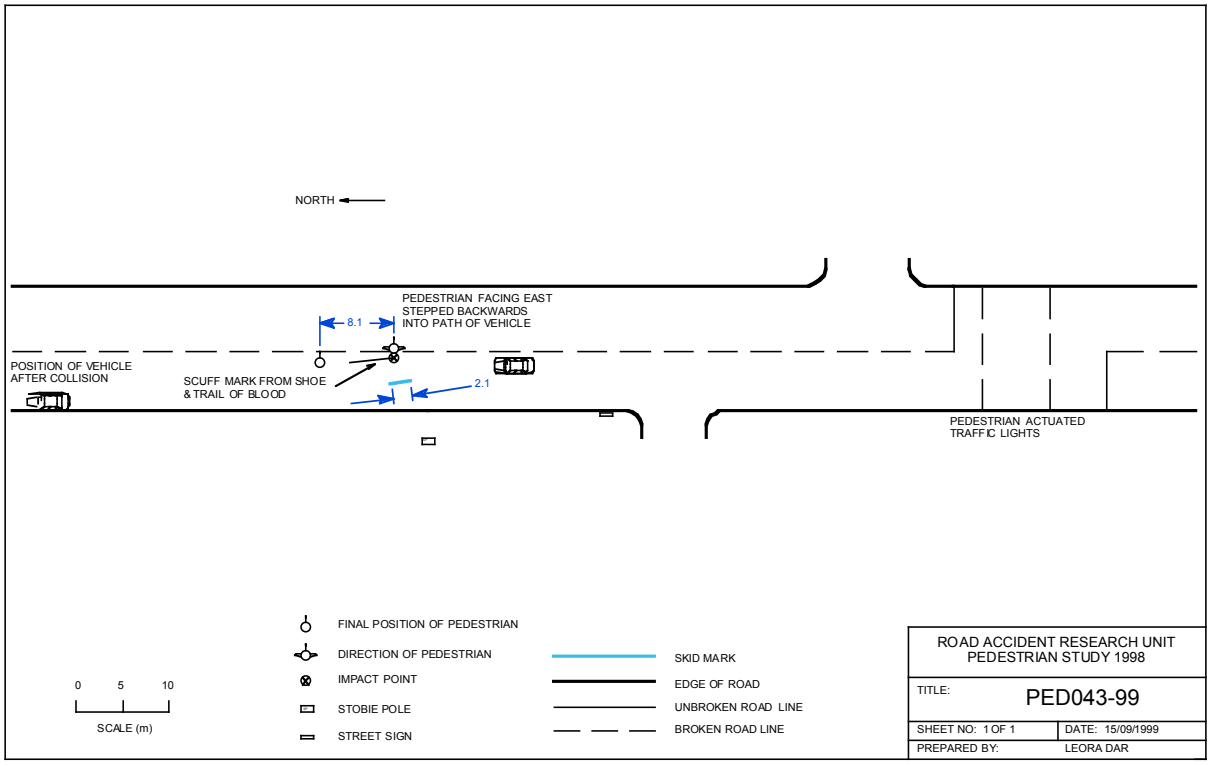

Figure 10-1 Site diagram of the collision in Case PED043-99.

10.2 PEDESTRIAN INJURIES

The pedestrian died as a result of the collision. He experienced loss of consciousness at the scene, paramedics rating his loss of consciousness with a Glasgow Coma Score of 4-5/15. His airway and circulatory systems were also compromised. His most significant injuries were

A fracture to the right parietal bone and the base of the skull (open and closed),

An extradural and subdural haematoma and other brain haemorrhages and contusions,

A splenic laceration,

Fractured ribs to his right side (5-7),

And an open 30 mm laceration to the right hip and contusions to the right ankle.

10.3 ACCIDENT RECONSTRUCTION

The point on the road at which the pedestrian was struck could be identified by the presence of a scuff mark, caused by the twisting and sliding of the sole of the pedestrian's shoe resulting from the impact between the vehicle and the pedestrian's leg. A distance of 8.1 m separated this point from the point at which the pedestrian came to rest after the collision. This distance implies an impact speed of approximately 33 km/h, based on throw distance calculations.

The damage to the right front of the vehicle (cracked headlamp, deformed leading edge of the bonnet) was the source of the pedestrian's wound to his thigh and hip. The significant depression in the right trailing edge of the bonnet was the source of the pedestrian's head and brain injuries.

The driver of the car that struck the pedestrian described the pedestrian as being stationary in the centre of the road prior to the collision, whereupon he stepped back into the path of the vehicle.

10.4 MADYMO SIMULATION

A 1992 Ford Fairmont was obtained for the physical reconstruction of this collision. The car was measured to obtain the geometry of the vehicle for the simulation. The procedure used to do this is described in Section 3.3.4. The geometry was represented by a series of planes and elliptical cylinders, as illustrated in Figure 10-2.

Table 10-1 Case details for reconstruction

Pedestrian details		
	Age, sex and height	52 year old male
	Orientation	Struck on right side, stepping backward into path of vehicle
Vehicle details		
	Year, Make and model	1992 Ford Fairmont
	Impact speed	33 km/h (determined from projection distance)

Two simulations were designed to represent the pedestrian stepping back into the path of the oncoming car. The first was designed to simulate the collision with the pedestrian having stepped back onto his left foot (PED043_g1a) and the second was designed to simulate a step back onto the right foot (PED043_g2a). These initial positions are shown in Figure 10-3.

The kinematics of the collision in these two accidents showed a significant involvement of the pedestrian's right arm in the collision. To see what effect this may have had on the head impact velocity, two further simulations were run. In these simulations, the right arm of the pedestrian was raised slightly and positioned forward of the trunk of the body, to minimise its involvement in the kinematics as the collision progressed (simulations PED043_g1b and PED043_g2b).

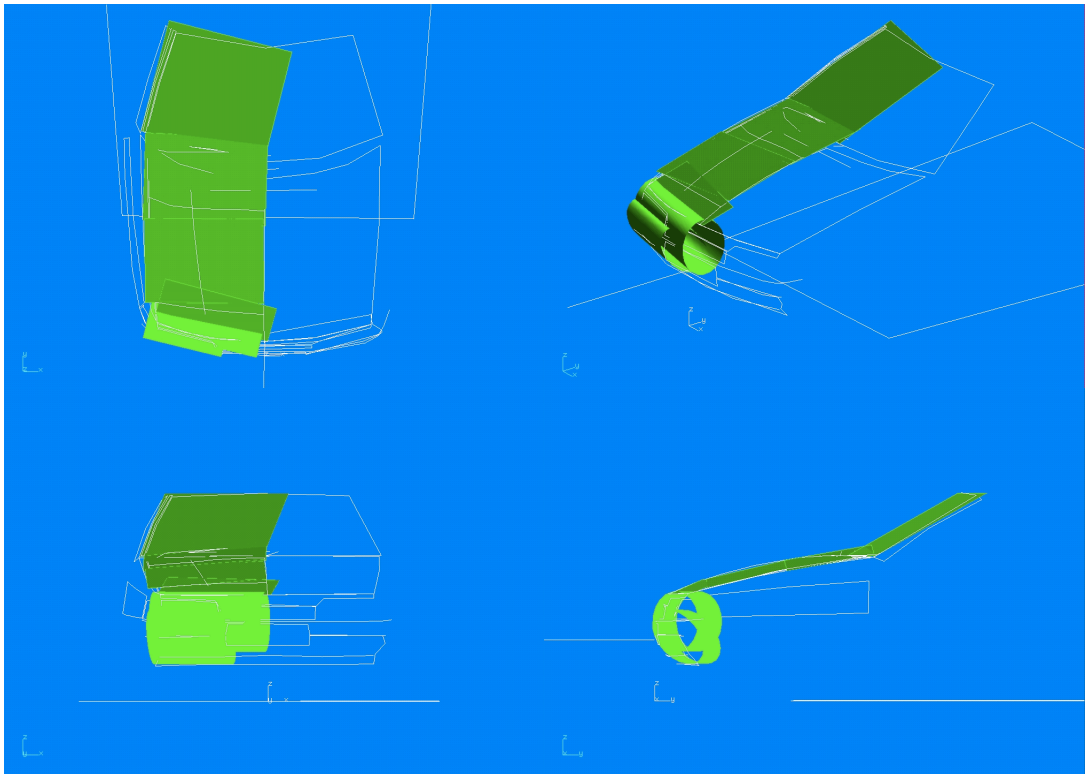

Figure 10-2 Geometry of the vehicle (shown in white). The approximation of this geometry for the simulation is shown by the shaded geometric entities.

10.5 SIMULATION RESULTS

The results of the simulations of the accident are listed in Table 10-3. It may be seen that the effect of the right arm's involvement in the collision with the car does not greatly affect the head impact velocity. As with PED018-99, the effective mass of the upper leg calculated from the simulation results was less than that achievable using the EEVC WG10 Legform. Consequently, the velocity was adjusted to produce an impact in the laboratory with equivalent energy to the elastic energy in the impact estimated by the simulation.

The average results of all simulations were used as the nominated test conditions for the tests.

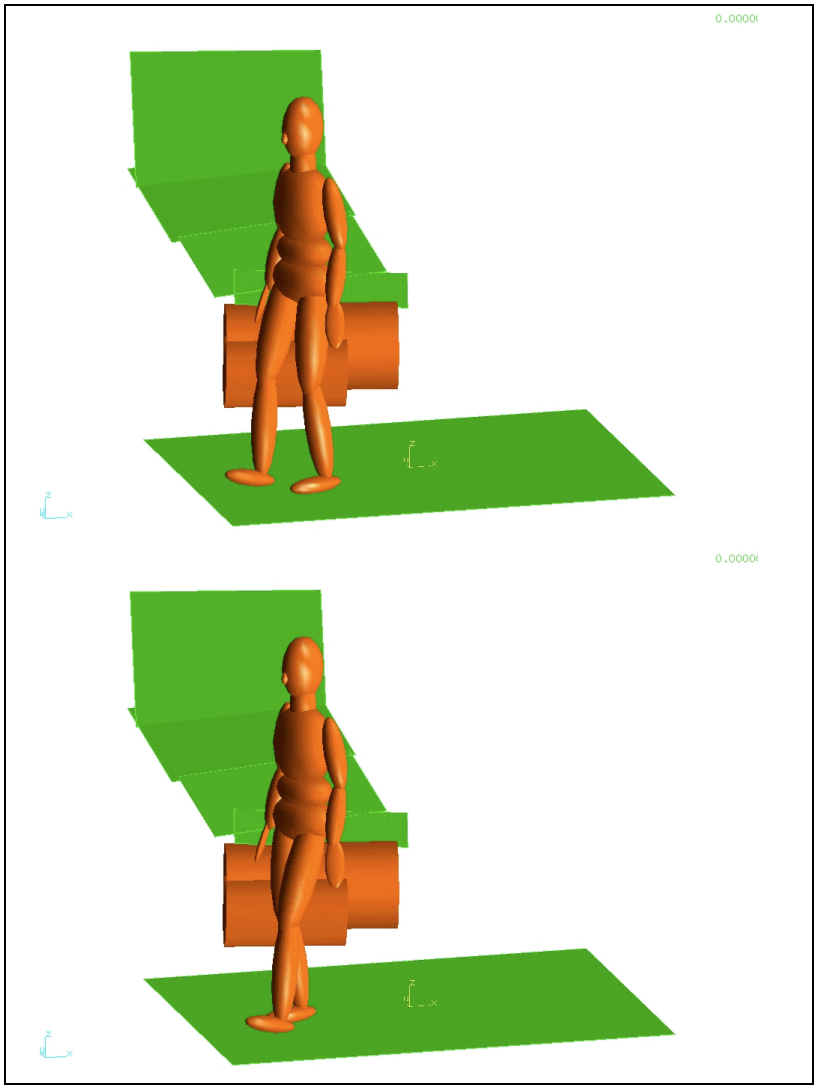

Figure 10-3 Initial position of the pedestrian and the vehicle in the simulations PED043-g1 to PED043-g2.

Table 10-2 Simulation results for PED043-99

Simulation number	Upper leg velocity	Upper leg impact angle	Elastic energy	Upper leg effective mass	Adjusted mass for test	Adjusted velocity for test	Head Velocity	Impact angle
	(m/s)	(deg.)	(J)	(kg)	(kg)	(m/s)	(m/s)	(deg.)
PED043_1a	9.18	59.60	198.59	4.72	8.75	6.74	9.81	46.13
PED043_1b	9.18	60.16	199.99	4.75	8.75	6.76	9.80	46.48
PED043_2a	9.17	60.78	203.27	4.83	8.75	6.82	10.25	47.65
PED043_2b	9.17	57.29	204.39	4.86	8.75	6.83	9.90	47.20
average	**9.17**	**59.46**	**201.56**	**4.79**	**8.75**	**6.79**	**9.94**	**46.86**

10.6 PHYSICAL RECONSTRUCTION

All three EEVC Working Group 10 sub-system impactors were used to simulate the impact between the different parts of the pedestrian and the vehicle, as described in Section 3.4.

The target of the Headform test was a point 540 mm from the bonnet centre-line, at a wrap-around-distance of 1700 mm from ground level. The target of the upper leg impact test was 530 mm from the centre-line and on the leading edge of the bonnet. The full leg test was aimed at a point on the bumper, 530 mm from the centreline. The full leg was fired at the speed estimated to be the vehicle's impact speed (9.2 m/s). The Headform velocity and the Upper Legform velocity were determined by the results of the MADYMO simulation.

10.6.1 Head impact reconstruction

Table 10-3 lists the test set-up conditions and results of the head impact reconstruction. Figure 10-4 contains a plot of the Headform acceleration, and Figure 10-5 shows the damage to the case vehicle alongside the damage created by the reconstruction test.

Table 10-3 Physical reconstruction parameters and results for the Headform test (test no. 01060101)

	Parameter	Value
Test set-up	Launch Angle	47°
	Measured velocity	9.76 m/s
Results	Peak acceleration	126 g
	HIC value (interval)	1177 (10.2 ms)

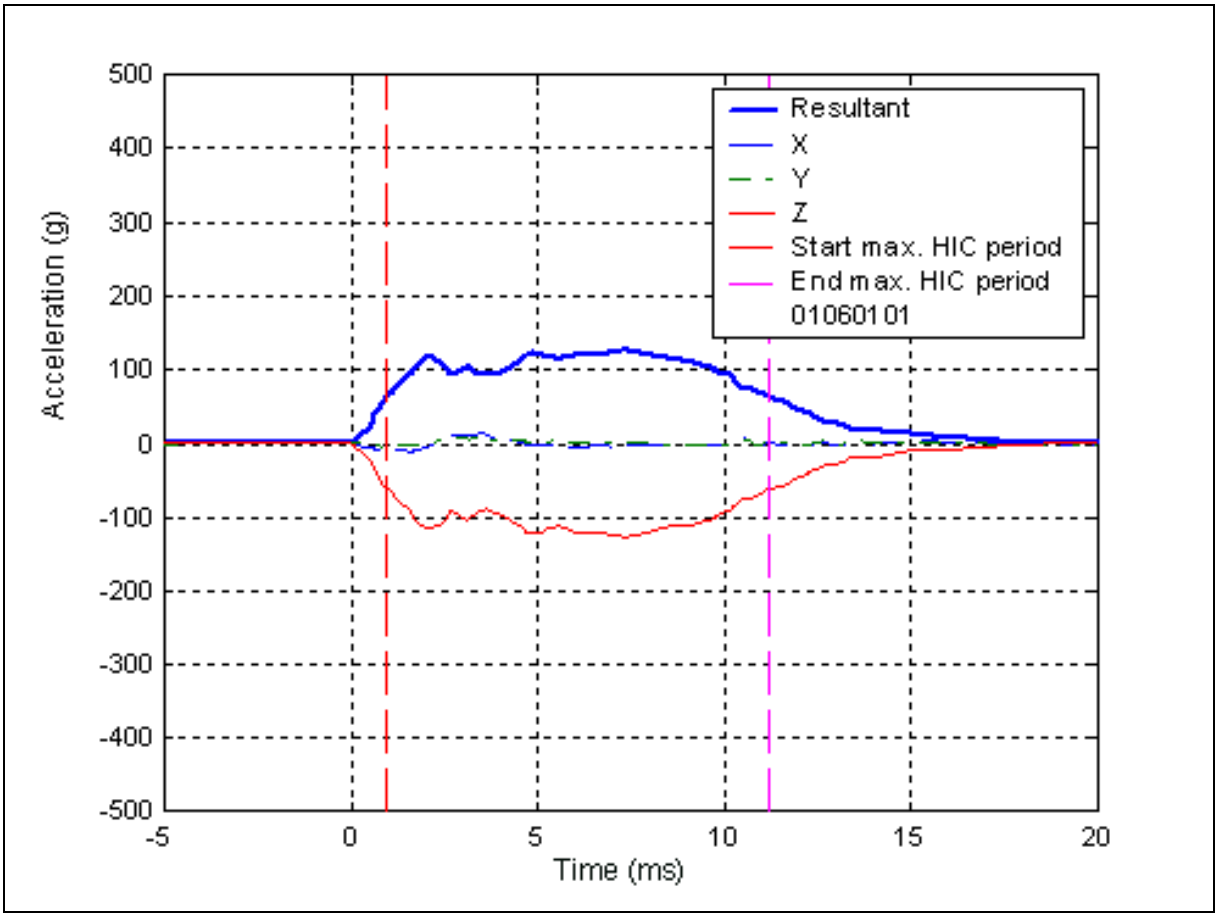

Figure 10-4 The acceleration recorded in the physical reconstruction of case PED043-99.

Figure 10-5 A side view of the vehicle involved in case PED043-99, showing where the head impact occurred (left) and the damage as produced by the reconstruction (right).

10.6.2 Full leg impact reconstruction

The impact with the pedestrian's leg was reconstructed using the Full Legform. The target velocity of the Legform was that which was estimated to be the striking speed of the vehicle, 33 km/h (9.16 m/s). The measured velocity and the results of the test are given in Table 10-4, and Figure 10-6 to Figure 10-8 contain plots of the acceleration of the tibia, and the knee bending angle and the knee shear displacement.

Table 10-4 Physical reconstruction parameters and results for the Legform test (test no. 07060102)

	Parameter	Value
Test set-up	Measured velocity	9.74 m/s
Results	Tibia acceleration	293.4 g
	Knee bending angle	32.2˚
	Knee shear displacement	n.a.

Note: There was no shear displacement data recorded for this test due to a faulty transducer lead.

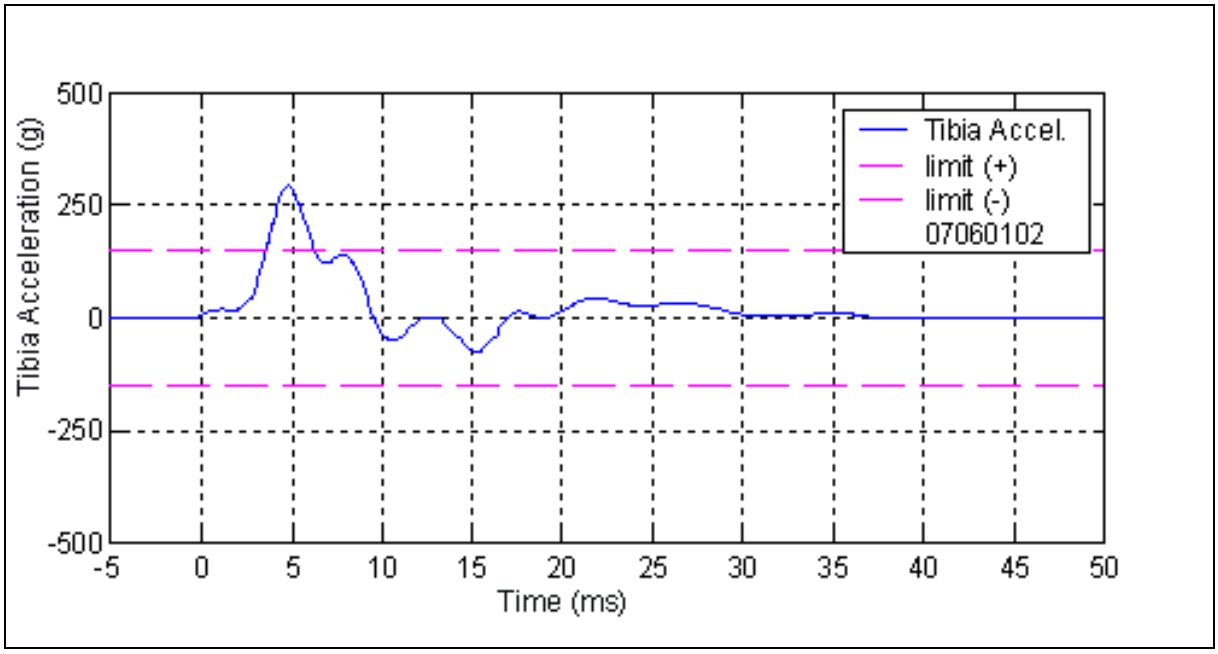

Figure 10-6 The tibia acceleration recorded in the physical reconstruction of case PED043-99.

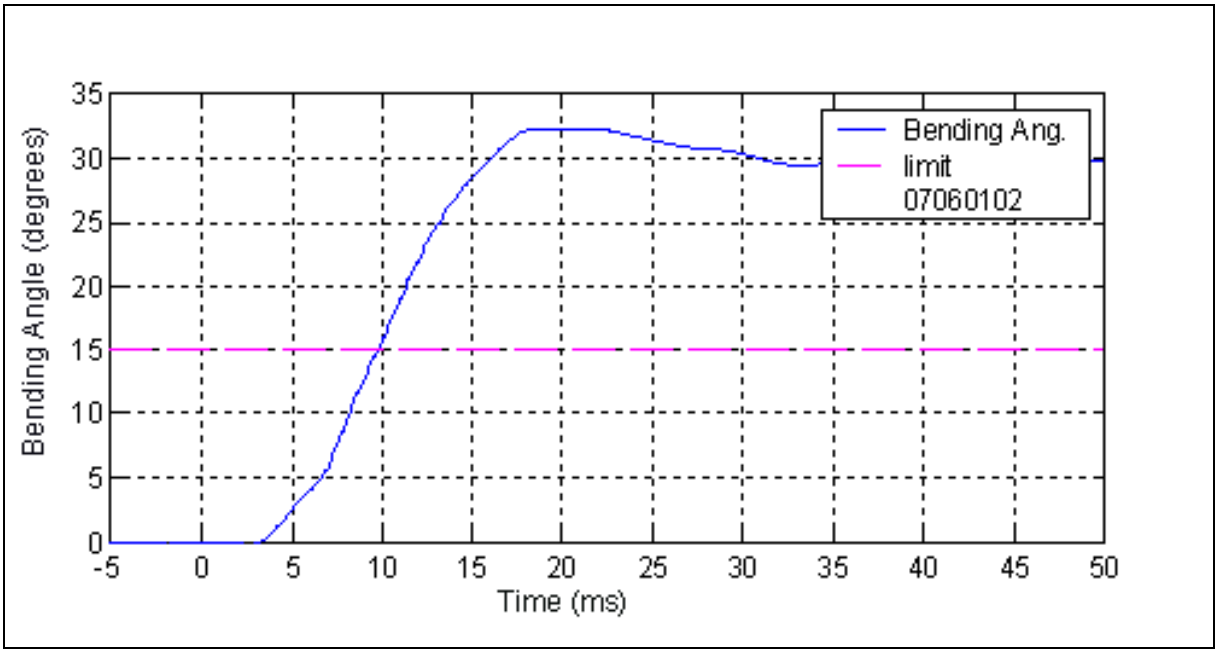

Figure 10-7 Knee bending angle recorded for the physical reconstruction of case PED043-99.

10.6.3 Upper leg impact reconstruction

In addition to the full leg impact reconstruction, the impact with the pedestrian's upper leg was reconstructed. The test conditions that were determined from the results of the simulation are given in Table 10-5. The support forces and the bending moment across the femur section are plotted in Figure 10-8 and Figure 10-9. Figure 10-10 shows a comparison between the accident damage and that caused by the reconstruction test.

Table 10-5 Physical reconstruction parameters and results for the Upper Legform test (test no.04060100)

	Parameter	Value
Test set-up	Launch Angle	50˚
	Impactor mass	8.75 kg
	Target velocity	6.8 m/s
	Actual velocity	6.6 m/s
Results	Maximum force	4.5 kN
	Bending Moment	344 Nm

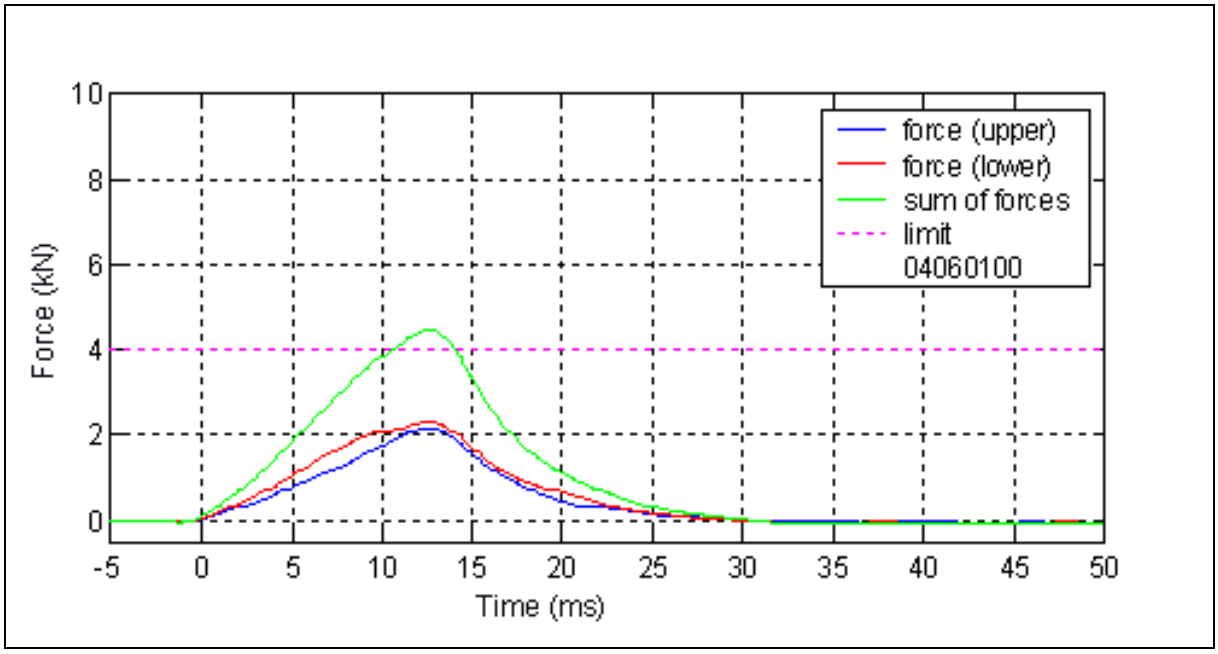

Figure 10-8 Upper leg force recorded in the physical reconstruction of case PED043-99.

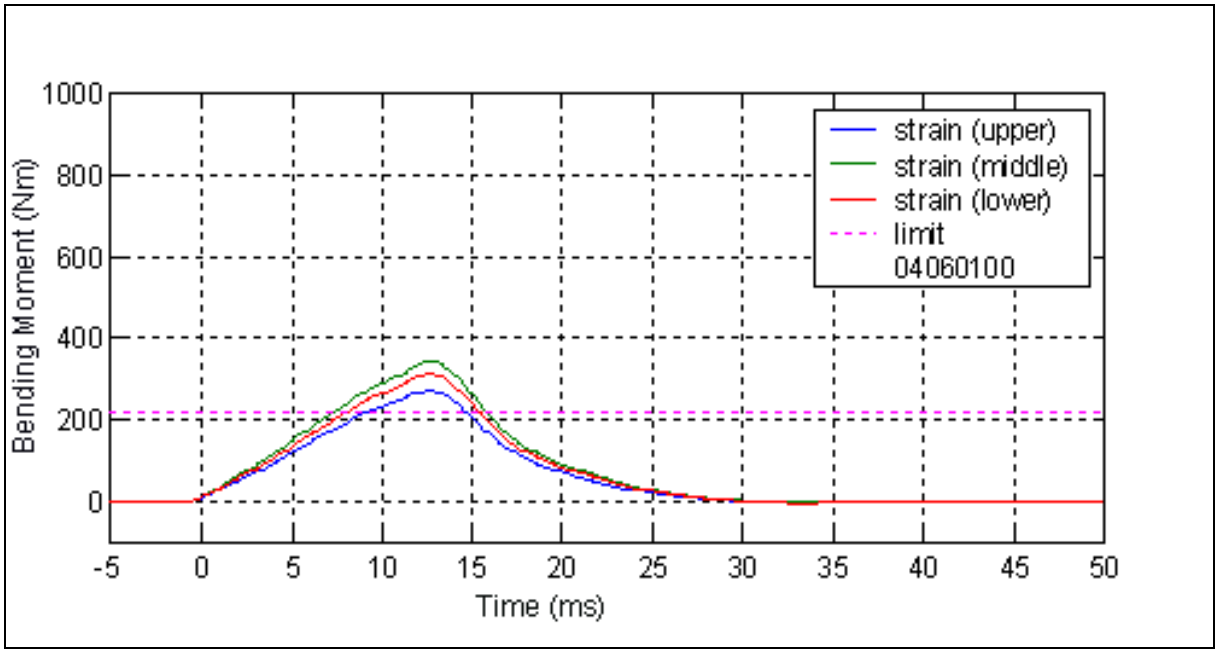

Figure 10-9 Bending moment recorded in the physical reconstruction of case PED043-99.

Figure 10-10 The accident damage caused by impact with the pelvic area (left) and the damage produced by the reconstruction with the Upper Legform impactor (right) of case PED043-99.

10.7 SUMMARY OF RECONSTRUCTION RESULTS AND INJURY DIAGNOSIS

The results of both of the Legform tests show that the vehicle fails the criteria set for each test. The autopsy did not reveal any femur, tibia or knee injuries that might be associated with such test results. Although the result of the head impact reconstruction failed the criteria, the HIC value appears low when compared to the injuries sustained by the pedestrian. Table 10-6 summarises the results of the tests and lists the pedestrian's injuries that are relevant to each test.

Table 10-6 Summary of test results and relevant injuries

Test	Measure	Result	Relevant Injury
Full leg	Tibia acceleration	293.4 g	Right ankle contusions, no skeletal injuries identified.
	Knee bending	32.2°	
	Knee shear	n.a.	
Upper leg	Support forces	4.5 kN	Laceration to skin on hip, no skeletal injuries identified
	Maximum bending moment	344 Nm	
Head	HIC	1177	Fatal head injury, AIS 5

Indicates a result which exceeds a safe limit according to EEVC WG10

11 Case PED049-99

11.1 CASE DESCRIPTION

The vehicle involved was travelling west in the left-hand lane of an arterial road and was approaching a T-intersection. The traffic lights at the intersection were green for traffic heading west. The driver saw a pedestrian running south across the intersection at a pedestrian crossing. The driver braked but collided with the pedestrian in the middle of the crossing.

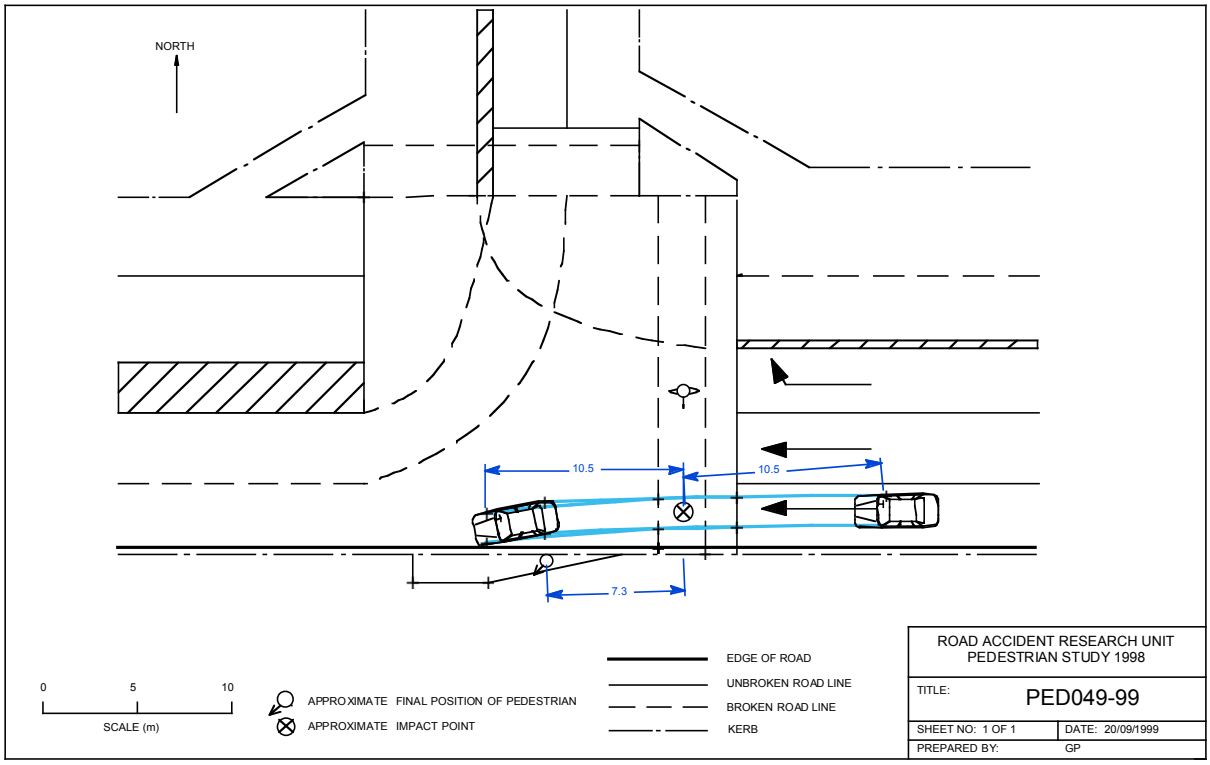

Figure 11-1 Site diagram of the collision in Case PED049-99.

11.2 PEDESTRIAN INJURIES

The pedestrian was hospitalised as a result of her injuries. She lost consciousness at the scene but regained consciousness by the time she was attended to by ambulance officers. She was diagnosed at hospital as suffering a concussion. Radiology confirmed a closed base fracture of the skull. A brain injury occurred secondary to this fracture but the extent of injury was undetermined. There were contusions to her knee. She was discharged from hospital ten days following the accident with an unknown prognosis for her head injuries.

11.3 ACCIDENT RECONSTRUCTION

An impact point was established based on the driver's estimate and verified by another person who had been accompanying the pedestrian. The impact speed of the vehicle was estimated based on the vehicle's post-impact skid mark, which was 10.5 m in length, the vehicle coming to a complete stop after the collision. This skid mark length implies an impact speed of 43 km/h.

There was an obvious head impact on the left side of the base of the windscreen and left windscreen wiper blade. It is reasonable to assume that this impact was the cause of the pedestrian's concussion, skull base fracture and brain injury. The impact with the car's bumper was the most likely cause of the pedestrian's knee contusion, although there was no evidence of contact on the bumper. There was a dent in the bonnet that was probably caused by the pedestrian's upper leg and pelvis but there was no injury associated with this contact.

11.4 MADYMO SIMULATION

A summary of the detail used to set up the simulation is contained in Table 11-1. The geometry of a 1997 Ford Falcon was measured using a Geodimeter. This measurement technique is described in Section 3.3.4. The geometry that was produced in this way was approximated by a series of elliptical cylinders and planes, and the resulting model is illustrated in Figure 11-2. The mass and moments of inertia of the pedestrian model were produced based on the 50th percentile female anthropometry of a 15 year old female, as produced by GEBOD (Section 3.3.3).

Table 11-1 Case details for reconstruction

Pedestrian details		
	Age, sex and height	15 year old female
	Orientation	Struck on left side
Vehicle details		
	Year, Make and model	1997 Ford Falcon EL
	Impact speed	43 km/h (determined from skid mark analysis)

As with previous cases, the stature of the pedestrian was modelled as a series of postures representative of the human gait cycle. In every case the pelvis was positioned 230 mm from the centre-line, a position corresponding with damage on the bonnet of the car from the impact with the pedestrian's pelvis and upper leg. The initial positions of the vehicle and pedestrian in each of the six simulations are shown in Figure 11-3.

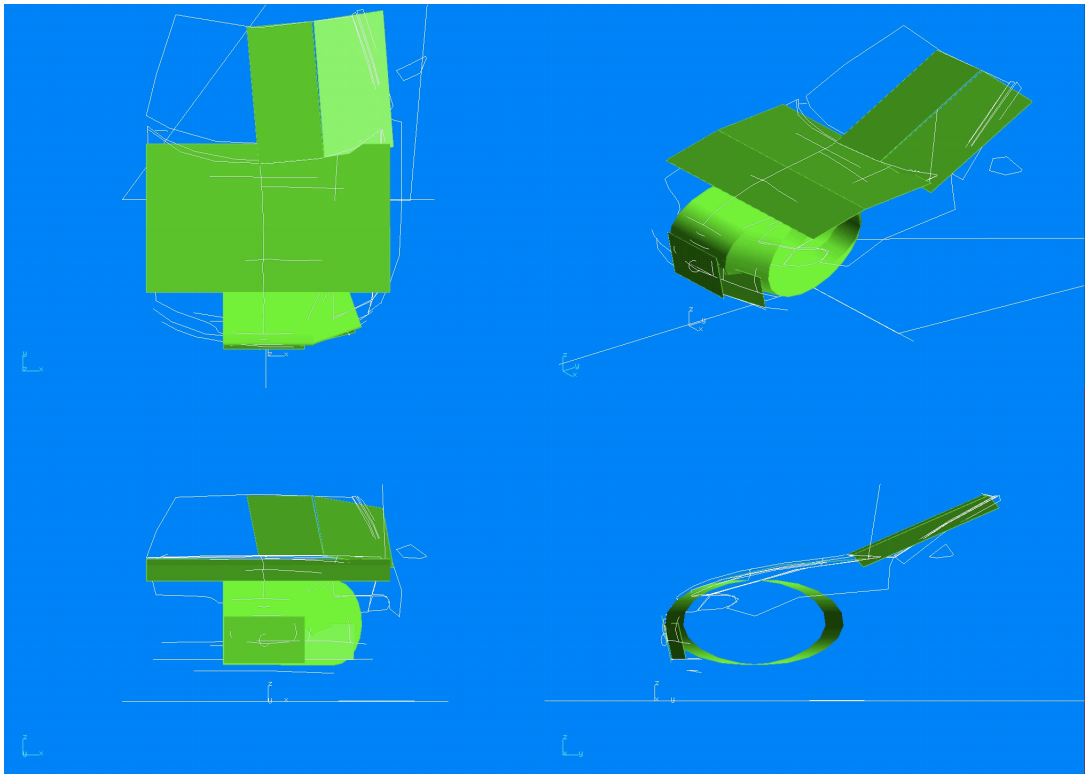

Figure 11-2 Geometry of the vehicle measured, shown in white. The approximation of this geometry for the simulation is shown by the shaded geometric entities.

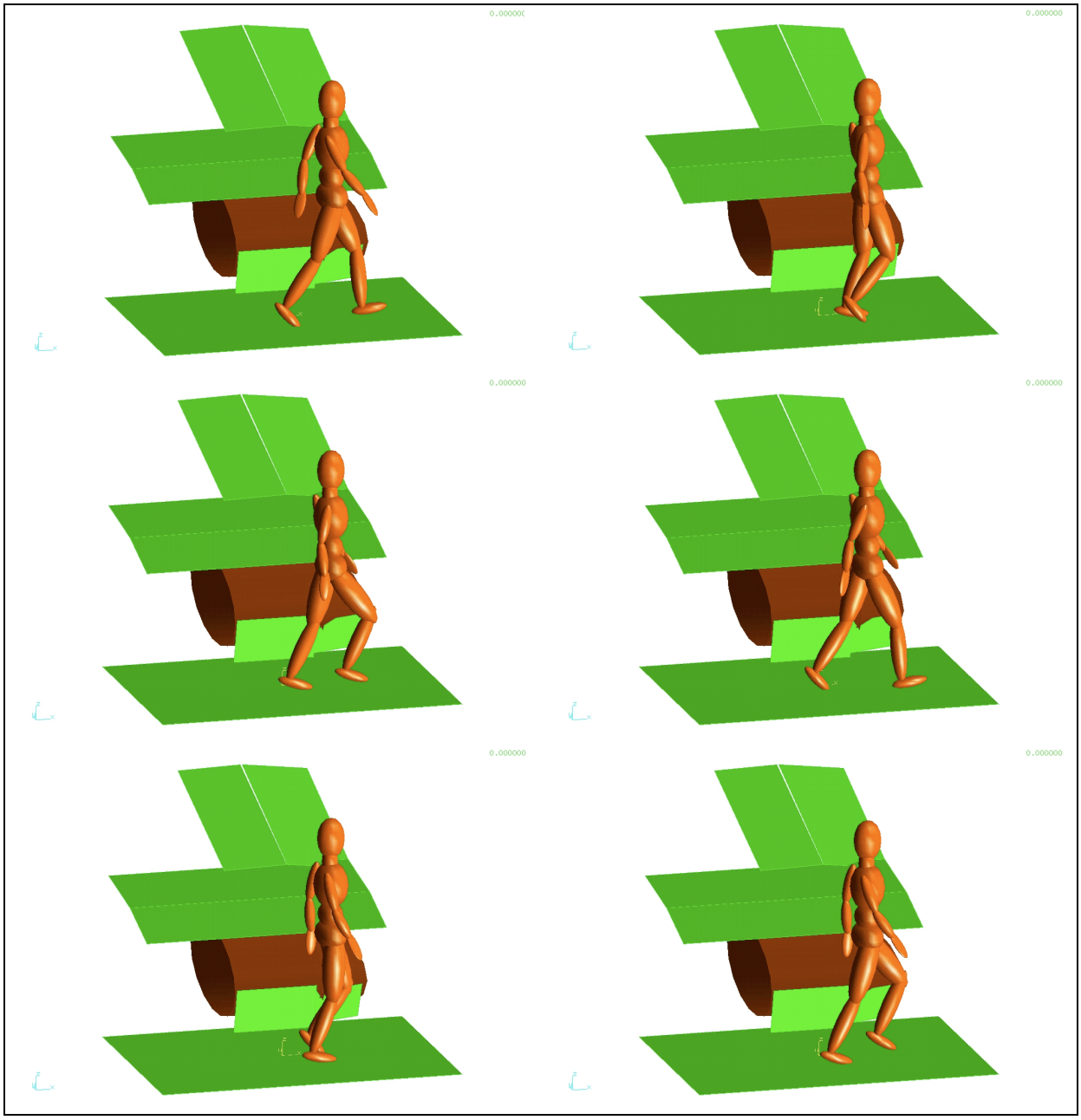

Figure 11-3 Initial position of the pedestrian and vehicle in the simulations PED049-g1 through PED049-g6 (*left to right and top to bottom*).

11.5 SIMULATION RESULTS

A summary of the simulation results is given in Table 11-2. The variations in stance give estimates of the head impact velocity in the range of 9.6 to 12.1 m/s. This range of head impact velocities is relatively large compared with the results of other simulations in this report. Nevertheless, no single simulation appeared more or less plausible than the others, and so the average of the six simulations was nominated as the target test condition for the head impact test.

Table 11-2 Simulation results for PED049-99

Simulation number	Head Velocity	Impact angle
	(m/s)	(deg.)
ped049_g1	9.95	44.75
ped049_g2	10.82	41.62
ped049_g3	9.88	50.71
ped049_g4	9.58	46.40
ped049_g5	12.05	42.14
ped049_g6	11.09	49.45
Average	**10.56**	**45.84**

11.6 PHYSICAL RECONSTRUCTION

The EEVC Working Group 10 sub-system impactors were used to simulate the impact between the head of the pedestrian and the vehicle as well as the leg of the pedestrian and the vehicle, as outlined in Section 3.4. The striking speed of the vehicle (43 km/h) was chosen for the speed of the Legform. The target head velocity was determined from the average of the MADYMO simulation models.

11.6.1 Head impact reconstruction

The Headform was fired at the windscreen at the same location identified on the case vehicle as the head impact point. This point was 390 mm from the bonnet centre-line, at a wrap-around-distance of 2020 mm. The results of the Headform tests are given in Table 11-3 and the recordings of the head acceleration are shown in Figure 11-5. A comparison between the damage to the vehicle created in the test and in the actual case is shown in Figure 11-6.

Figure 11-4 A general view of the accident damage (left) and the damage produced by the reconstruction (right) of case PED049-99.

Table 11-3 Physical reconstruction parameters and results Headform test (test no. 19060101)

	Parameter	Value
Test set-up	Launch Angle	46˚
	Measured velocity	10.37 m/s
Results	Peak acceleration	193 g
	HIC value (interval)	1678 (9.4 ms)

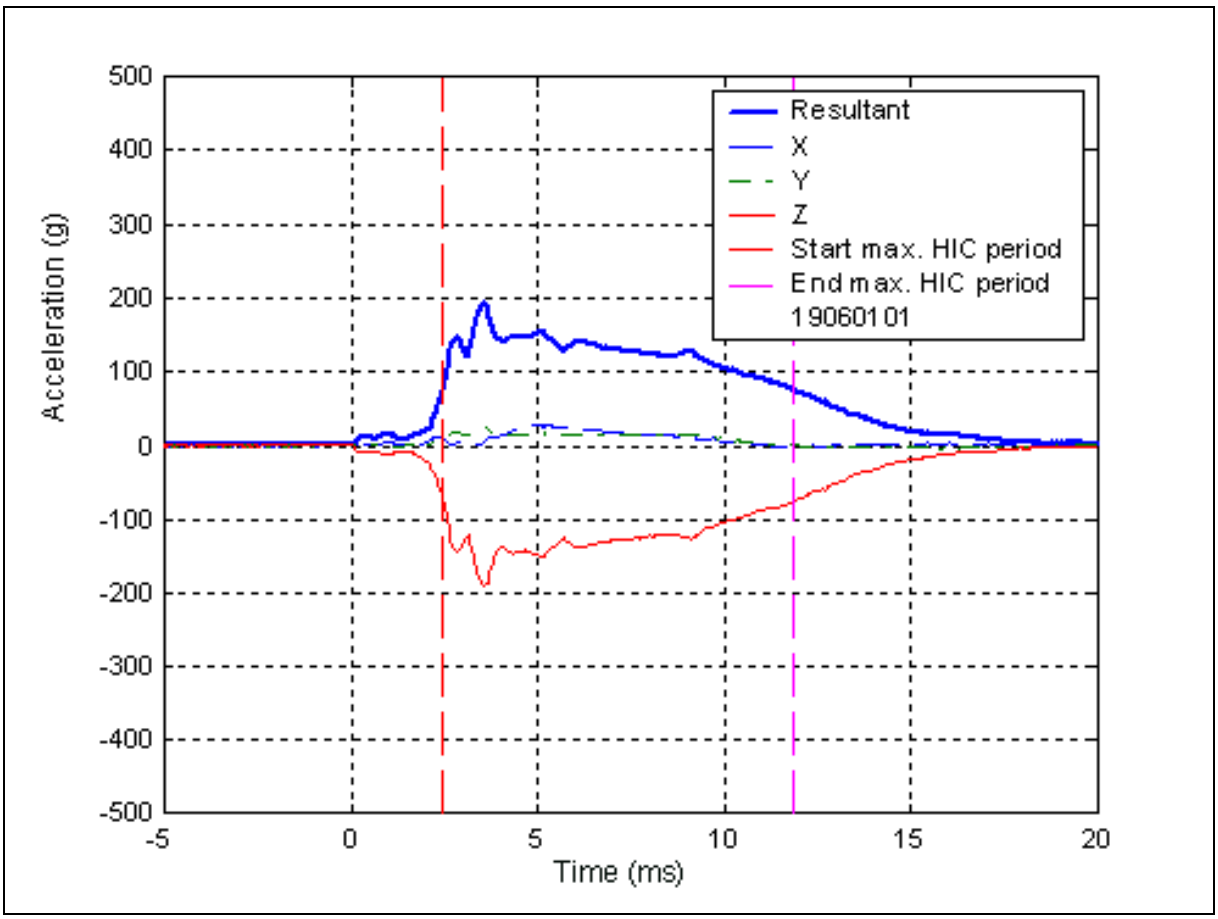

Figure 11-5 The acceleration recorded in the physical reconstruction of case PED049-99.

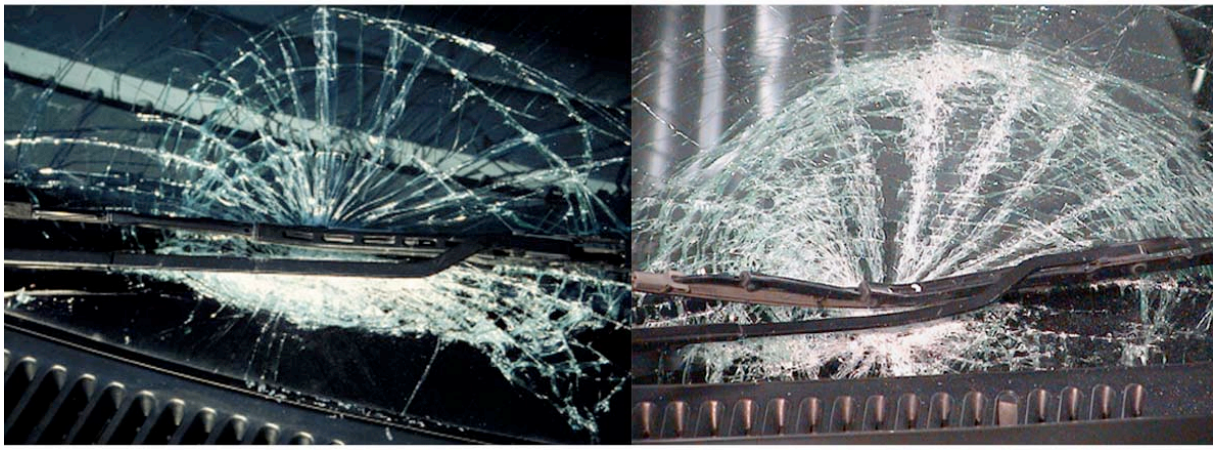

Figure 11-6 The accident damage caused by the impact with the head of the pedestrian (*left*) and the physical reconstruction damage of the head impact (*right*) in case PED049-99.

11.6.2 Leg impact reconstruction

The Full Legform was aimed at a point on the bumper 230 mm from the bumper's centreline (in line with the upper leg damage identified on the case vehicle). The results of the Legform tests are given in Table 11-4, and the recordings of the tibia acceleration and knee kinematics are shown in Figure 11-7 to Figure 11-9.

Table 11-4 Physical reconstruction parameters and results of the Legform test (test no. 14060102)

	Parameter	Value
Test set-up	Measured velocity	11.55 m/s
Results	Tibia acceleration	165.8 g
	Knee bending angle	32.5°
	Knee shear displacement	3.9 mm

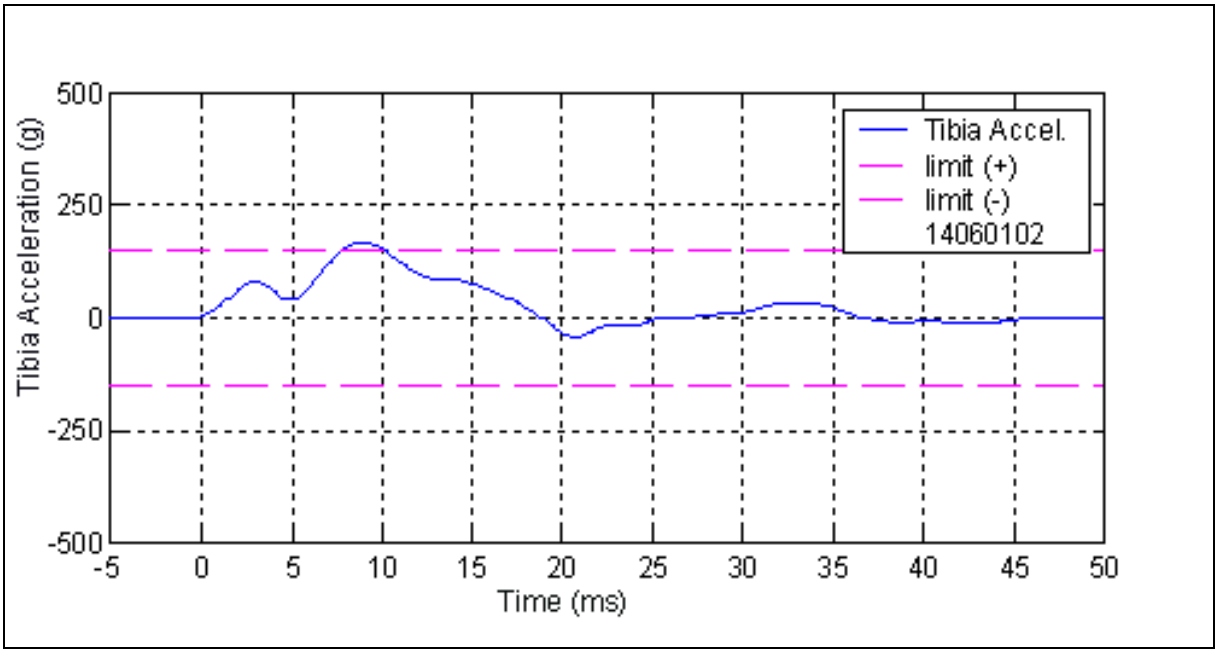

Figure 11-7 The tibia acceleration recorded in the physical reconstruction of case PED049-99.

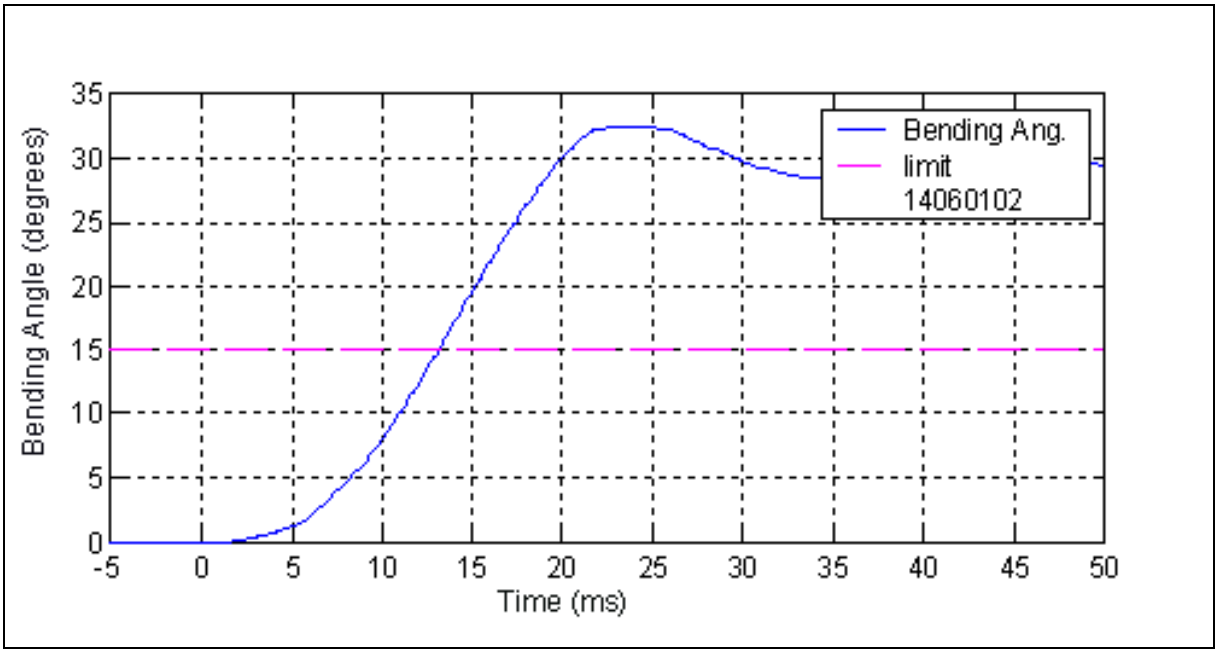

Figure 11-8 Knee bending angle recorded for the physical reconstruction of case PED049-99.

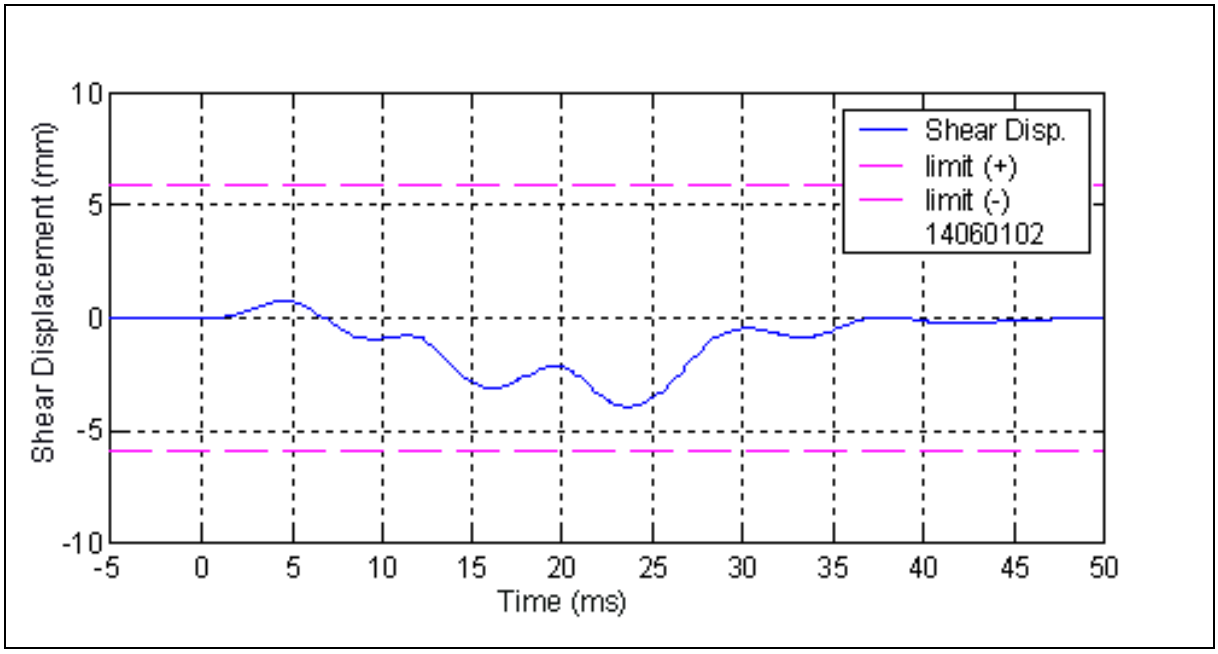

Figure 11-9 Knee shear displacement recorded for the physical reconstruction of case PED049-99.

Figure 11-10 The accident damage caused by the pedestrian's leg (left - negligible) compared with the physical reconstruction damage of the full leg impact (right) in case PED049-99.

11.7 SUMMARY OF RECONSTRUCTION RESULTS AND INJURY DIAGNOSIS

A summary of the test results from the reconstruction of this case and the corresponding injuries that were identified on the pedestrian are given in Table 11-5. The result of the leg impact reconstruction would suggest a more significant injury than was caused to the pedestrian in the accident, although the tibia acceleration is close to the limit specified by the EEVC. The head impact reconstruction is consistent with the injuries diagnosed as a result of the crash.

Table 11-5 Summary of reconstruction results and relevant injuries in PED049-99

Test	Measure	Result	Relevant Injury
Full leg	Tibia acceleration	165.8 g	Contusion to knee
	Knee bending	32.5°	
	Knee shear	3.9 mm	
Head	HIC	1678	Closed base fracture of the skull and secondary brain injury

Indicates a result which exceeds a safe limit according to EEVC WG10

12 Case PED056-99

12.1 CASE DESCRIPTION

The involved vehicle was travelling north in the right side of a wide lane and moved to the left because another vehicle in front was turning right into a petrol station. The driver of the vehicle did not see the pedestrian who was crossing the road from east to west and the vehicle struck the pedestrian on its front left-hand side of the vehicle. The pedestrian was flipped up onto the bonnet, striking the windscreen before falling to the roadway.

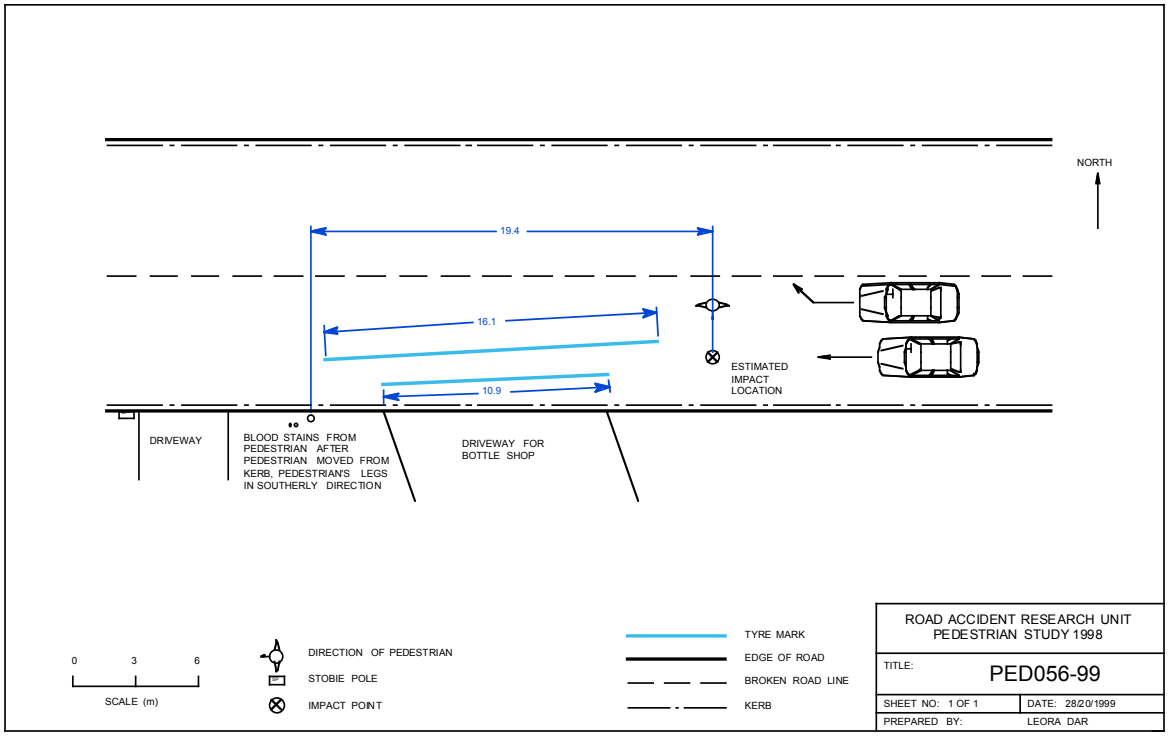

Figure 12-1 Site diagram of the collision in Case PED056-99.

12.2 PEDESTRIAN INJURIES

The pedestrian was transported by ambulance to hospital as a result of his injuries. He remained conscious after the accident. His most significant injuries were

An open fracture to his left tibia and fibula - the 3 cm puncture site was 36-39 cm from ground level.

Grazes to the left aspect of the head, behind the left ear and extending down lateral aspect of neck

Grazing to the left shoulder, the left hand, both elbows and both knees.

12.3 ACCIDENT RECONSTRUCTION

The circumstances surrounding this accident are not completely clear, but in the interview that the pedestrian gave for this study, two pertinent statements were made. First, he was waiting on a median before crossing the lanes in which he was hit. Second, he had a clear recollection of the entire collision and specifically remembers the brakes of the car coming on and screeching while he was on the surface of the vehicle. The only median in the vicinity terminates before the commencement of the skid marks. This means that if the pedestrian had crossed even at the end of the median, the car probably struck him before any braking had taken place. This is consistent with his statement regarding the braking of the car. The skid marks left by the vehicle would suggest that the car was travelling at 60 km/h prior to the collision.

Although there was no evidence of contact on the steel bumper bar of the vehicle that struck the pedestrian, open fractures to the shaft of the tibia and fibula, with an exit point of fracture 36-39 cm from ground level indicates that a significant contact with the bumper bar did occur. The pedestrian's shoulder impact with the base of the windscreen resulted in various grazing and bruising. The pedestrian suffered grazing immediately behind the left ear and extending along the lateral aspect of the neck. This probably resulted from impact with the lower corner of the left side of the windscreen.

The target of the Full Legform test was a point 290 mm from the centre of the vehicle, in line with the head impact point on the vehicle, in the absence of any distinguishing marks or dents in the bumper of the case vehicle.

12.4 MADYMO SIMULATION

A summary of the details used to set up the simulation is contained in Table 12-1. The geometry of a 1983 Holden Commodore was measured using a Geodimeter. This measurement technique is described in Section 3.3.4. The geometry that was produced in this way was approximated by a series of elliptical cylinders and planes, and the resulting model is illustrated in Figure 12-2. The mass and moments of inertia of the pedestrian model were produced based on the anthropometry of an adult male 178 cm high and weighing 81 kg, as produced by GEBOD (Section 3.3.3).

Table 12-1 Case details for reconstruction

Pedestrian details	
Age, sex and height	35 year old male, 178 cm, 81 kg
Orientation	Struck on left side
Vehicle details	
Year, Make and model	1983 Holden VH Commodore
Impact speed	60 km/h

As the stature of the pedestrian could not be determined from the accident investigation, it was modelled as a series of postures representative of the human gait cycle. The initial positions of the vehicle and pedestrian in each of the six simulations are shown in Figure 12-3. The pedestrian gave

a detailed description of the collision, and described how his left arm slid over the bonnet before his head struck the windscreen. He described how his arm subsequently struck the broken windscreen. Each of the simulations produced slightly different head impact locations, and several also produced heavy impacts between the left elbow and the bonnet. The simulation that best reflected the pedestrian's description of the collision, and the head impact point in the case, was modified so that the left arm slid over the bonnet, rather than digging into it, while maintaining the correct head impact location. In this simulation, the left arm of the pedestrian went on to strike the windscreen in a manner consistent with the pedestrian's description, and with the damage to the windscreen caused by this second impact. The results of this simulation were used to determine the initial conditions for the reconstruction of the head impact.

Table 12-2 Simulation results for PED056-99

Simulation number	Head Velocity	Impact angle
	(m/s)	(deg.)
ped056_g1	15.03	45.23
ped056_g2	10.78	64.43
ped056_g3	11.09	55.21
ped056_g4	11.62	58.35
ped056_g5	16.04	51.12
ped056_g6	16.47	46.16
ped056_final	**15.51**	**45.32**

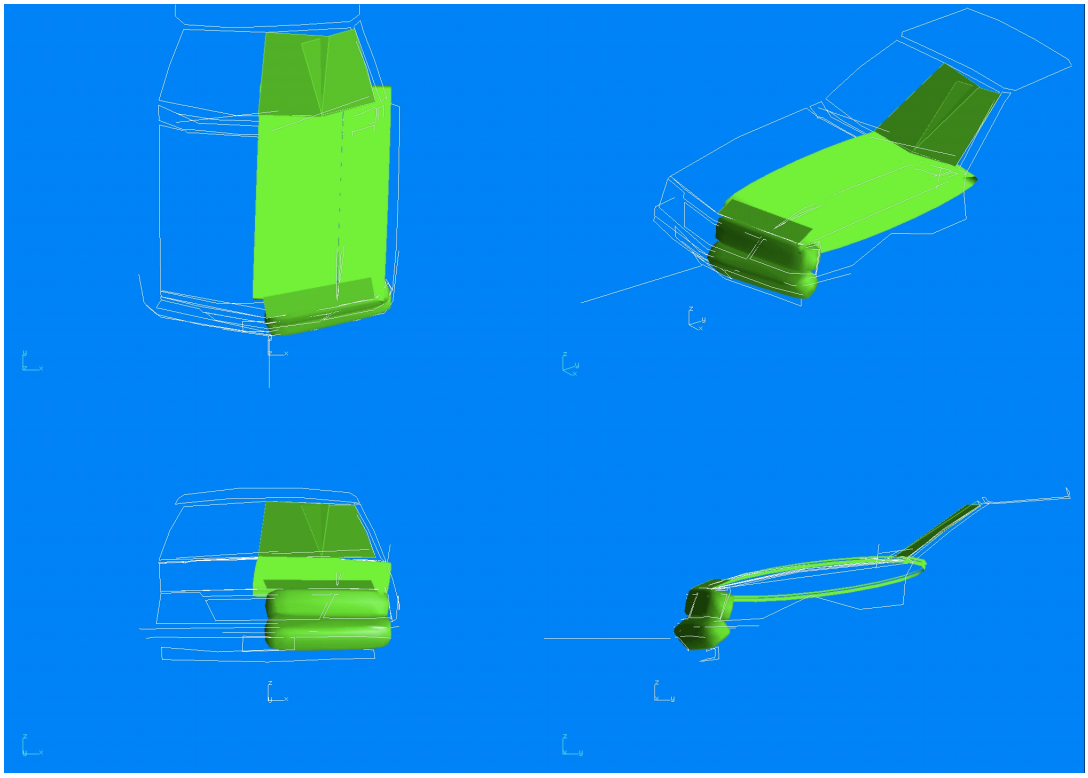

Figure 12-2 Geometry of the vehicle measured, shown in white. The approximation of this geometry for the simulation is shown by the shaded geometric entities.

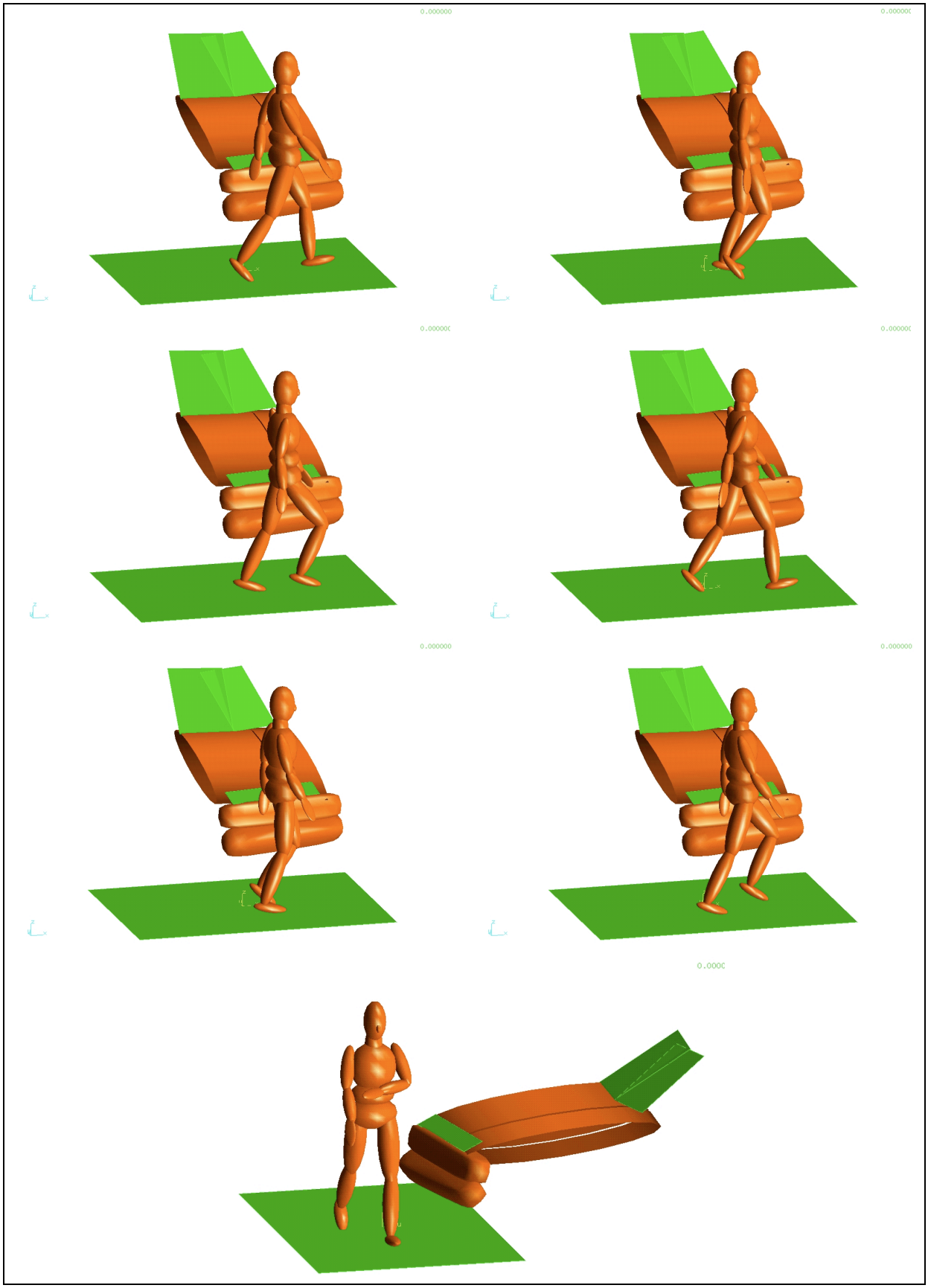

Figure 12-3 Initial position of the pedestrian and vehicle in the simulations PED056-g1 through PED056-g6 (*left to right and top to bottom*), and the final posture based on head impact position and arm kinematics.

12.5 PHYSICAL RECONSTRUCTION

The EEVC WG10 Adult Headform and Full Legform were used to simulate the impact between the head of the pedestrian and the windscreen, and the leg of the pedestrian and the bumper. Because of the expected severity of the leg impact reconstruction, the Legform was fired at a lower speed than that of the impact speed of the car, to avoid damaging the test tool. A general view of the damage caused in the collision and that produced from the reconstruction is shown in Figure 12-4.

Figure 12-4 A general view of the accident damage (left) and the damage produced by the reconstruction (right) of case PED056-99.

12.5.1 Head impact reconstruction

Table 12-3 lists the set-up of the head impact reconstruction and the results of the test. The head impact was of relatively low severity with a HIC value of 534. The acceleration recorded in the test (Figure 12-5) was typical of a windscreen impact with a short spike of acceleration prior to the fracture of the windscreen, followed by a long period of low acceleration. The damage caused by the reconstruction test and that caused to the windscreen in the actual accident is shown in Figure 12-6.

Table 12-3 Physical reconstruction parameters and results for the Headform test (test no.31070100)

	Parameter	Value
Test set-up	Launch Angle	45˚
	Measured velocity	15.32 m/s
Results	Peak acceleration	168 g
	HIC value (interval)	524 (31.0 ms)

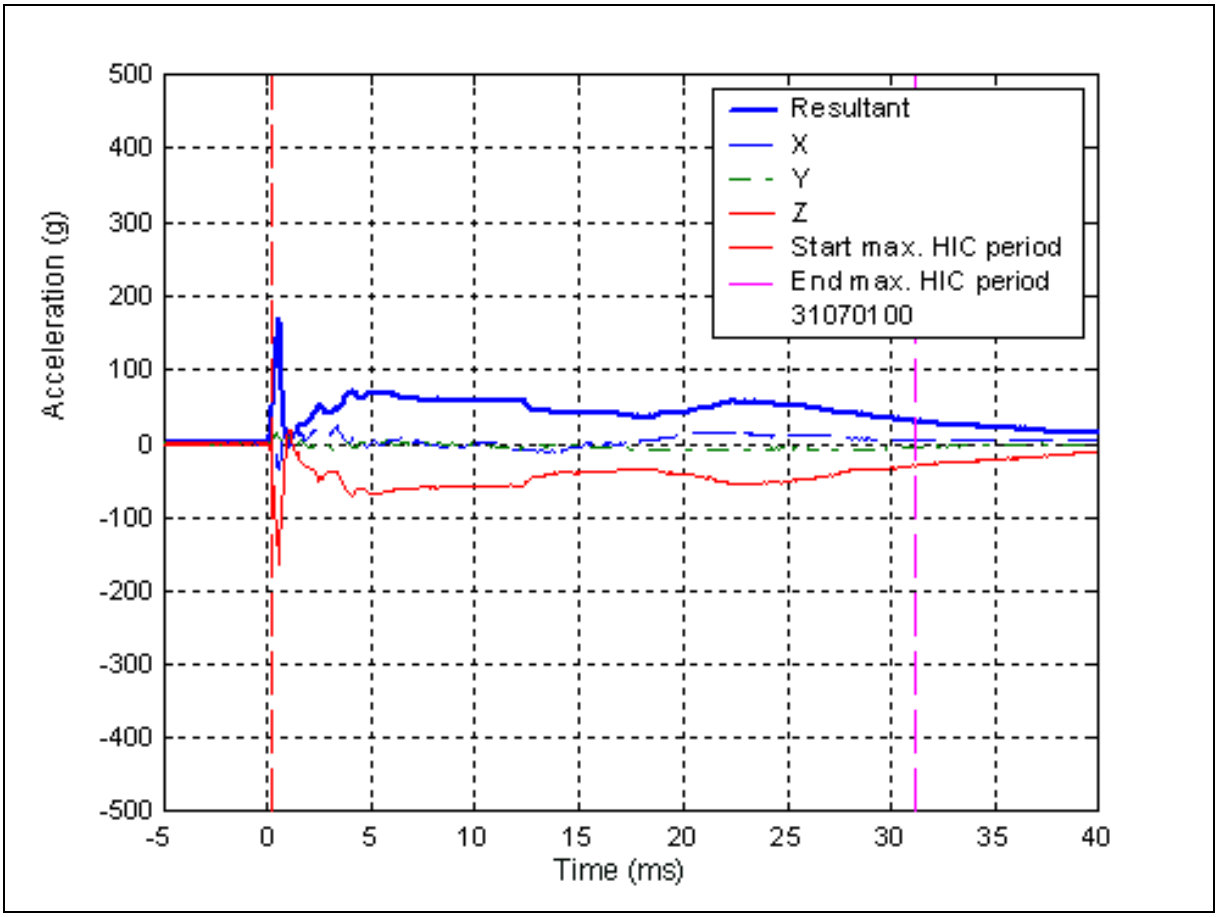

Figure 12-5 The acceleration recorded in the physical reconstruction of case PED056-99.

Figure 12-6 The accident damage caused by the impact with the head of the pedestrian (*left*) and the physical reconstruction damage of the head impact (*right*) in case PED056-99.

12.5.2 Leg impact reconstruction

The bumper of this car is very stiff. Because of this, the impact speed of the legform was reduced to avoid damage to the test tool. Nevertheless, the tibia acceleration was high, and consistent with the compound fracture of the pedestrian's left tibia and fibula.

The recordings of the tibia acceleration and the knee kinematics are shown in Figure 12-7 to Figure 12-9. A comparison of the damage caused by the reconstruction and the actual leg impact is shown in Figure 12-10.

Table 12-4 Physical reconstruction parameters and results for the Legform test (test no.30070101)

	Parameter	Value
Test set-up	Measured velocity	11.8 m/s
Results	Tibia acceleration	283.7 g
	Knee bending angle	33.1˚
	Knee shear displacement	7.5 mm

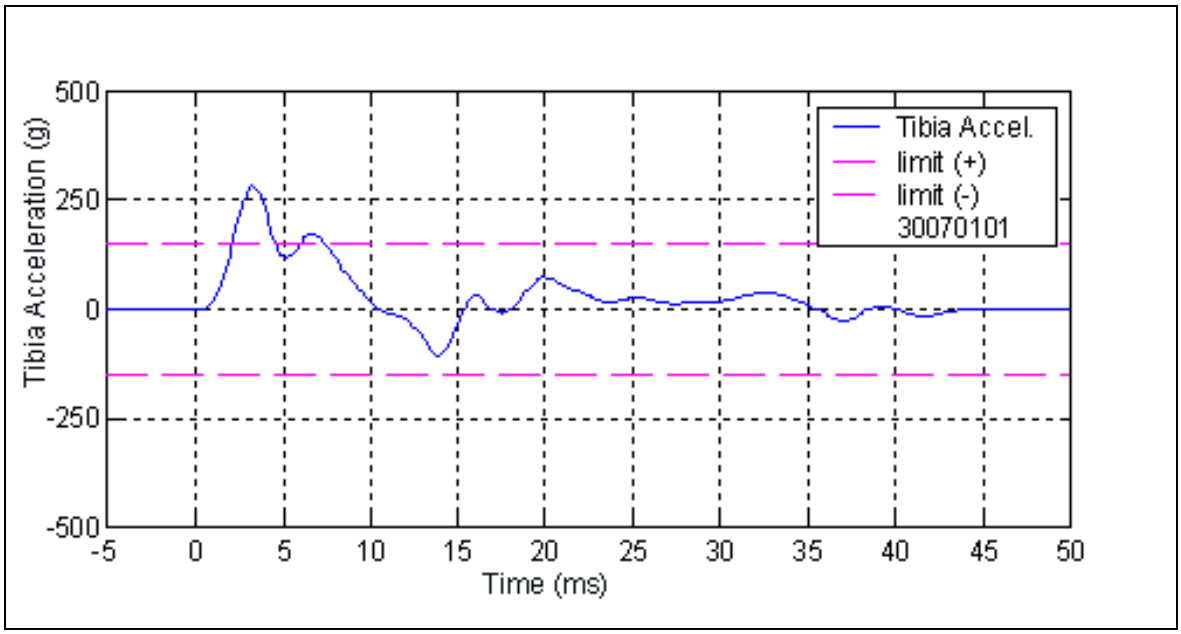

Figure 12-7 The tibia acceleration recorded in the physical reconstruction of case PED056-99.

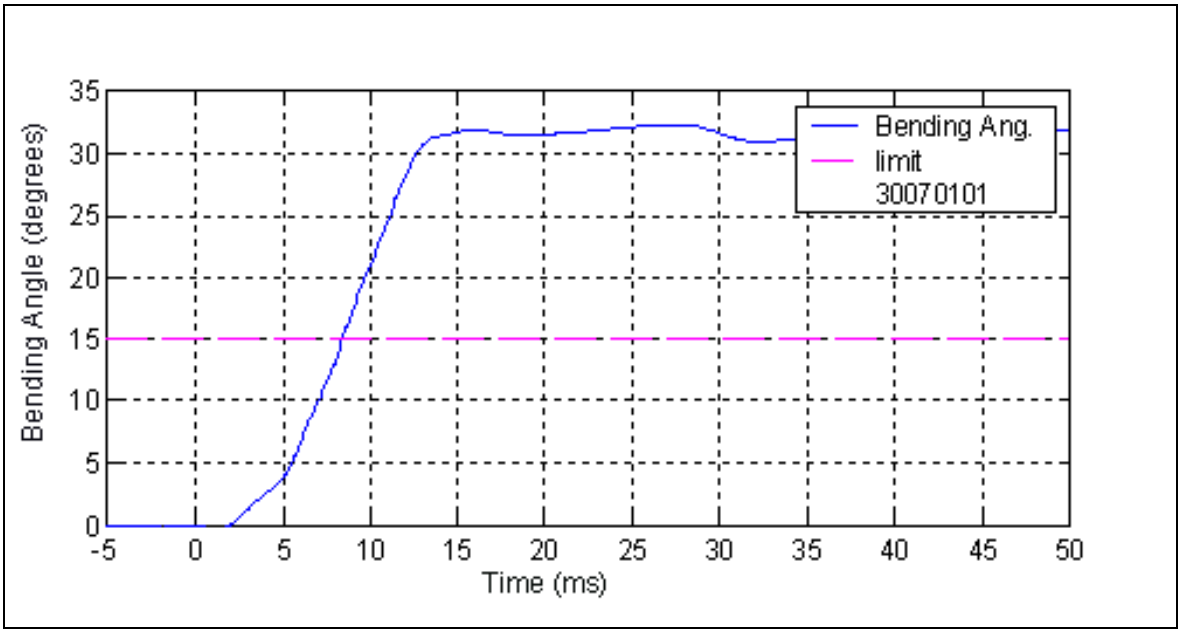

Figure 12-8 Knee bending angle recorded for the physical reconstruction of case PED056-99.

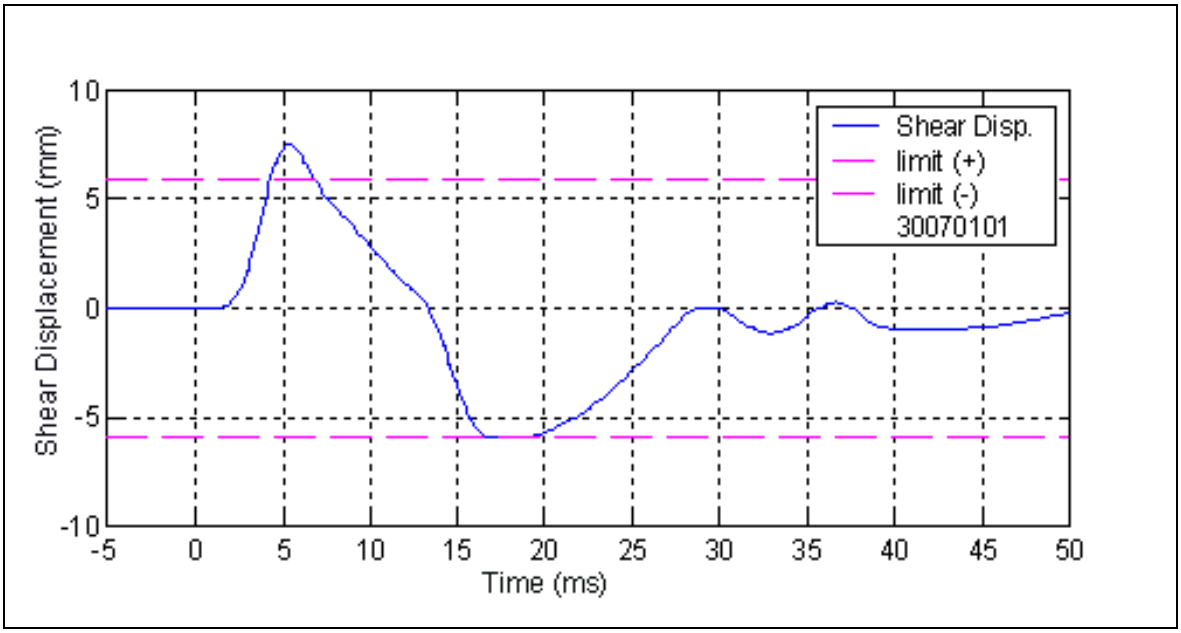

Figure 12-9 Knee shear displacement recorded for the physical reconstruction of case PED056-99.

Figure 12-10 Close-up view of the vehicle involved in the actual pedestrian impact compared with the reconstruction of case PED056-99, very minor denting on the steel bumper bar in both cases.

12.6 SUMMARY OF RECONSTRUCTION RESULTS AND INJURY DIAGNOSIS

The left tibia and fibula of the pedestrian was badly broken by the impact with the bumper of the car. Although the legform was fired at a lower speed than the impact speed of the car, a high acceleration was recorded. A more representative impact would have produced an even higher acceleration, which is commensurate with the severity of the pedestrian's lower leg fractures.

The pedestrian suffered no head injury or concussion as a result of this accident, despite the high impact speed. This is reflected in the result of the head impact reconstruction. The results of the reconstructions and the related injuries from the case are presented in Table 12-5.

Table 12-5 Summary of test results and relevant injuries

Test	Measure	Result	Relevant Injury
Full leg	Tibia acceleration	283.7 g	Compound fracture of tibia and fibula
	Knee bending	33.1˚	No knee injury diagnosed
	Knee shear	7.5 mm	
Head	HIC	524	No head injury diagnosed, skin abrasions

Indicates a result which exceeds a safe limit according to EEVC WG10

13 Case PED057-99

13.1 CASE DESCRIPTION

Two pedestrians, a young male and female, were crossing northwest across the road when the female pedestrian dashed across into the right-hand lane. A vehicle that was travelling southwest in the right-hand lane struck the female pedestrian. The driver of the vehicle applied the brakes prior to colliding with the pedestrian. The pedestrian collided heavily with the leading edge of the vehicle then struck her head on the trailing edge of the bonnet, before being vaulted over the vehicle. The vehicle did not come to a complete stop before driving off. The driver did not stop at the scene.

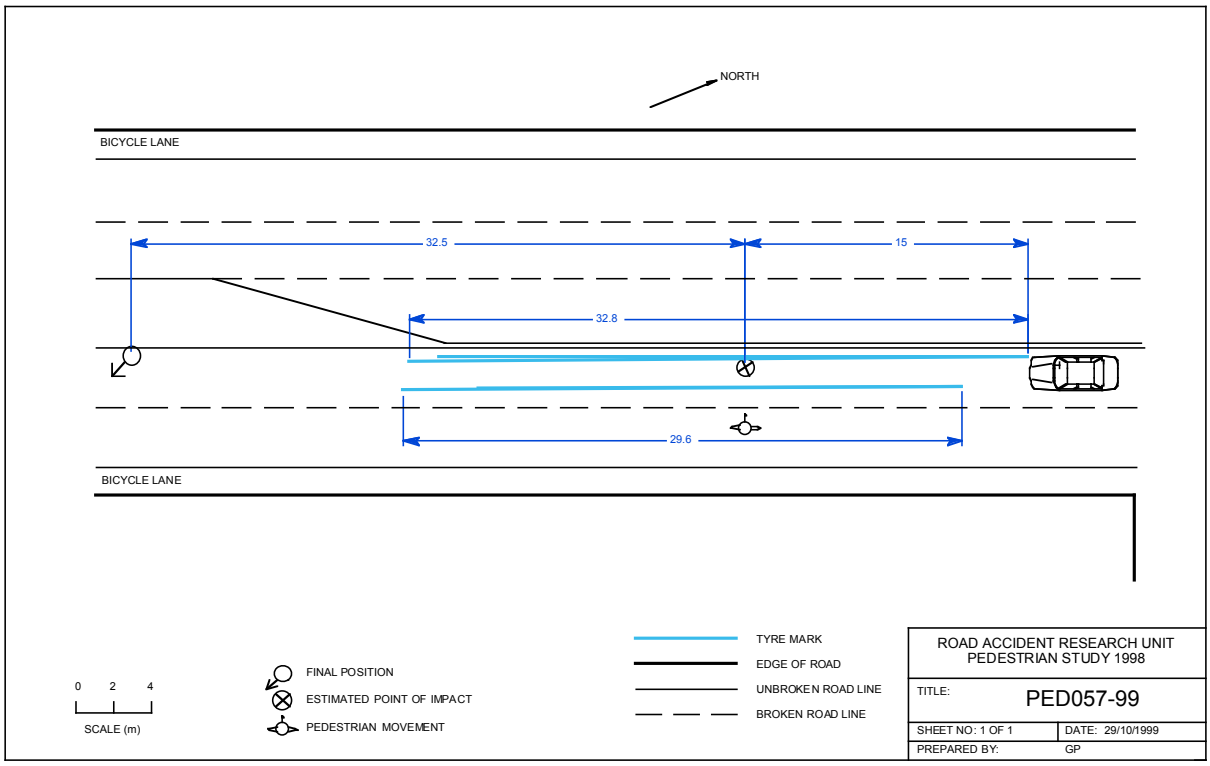

Figure 13-1 Site diagram of the collision in Case PED057-99.

13.2 PEDESTRIAN INJURIES

The pedestrian was transported by ambulance and admitted to hospital as a result of her injuries. She experienced brief loss of consciousness at the scene but regained consciousness, having a Glasgow Coma Score 13-15/15 prior to admission to hospital. She remained in hospital for 19 days before being discharged. Her most significant injuries were:

A closed fracture of the pelvis (acetabular),

A fracture to the first metatarsal (base fracture),

An open wound to the right knee, and

Abrasions to her trunk hip and leg.

13.3 ACCIDENT RECONSTRUCTION

An impact point was marked by police based on the evidence given by a number of witnesses, including the pedestrian's companion. This point is close to where the front and rear skid marks started to diverge, possibly caused by the momentum transfer during the collision. Two impact speeds were calculated, one based on the distance the pedestrian was thrown (32.5 m) and one based on skid mark analysis. The throw distance method suggests that the impact speed of the vehicle was in the range of 60-70 km/h (average estimate was 65 km/h). The method that uses the length of the skid marks after the impact point (17.8 m) gives an impact speed of 56 km/h. The latter calculation is conservative because the vehicle did not come to a complete rest at the end of the skid marks (the appearance of the end of the skid marks suggests that the vehicle's brakes were released prior to the vehicle coming to a stop). In the simulation and reconstruction, 56 km/h was used as a conservative estimate of the impact speed and 65 km/h was used as a more likely impact speed.

As the vehicle immediately left the scene, we were unable to measure or photograph it at the time of the collision. The South Australian Police eventually recovered the vehicle some time later, with the accident damage intact. We obtained copies of photographs that had been taken by the police as part of their investigation. This allowed us to complete the reconstruction.

The open wound to the knee and the fracture to the first metatarsal at base were probably associated with the contact with the bumper of the vehicle. However, there was no obvious bumper contact. The pelvic fracture and abrasions to the hip and leg were associated with the contact with the leading edge and there was a significant dent on the leading edge of the bonnet. There was also a deformation in the bonnet toward its trailing edge. This damage was very probably caused by an impact with the head of the pedestrian, who suffered concussion as a result of the accident.

13.4 MADYMO SIMULATION

A summary of the detail used to set up the simulation is contained in Table 13-1. The geometry of a 1973 Holden HQ Kingswood was measured using a Geodimeter. This measurement technique is described in Section 3.3.4. The geometry that was produced in this way was approximated by a series of elliptical cylinders and planes, and the resulting model is illustrated in Figure 13-2. The mass and moments of inertia of the pedestrian model were produced based on the 50^{th} percentile female anthropometry of a 15 year old female, as produced by GEBOD (Section 3.3.3).

As with previous simulations, six postures representative of the human gait cycle were used to examine the possible range of values for the head impact velocity. Two sets of simulations were made in this way: one with a vehicle impact speed of 56 km/h and the other set with a vehicle impact speed of 65 km/h. The results of these simulations are summarised in Table 13-2.

Table 13-1 Case details for reconstruction

Pedestrian details	
Age, sex and height	15 year old female
Orientation	Struck on right side
Vehicle details	
Year, Make and model	1973 Holden HQ Kingswood
Impact speed	65 km/h (determined from throw distance) conservative estimate of 56 km/h (determined from skid mark analysis)

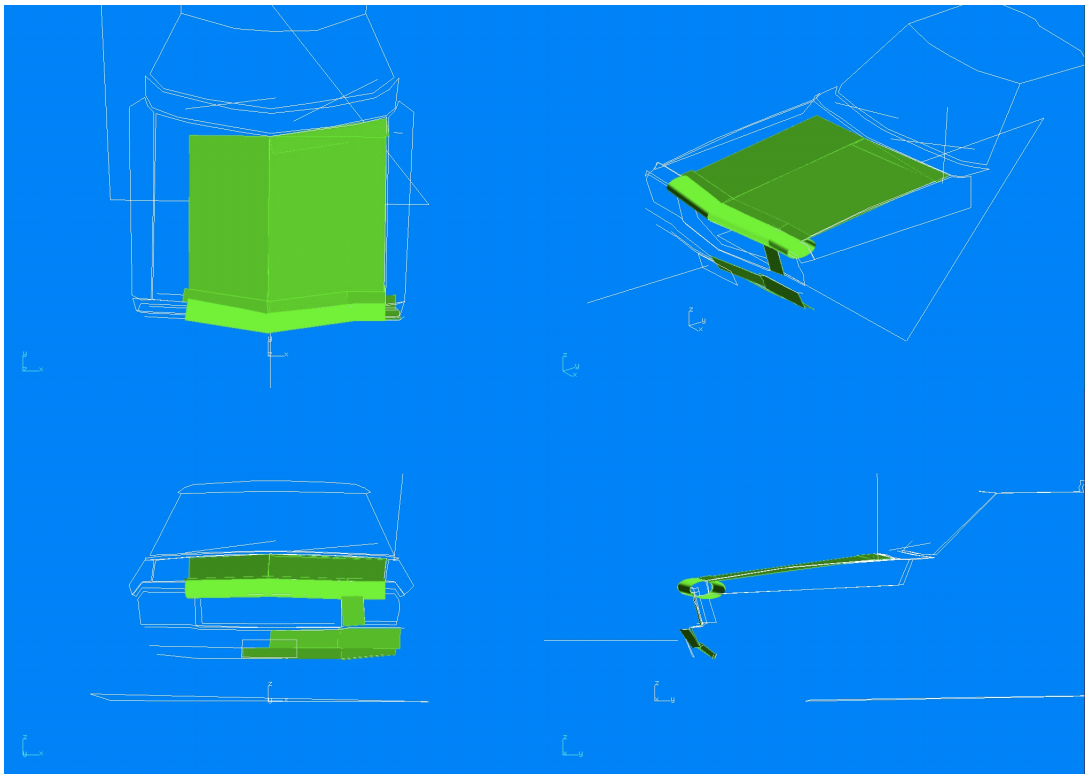

Figure 13-2 Geometry of the HQ Holden Kingswood. The approximation of this geometry for the simulation is shown by the shaded geometric entities.

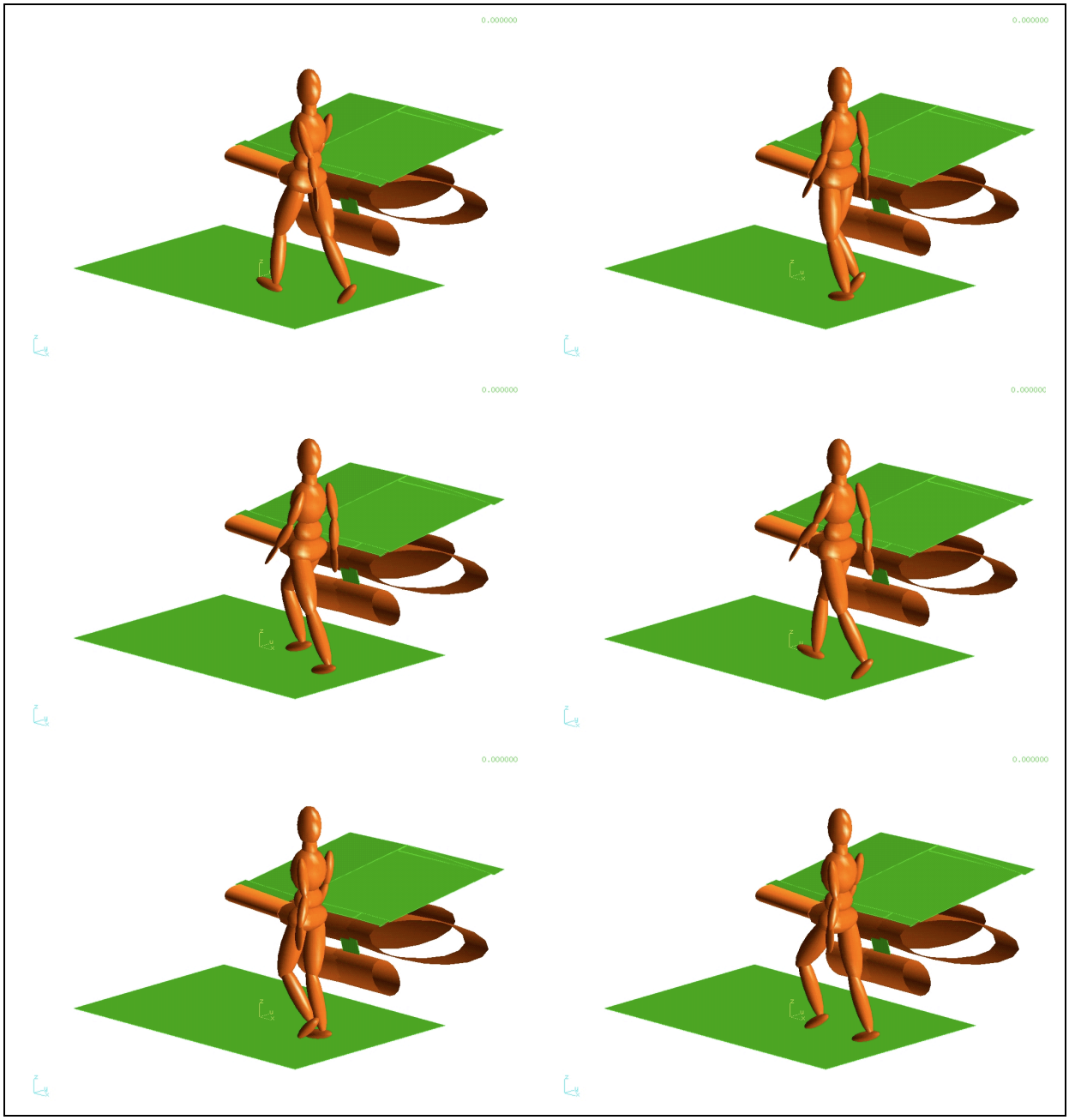

Figure 13-3 Initial position of the pedestrian and vehicle in the simulations PED057-g1 through PED057-g6 (*left to right and top to bottom*).

Table 13-2 Simulation results for PED057-99

Simulation number	Upper leg velocity	Impact angle	Energy	Effective mass	Corrected mass for test	Corrected velocity for test	Head Velocity	Impact angle
	(m/s)	(deg.)	(J)	(kg)	(kg)	(m/s)	(m/s)	(deg.)
PED057g1	18.14	38.30	1262.90	7.68	8.75	16.99	12.54	56.38
PED057g2	18.14	36.22	1446.60	8.80	8.80	18.14	16.06	53.63
PED057g3	18.14	42.53	1198.60	7.29	8.75	16.55	16.45	58.28
PED057g4	18.14	39.26	1438.60	8.75	8.75	18.13	15.22	51.09
PED057g5	18.14	34.50	1448.00	8.81	8.81	18.14	10.73	49.85
PED057g6	18.12	36.25	1363.90	8.31	8.75	17.66	12.01	53.41
Average	**18.13**	**37.84**	**1359.77**	**8.27**	**8.77**	**17.60**	**13.83**	**53.77**
PED057g1_56	15.69	28.31	1062.60	8.63	8.75	15.58	10.89	56.79
PED057g2_56	15.69	28.37	1241.00	10.09	10.09	15.69	14.13	56.55
PED057g3_56	15.69	34.28	984.64	8.00	8.75	15.00	14.82	58.35
PED057g4_56	15.69	29.78	1206.10	9.80	9.80	15.69	13.60	52.86
PED057g5_56	15.69	33.90	1272.10	10.34	10.34	15.69	9.80	52.57
PED057g6_56	15.67	27.26	1135.60	9.25	9.50	15.46	10.67	55.09
Average	**15.69**	**30.32**	**1150.34**	**9.35**	**9.54**	**15.52**	**12.32**	**55.37**

13.5 PHYSICAL RECONSTRUCTION

The EEVC Working Group 10 sub-system impactors were used to simulate the impact between the different parts of the pedestrian and the vehicle. The velocity of the headform was set to the average of the results of all the MADYMO simulation models.

The impact locations were scaled off the photographs taken by the SA Police. The head impact was estimated to be 250 mm from the centre-line of the vehicle at a wrap-around-distance of 2000 mm. The upper leg impact point was estimated to be at 400 mm from the centre-line and on the leading edge of the vehicle.

13.5.1 Head impact reconstruction

Two headform tests were performed: the first assumed a vehicle impact speed of 65 km/h, and the second assumed an impact speed of 57 km/h.

Table 13-3 and Table 13-4 give the set-up parameters and the results of the head impact reconstructions. The associated Headform acceleration from each impact is shown in Figure 13-5 and Figure 13-6.

Figure 13-4 The accident damage from the impact (left) and the damage produced in the physical reconstruction (right) of case PED057-99.

Table 13-3 Physical reconstruction parameters and results for the Headform test (test no. 05060102; assuming a vehicle impact speed of 65 km/h)

	Parameter	Value
Test set-up	Launch Angle	54˚
	Measured velocity	13.65 m/s
Results	Peak acceleration	326 g
	HIC value (interval)	3558 (6.9 ms)

Table 13-4 Physical reconstruction parameters and results for the Headform test (test no. 05060103; assuming a vehicle impact speed of 57 km/h)

	Parameter	Value
Test set-up	Launch Angle	55.5˚
	Measured velocity	12.21 m/s
Results	Peak acceleration	319 g
	HIC value (interval)	4109 (5.2 ms)

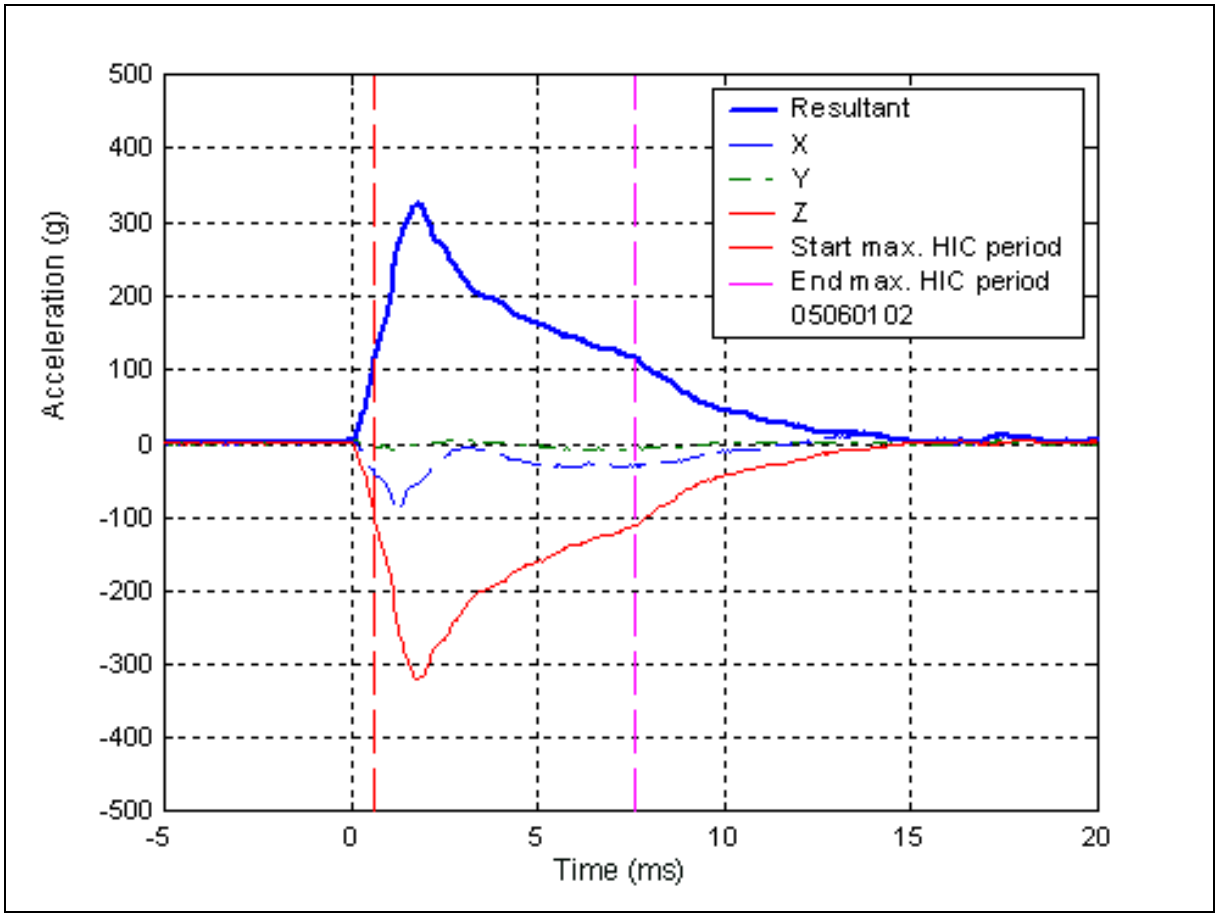

Figure 13-5 The acceleration recorded in the physical reconstruction of case PED057-99 for higher impact speed of the range.

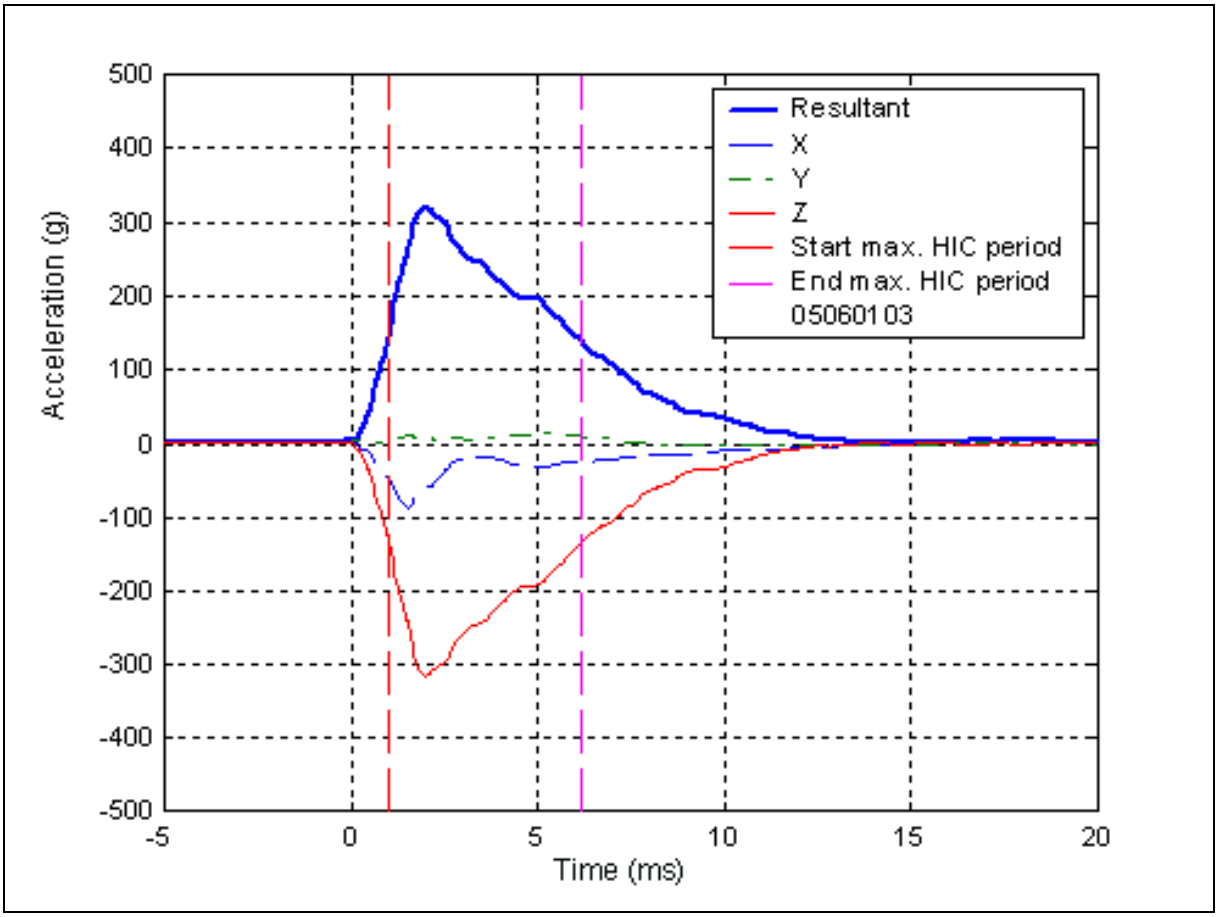

Figure 13-6 The acceleration of the Headform recorded in the physical reconstruction of case PED057-99 for lower impact speed of the range.

13.5.2 Upper leg impact reconstruction

The simulations predicted that the impact between the pedestrian and the leading edge would have been severe. The reconstruction speed was lowered as it was thought that an impact at the speed estimated by the MADYMO simulation would damage the test tool. The test conditions used in the test, and the results of the test are given in Table 13-5, and the support forces and bending moment are plotted in Figure 13-7 and Figure 13-8

Figure 13-9 and Figure 13-10 show the damage caused by the reconstruction of the upper leg impact and the damage caused in the collision. Despite the lower impact speed and less damage to the vehicle, the results of the test exceeded the EEVC limits in the test by a significant amount.

Table 13-5 Physical reconstruction parameters and results for the Upper Legform test (test no. 07060100)

	Parameter	Value
Test set-up	Launch Angle	30˚
	Impactor mass	9.5 kg
	Simulation velocity	15.5 m/s
	Actual velocity	12.1 m/s
Results	Maximum force	8 kN
	Bending Moment	605 Nm

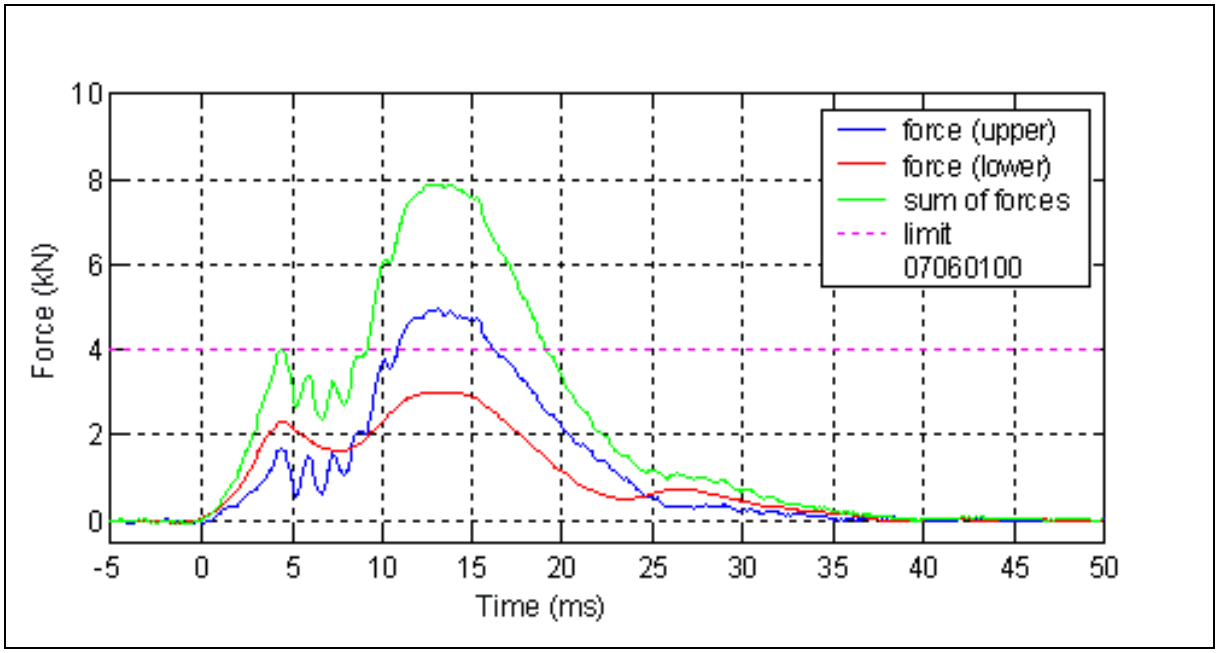

Figure 13-7 Force recorded in the Upper Legform in the physical reconstruction of case PED057-99

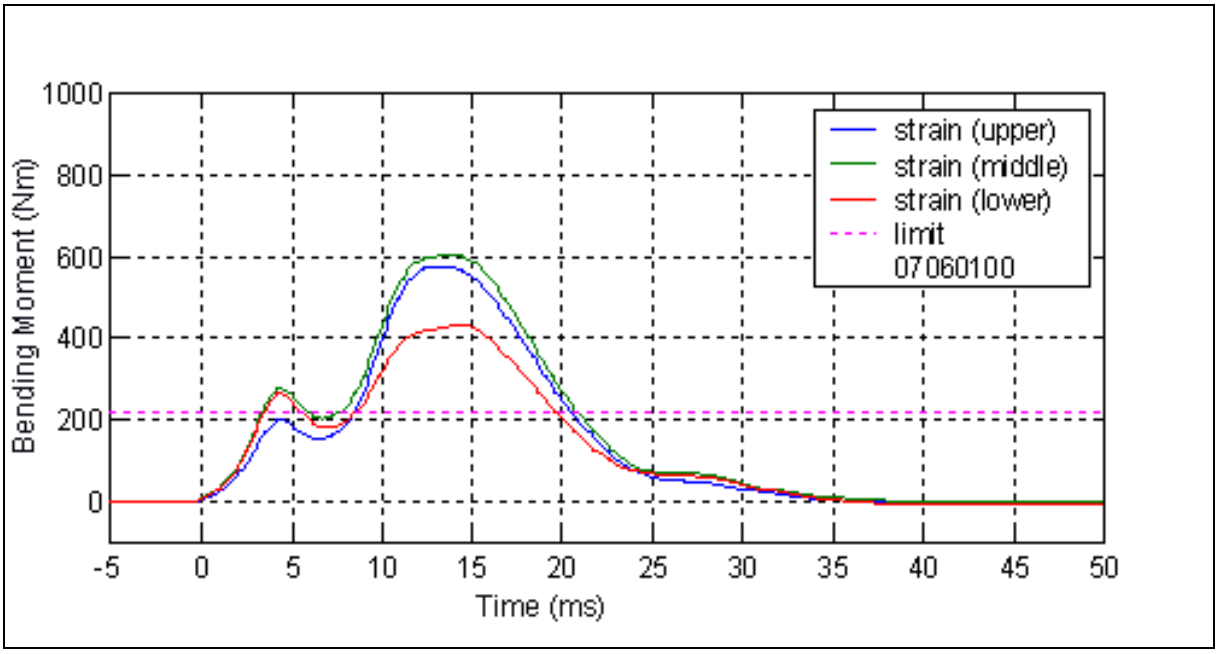

Figure 13-8 Bending moment recorded in the physical reconstruction of case PED057-99.

Figure 13-9 A close up front view of the accident damage from impact with the pelvic area (left) and the damage from the reconstruction with the Upper Legform (right) of case PED057-99.

Figure 13-10 Close up angle view after the physical reconstruction with the Upper Legform impactor of case PED057-99.

13.6 SUMMARY OF RECONSTRUCTION RESULTS AND INJURY DIAGNOSIS

This case was unusual in that the pedestrian was not as severely injured as we might have expected, given the high speed at which she was struck. It appears that the extent of the deformation created in the car may have prevented a worse outcome than might have otherwise occurred. The deformation in the car involved in the collision is shown in Figure 13-4. This figure also shows the car used in the reconstruction of this case, after the impact reconstructions. The bonnet of the car involved in the collision was pushed upward some distance by the initial impact at the front of the bonnet. It is possible that this increased the clearance between the bonnet and the car structure beneath. This increased clearance may have softened the impact considerably.

The impact between the pedestrian and the leading edge was severe, and caused significant deformation of the vehicle. The reconstruction test was performed at a lower speed and did not cause as much deformation. Nevertheless, very high loads were placed on the Upper Legform during the impact, and would have been much higher to cause the amount of deformation seen in the case vehicle. Although the pedestrian's pelvis was fractured as a result of this impact (AIS 2), the loads measured in the reconstruction would be expected to be associated with a more severe injury.

Table 13-6 Summary of test results and relevant injuries

Test	Measure	Result	Relevant Injury
Upper leg	Support forces Maximum bending moment	8 kN 605 Nm	Pelvic (acetabular) injury
Head	HIC	3558 (higher impact speed) 4109 (lower impact speed)	Brief unconsciousness

Indicates a result which exceeds a safe limit according to EEVC WG10

14 Case PED061-99

14.1 CASE DESCRIPTION

A vehicle was travelling north when it struck two children (male and female) who were crossing from the driver's left-hand side. The left-hand side of the vehicle struck the female, and her forehead struck the left-hand edge of the bonnet. The impact with the bonnet resulted in skull fractures and brain injuries. She was then dragged along the road, the skin from her shoulder and head leaving scuffmarks on the road. She died of secondary brain injury. The male pedestrian appears to have been struck closer to the centre of the car, thrown onto the bonnet before being thrown forwards. He suffered serious head injuries as a result of the accident.

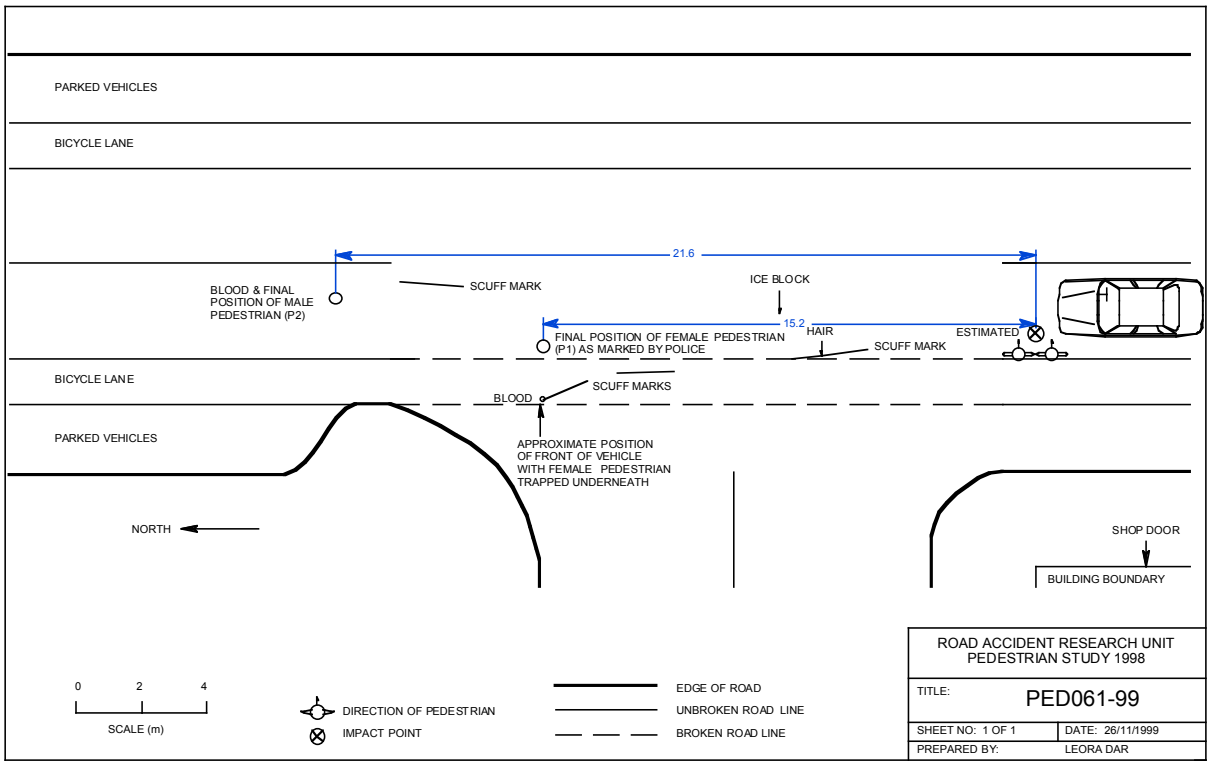

Figure 14-1 Site diagram of the collision in Case PED061-99.

14.2 PEDESTRIAN INJURIES

The female pedestrian was transported by ambulance and admitted to the Intensive Care Unit as a result of her injuries but died the following day. She experienced loss of consciousness at the scene and presented with airway compromise. She had a Glasgow Coma Score 0/15 at the scene. The cause of death was determined to be hypoxic ischaemic encephalopathy secondary to closed head injuries.

Her other significant injuries were:

Fractures of the right frontal bone of the skull

Kidney laceration with haematoma

Haematoma over right fronto-temporal area of scalp

Multiple abrasions to her right ear, neck, shoulder, hip and thigh

14.3 ACCIDENT RECONSTRUCTION

An estimated impact point was marked by police based on the evidence given by a number of witnesses. Both pedestrians walked out from in front of a parked car and into the path of the striking vehicle. There was no evidence of pre-impact or post-impact braking. The total throw distance for the fatally injured pedestrian was 15.2 m. The travel speed and impact speed of the vehicle was calculated to be 41-48 km/h, based on the distance the pedestrian was thrown. The second pedestrian was thrown 21.6 m, implying a range of impact speeds of 49 - 57 km/h.

One equation that is used to calculate impact speed assumes, that the pedestrian will slide the whole distance between the impact point and the final position. This gives an estimation of the highest possible impact speed for a given trajectory. The second equation assumes that the pedestrian was thrown in a ballistic fashion to the final position. This latter equation provides an estimate of the lowest possible impact speed. Usually the average of the speeds given by these methods provides a reasonable estimate of impact speed. In this case, the fatally injured pedestrian mostly slid to her final position, and the other was mostly thrown. Therefore, an appropriate estimate of speed is one consistent with the upper bound given by the throw distance of the fatally injured pedestrian, and the lower bound given by the trajectory of her companion. This implies an impact speed of approximately 49 km/h. This speed also supports the estimate of speed given by the driver of the vehicle, who claimed to be travelling about 50 km/h.

Abrasions to the pedestrian's hip and thigh and a lacerated kidney were associated with the dent on the leading edge of the bonnet, and damage to the left hand headlight and front corner of the mudguard. There was also a dent on the seam of the bonnet and left hand wing panel, which was the source of the head impact resulting in the brain injuries and the skull fracture of the pedestrian. The pattern of deformation on the impact point was matched to a bruise on the forehead of the pedestrian. The impact point on the vehicle measured 700 mm from the centre of the bonnet, and a wrap around distance of 1420 mm was measured from the ground to the impact point.

14.4 MADYMO SIMULATION

The simulation of this collision was designed to reproduce the location of the head impact. The left-hand corner of the car struck the pedestrian, but no evidence was seen of any sliding along the side of the car. Therefore, the initial position of the pedestrian was designed to reflect this. There was also no evidence of significant arm involvement in the collision. The simulation was adjusted to ensure that the arm did not unduly affect the head impact velocity.

The parameters that determined the models of the vehicle and pedestrian are given in Table 14-1, and illustrations of the vehicle and pedestrian models are shown in Figure 14-2 and Figure 14-3.

Table 14-1 Case details for reconstruction

Pedestrian details		
	Age, sex and height	10 year old female, 138 cm
	Orientation	Struck on right side
Vehicle details		
	Year, Make and model	1997 Mitsubishi Magna
	Impact speed	50 km/h

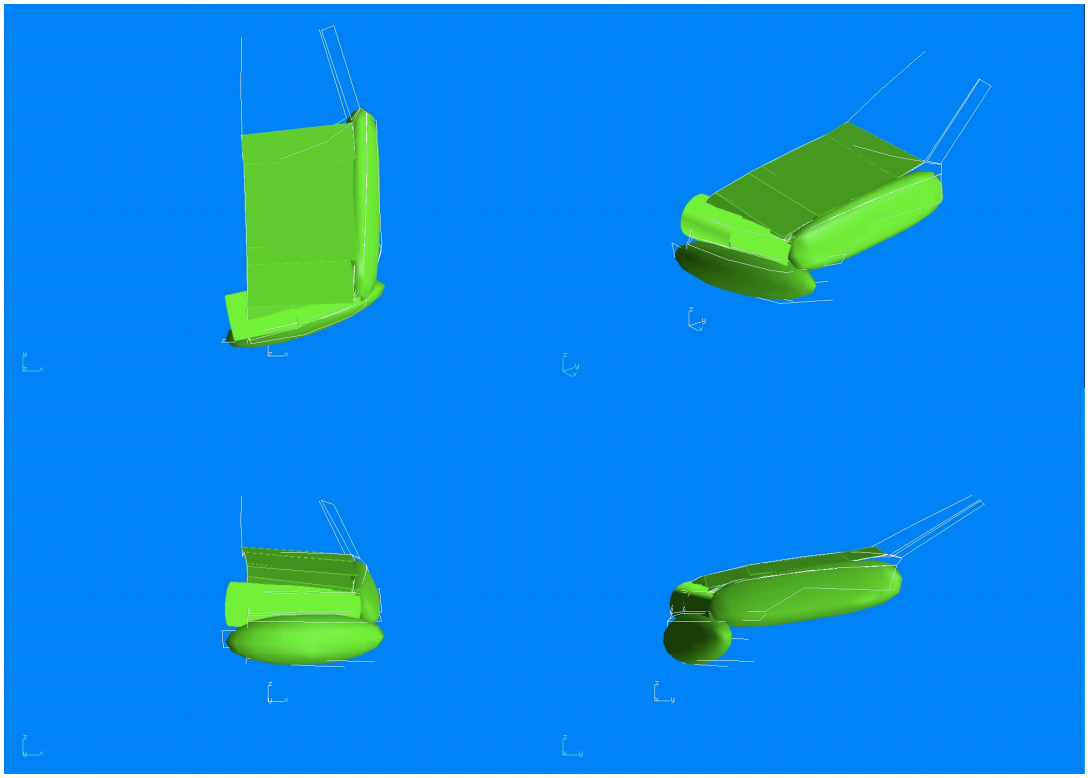

Figure 14-2 Geometry of the Mitsubishi Magna. The approximation of this geometry for the simulation is shown by the shaded geometric entities.

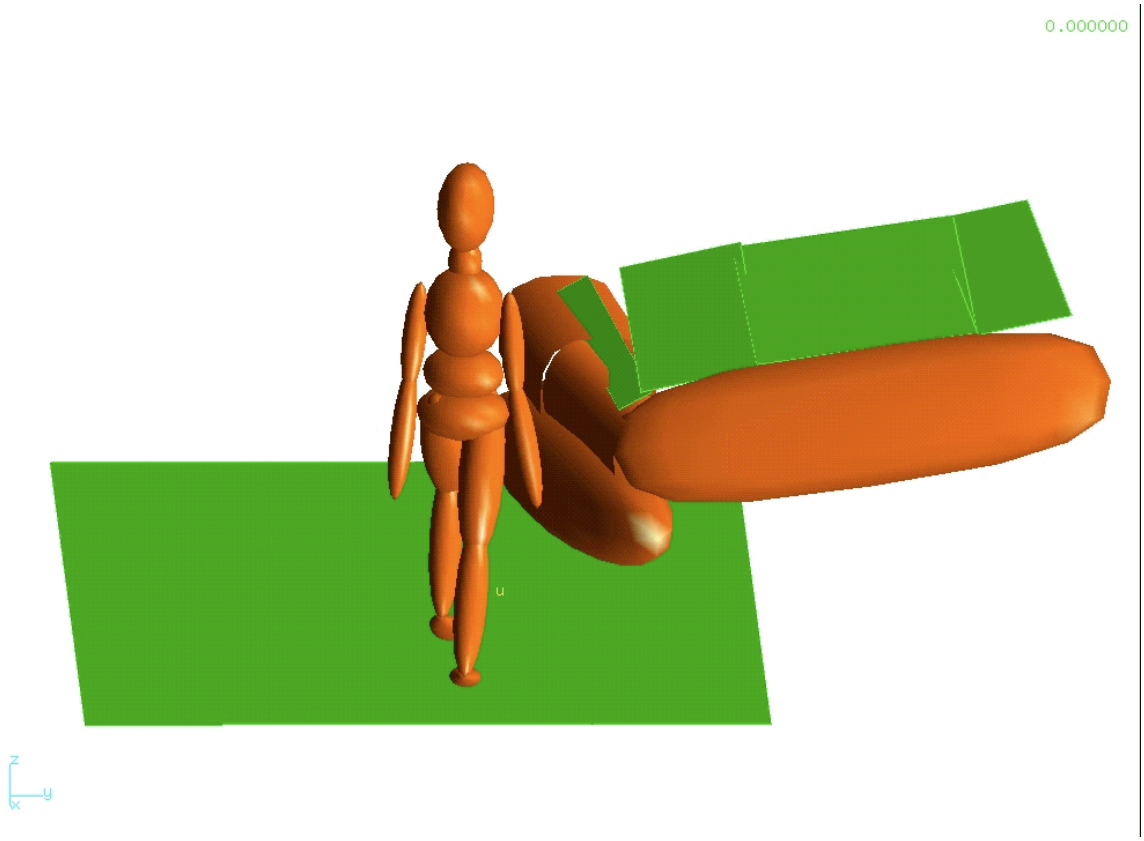

Figure 14-3 Initial position of vehicle and pedestrian in the simulation of Case PED061-99

Table 14-2 Simulation results for PED061-99

Simulation number	Head Velocity	Impact angle
	(m/s)	(deg.)
ped061_e	6.39	39.37

14.5 PHYSICAL RECONSTRUCTION

The head impact experienced by the pedestrian was reconstructed using Child Headform, which was fired at the impact point identified in the crash investigation. Figure 14-4 shows overall shots of the accident-involved vehicle and the vehicle used for the reconstruction.

Figure 14-4 A general view of the vehicle involved in case PED061-99 (left) and the general view after the physical reconstruction (right) of case PED061-99.

14.5.1 Head Impact reconstruction

The impact conditions of the reconstruction were set to those estimated by the MADYMO simulation. The set-up and result of the test is shown in Table 14-3. The result and the acceleration of the headform (Figure 14-5) are indicative of a very hard impact. The damage caused by the reconstruction is a close replica of that caused in the accident (Figure 14-6).

Table 14-3 Physical reconstruction parameters and results (test no. 22060100)

	Parameter	Value
Test set-up	Launch Angle	39.5˚
	Measured velocity	6.45 m/s
Results	Peak acceleration	229 g
	HIC value (interval)	1718 (3.8 ms)

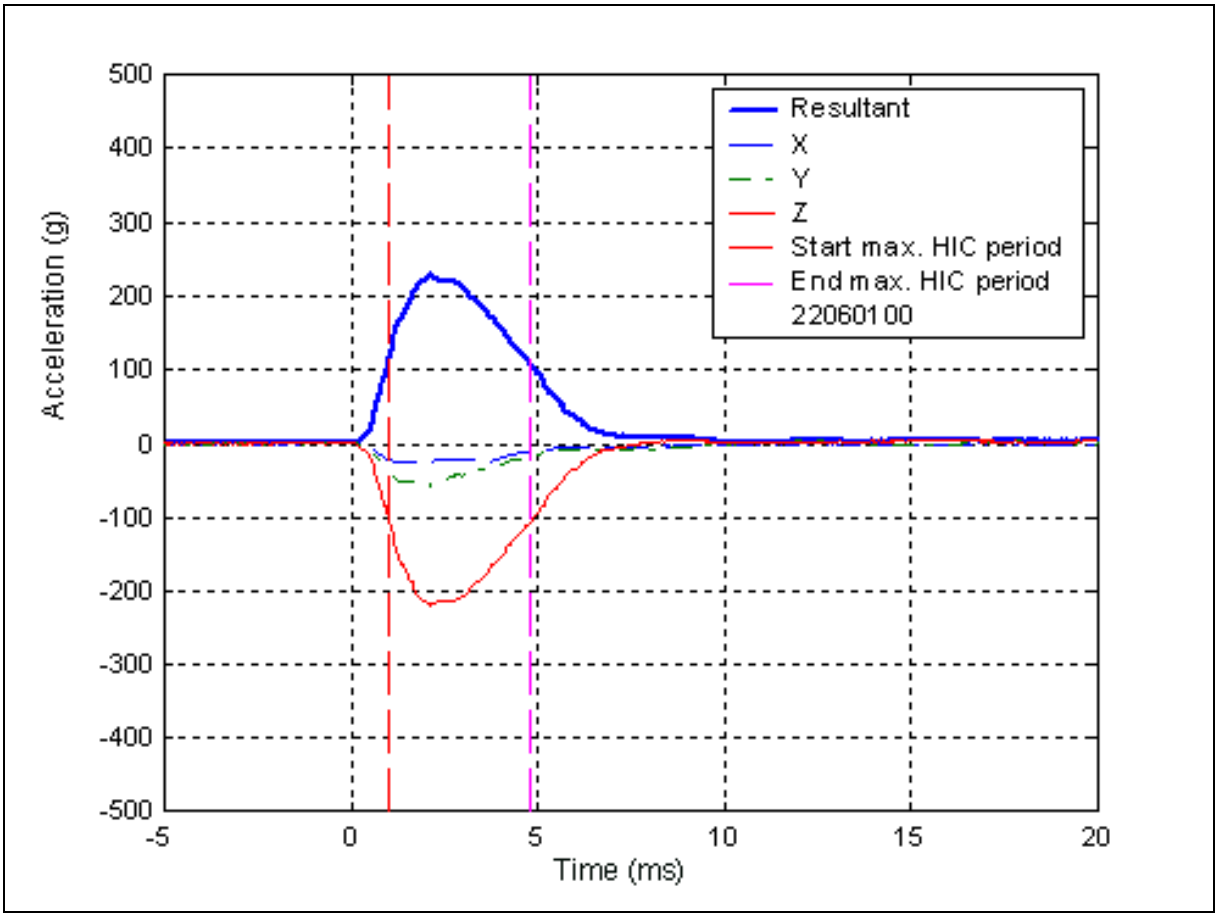

Figure 14-5 The acceleration recorded in the physical reconstruction of case PED061-99.

Figure 14-6 Close-up of the damage caused by impact with the child pedestrian's head (left) and the damage produced in the reconstruction (right) of case PED061-99.

14.6 SUMMARY OF RECONSTRUCTION RESULTS AND INJURY DIAGNOSIS

The result of the head impact reconstruction appears to be a good representation of the head impact in the accident. The head of the pedestrian struck a very stiff structure on the car, and the resulting head impact was severe. The estimated head impact severity reflects the serious nature of the pedestrian's head injuries (Table 14-4).

Table 14-4 Summary of test results and relevant injuries

Test	Measure	Result	Relevant Injury
Head	HIC	1718	Fatal brain injury

Indicates a result which exceeds a safe limit according to EEVC WG10

15 Case PED064-00

15.1 CASE DESCRIPTION

A vehicle, heading west in the right-hand lane of an arterial road, drove through an intersection while the traffic light signal was either amber or red. The driver saw a pedestrian crossing the road in front of her, sounded the horn and applied the brakes, which did not lock up. The vehicle collided with the pedestrian. The vehicle came to a stop with the pedestrian thrown approximately 3 m in front of the vehicle.

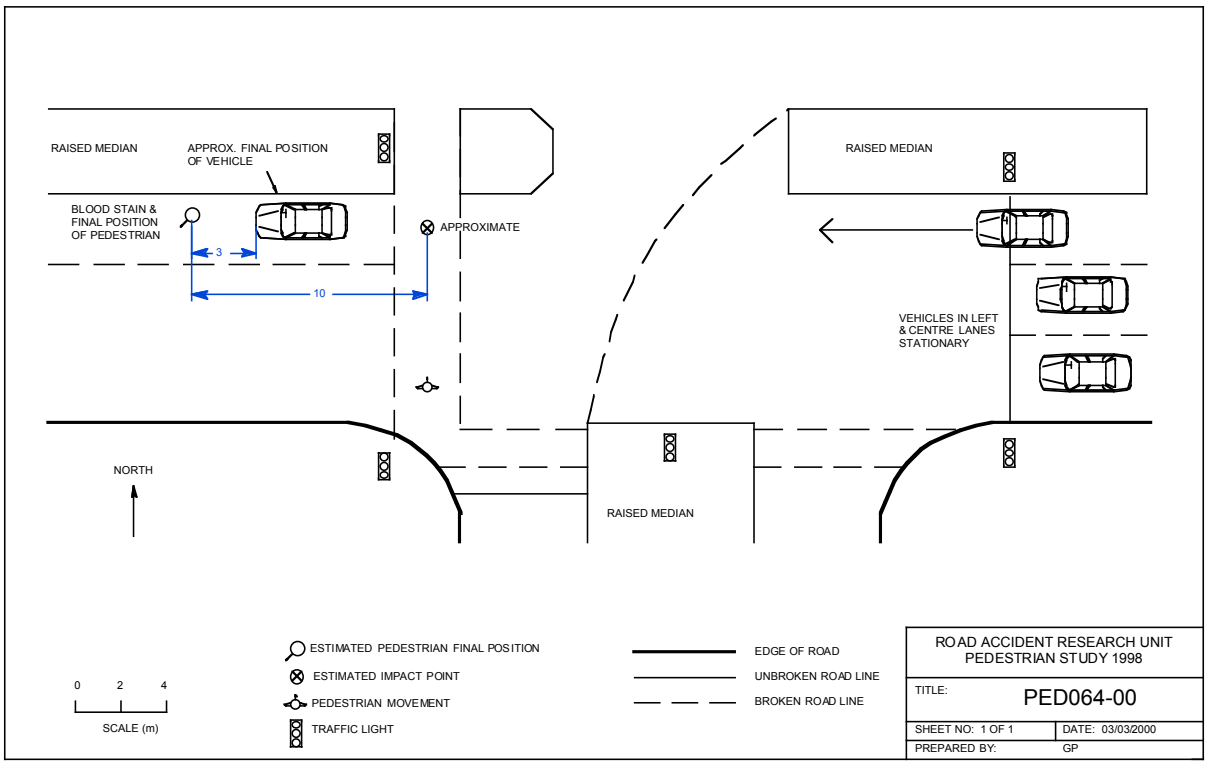

Figure 15-1 Site diagram of the collision in Case PED064-00.

15.2 PEDESTRIAN INJURIES

The pedestrian was transported by ambulance to hospital as a result of her injuries but was discharged from the Emergency Services Department after two hours. She remained conscious following the accident. Her most significant injuries were

scratches and grazes to her face and right ear

laceration to her chin area that required suturing

abrasion to her right elbow that required suturing

deep graze to her right hip and deep bruising in her left knee, which took approximately 8 weeks to resolve and continued to be stiff three months following accident.

15.3 ACCIDENT RECONSTRUCTION

An impact point was estimated from information received from the driver and witnesses. The pedestrian was thrown approximately 10 m, which implies an impact speed of 36 km/h. The stopping distance of the vehicle, 7 m, is consistent with this estimate of the impact speed (the driver claimed she braked but did not lock up the wheels of the car).

A scuff on the left side of the bumper indicated that this was the source of the bruising to the pedestrian's left knee. There was also scuffing on the bonnet, which was probably the source of the graze to the pedestrian's right hip. There were two obvious impacts with the windscreen. The lower impact was with the pedestrian's right elbow, which was lacerated. The second, and higher, impact was with the pedestrian's head. This impact caused scratches and grazes to the right side of her face and ear, and lacerations to her chin.

The head impact point measured to 125 mm from the vehicle centre-line and measured 2605 mm (wrap around distance) from the ground. The scuff from the leg impact was 470 mm from the centre-line of the vehicle.

15.4 MADYMO SIMULATION

The simulation was based on the information given in Table 15-1. The vehicle model, which was based on measurements made using the Geodimeter (Section 3.3.4), is shown in Figure 15-2. The simulation was required to produce an elbow impact with the lower edge of the windscreen, and a head impact further up the windscreen. This was achieved using the initial position illustrated in Figure 15-3.

The head impact velocity estimated by the simulation is given in Table 15-2.

Table 15-1 Case details for reconstruction

Pedestrian details		
	Age, sex and height	19 year old female,165 cm
	Orientation	struck on right side
Vehicle details		
	Year, Make and model	1993 Holden VP Commodore
	Impact speed	36 km/h

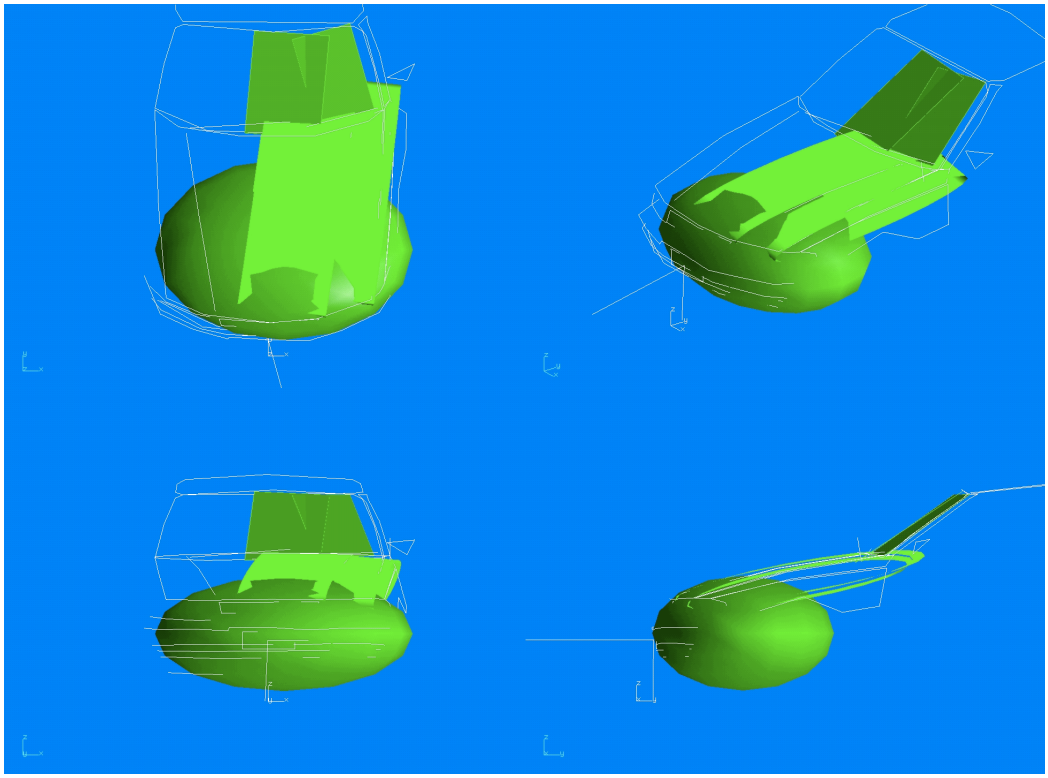

Figure 15-2 Geometry of the Holden VP Commodore. The approximation of this geometry for the simulation is shown by the shaded geometric entities.

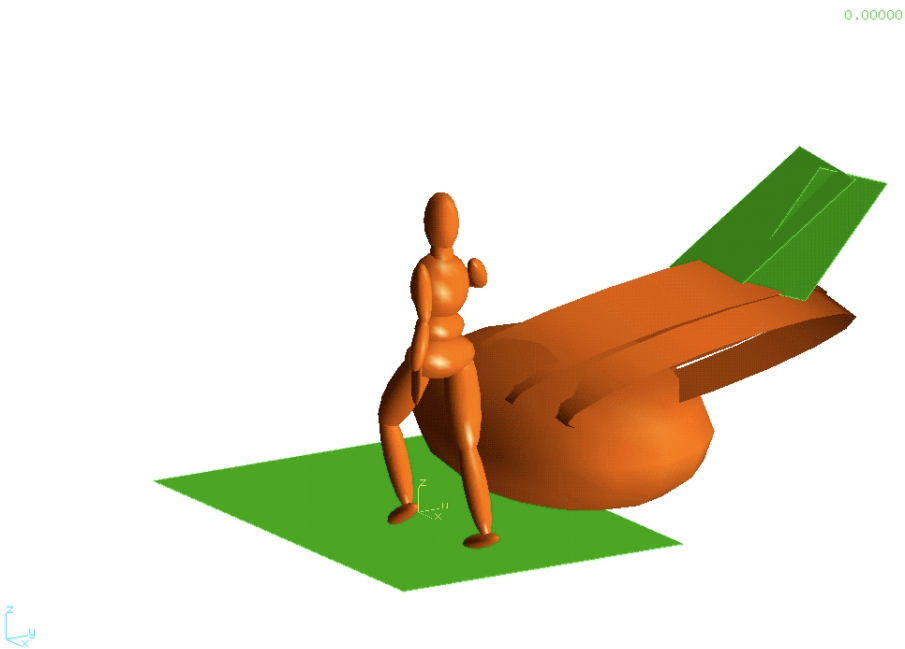

Figure 15-3 The initial position of the pedestrian and vehicle in the simulation of Case PED064-00

Table 15-2 Simulation results for PED064-00

Simulation number	Head impact velocity	Impact angle
	(m/s)	(deg.)
Ped064	6.46	46.58

15.5 PHYSICAL RECONSTRUCTION

15.5.1 Head impact reconstruction

The head impact reconstruction was performed based on the results of the simulation. The set-up and results of the test are shown in Table 15-3. The acceleration (Figure 15-4) and HIC value measured in the test indicate that the head impact in this collision was relatively soft. Figure 15-5 compares the damage created by the reconstruction and that caused by the head impact in the case.

Table 15-3 Physical reconstruction parameters and results for the Headform test (test no. 21060100)

	Parameter	Value
Test set-up	Launch angle	47˚
	Measured velocity	6.51 m/s
Results	Peak acceleration	96 g
	HIC value (interval)	136 (2.0 ms)

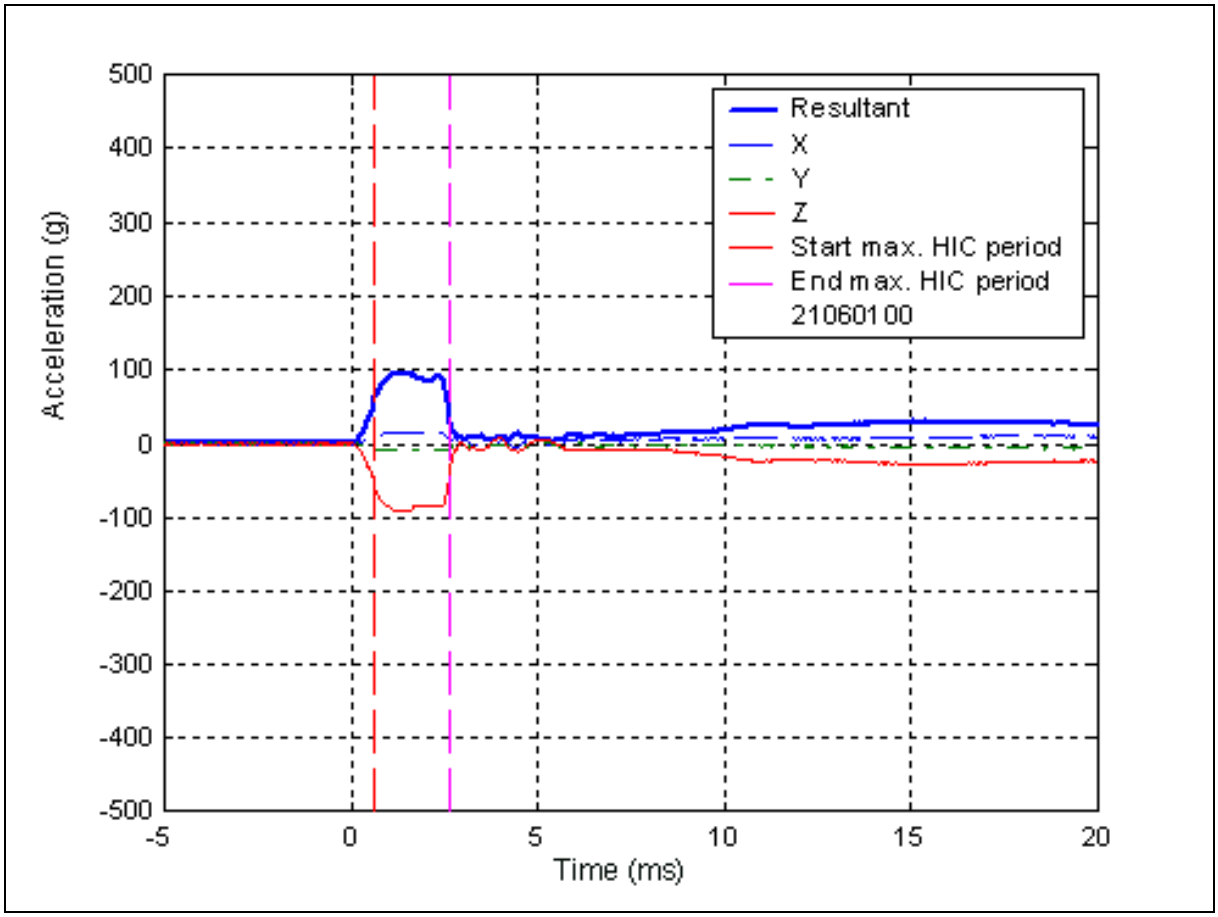

Figure 15-4 The acceleration recorded in the physical reconstruction of case PED064-00.

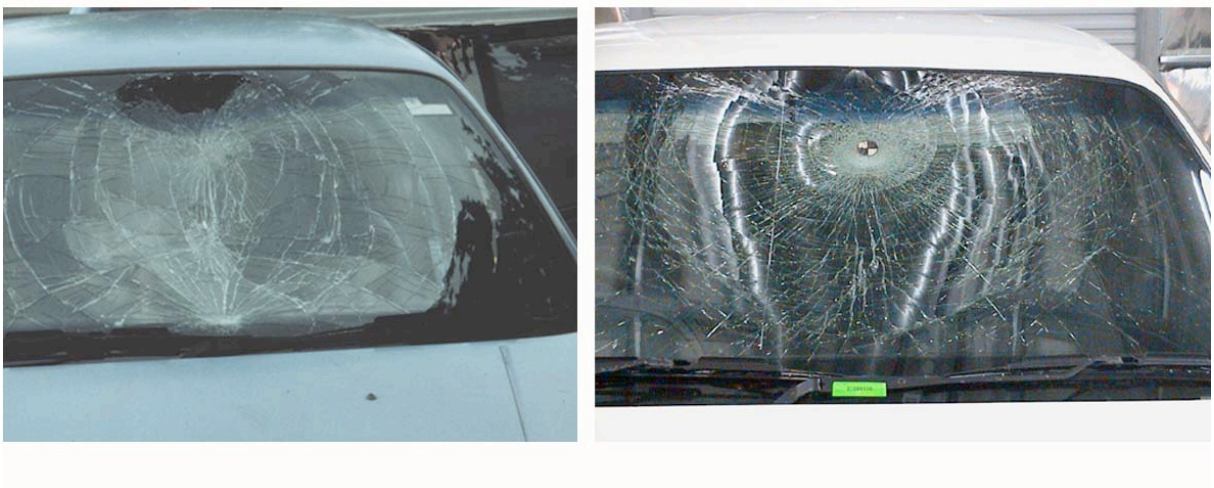

Figure 15-5 Damage caused by impact with the pedestrian's head (left) and the damage produced in the reconstruction (right) of case PED064–00.

15.5.2 Leg impact reconstruction

The Full Legform was fired a point 470 mm from the centreline of the bumper, the position of the scuffmark on the accident-involved car. The speed of the Legform was set to that of the striking speed of the car. The set-up and results of the test are given in Table 15-4.

The result of the test fails the limits set by the EEVC. The tibia acceleration would indicate that there would have been a high risk of tibia fracture resulting from such an impact. The bending of the knee would be expected to produce ligamentous damage. The tibia acceleration and the kinematics of the knee in the test are shown in Figure 15-6 to Figure 15-8. There was little sign of damage on the exterior of the car after the test, as was the case in the accident-involved car (Figure 15-9).

Table 15-4 Physical reconstruction parameters and results for the Legform test (test no.08060100)

	Parameter	Value
Test set-up	Measured velocity	10.0 m/s
Results	Tibia acceleration	199.4 g
	Knee bending angle	29.9°
	Knee shear displacement	2.8 mm

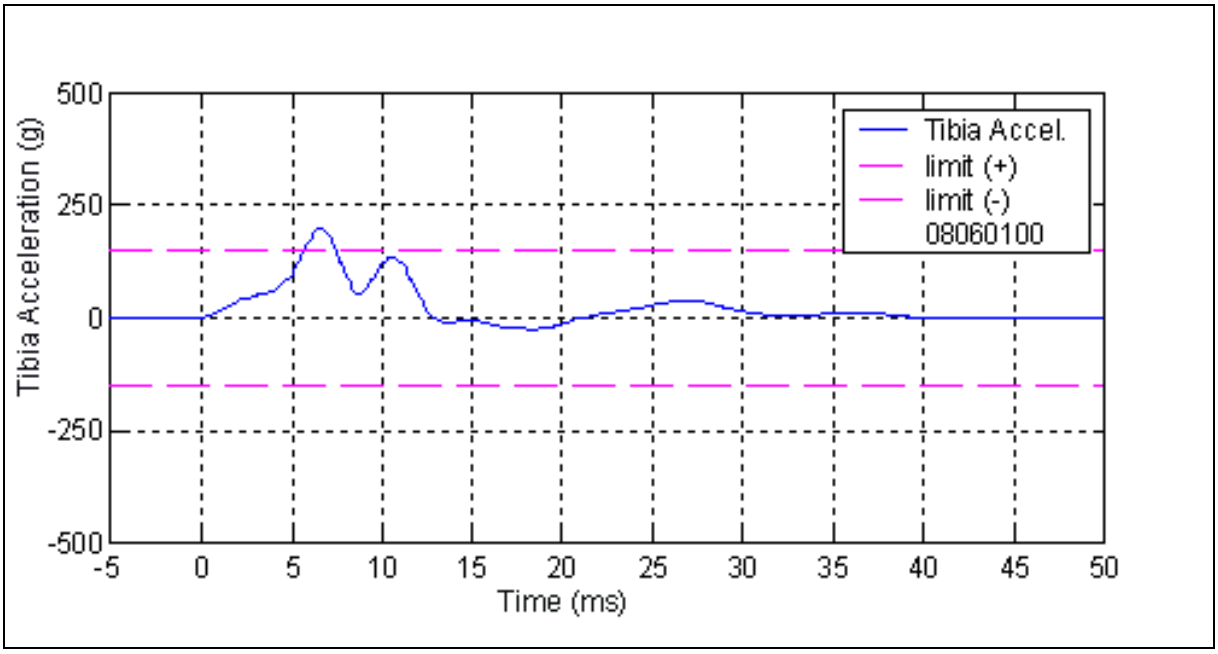

Figure 15-6 The acceleration recorded in the physical reconstruction of case PED064-00

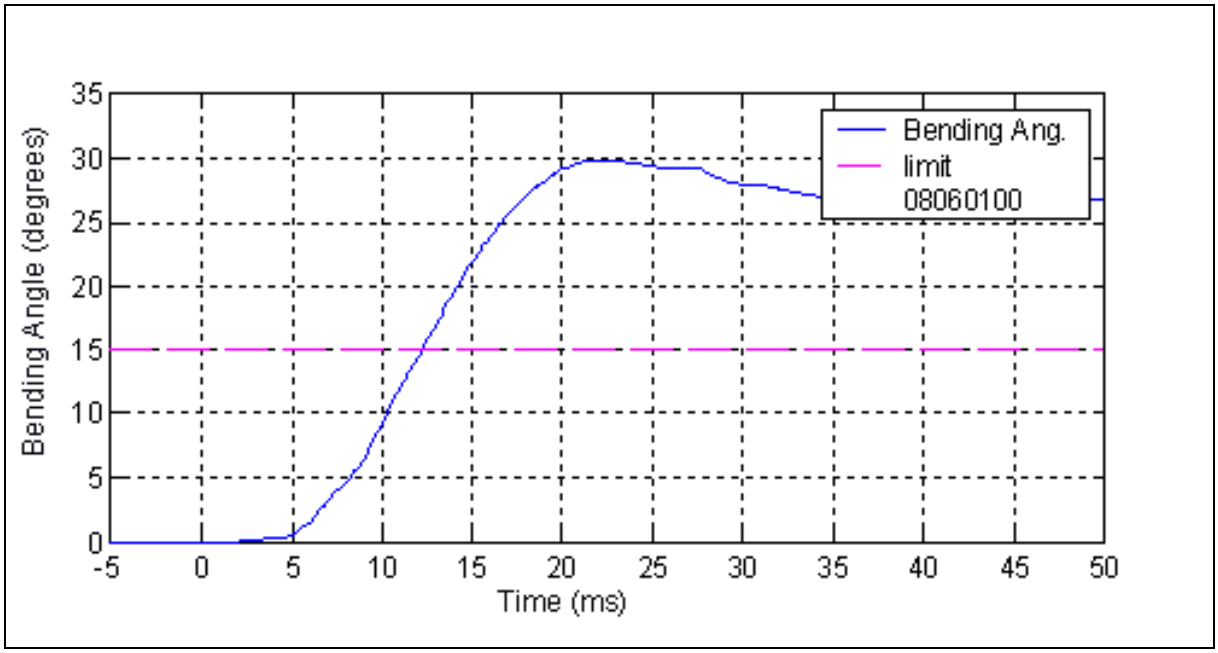

Figure 15-7 Knee bending angle recorded for the physical reconstruction of case PED064-00.

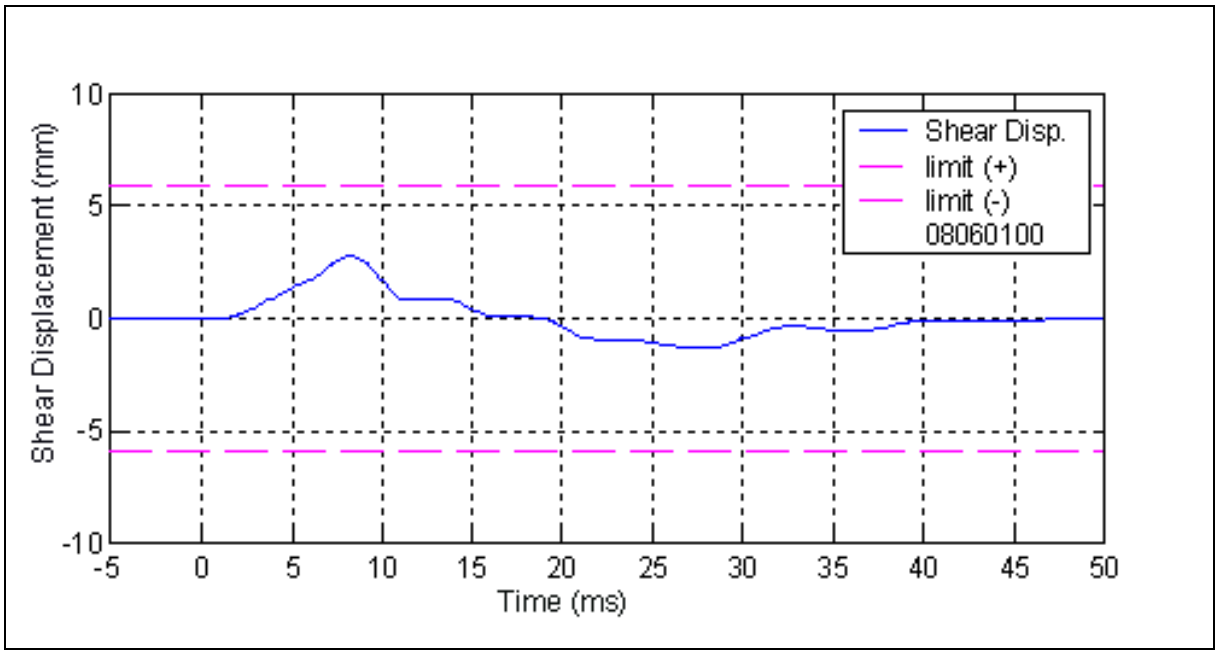

Figure 15-8 Knee shear displacement recorded for the physical reconstruction of case PED064-00.

Figure 15-9 Close up front view showing the accident damage to the bumper (left) and the damage produced by the reconstruction (right) with the Legform of case PED064–00.

15.6 SUMMARY OF RECONSTRUCTION RESULTS AND INJURY DIAGNOSIS

A summary of the results of the impact reconstructions and the injuries associated with the impacts in the case is given in Table 15-5. The knee of the pedestrian was badly bruised and caused her limited mobility for some months. The results of the test indicate that such an impact would cause ligamentous damage, although the injury might be expected to have been more severe. The head impact reconstruction, however, is consistent with the fact that the pedestrian's head was uninjured.

Table 15-5 Summary of test results and relevant injuries

Test	Measure	Result	Relevant Injury
Full leg	Tibia acceleration	199.4 g	Bruising of the knee
	Knee bending	29.9°	
	Knee shear	2.8 mm	
Head	HIC	136	No head injury, abrasions and lacerations to face

Indicates a result which exceeds a safe limit according to EEVC WG10

16 Case PED076-00

16.1 CASE DESCRIPTION

An elderly female pedestrian was crossing a road from west to east when struck by a vehicle that was travelling north in the left-hand lane of the double carriageway. The driver of the vehicle saw the pedestrian and braked heavily before the collision. The pedestrian was thrown forward landing on the road in front of the vehicle.

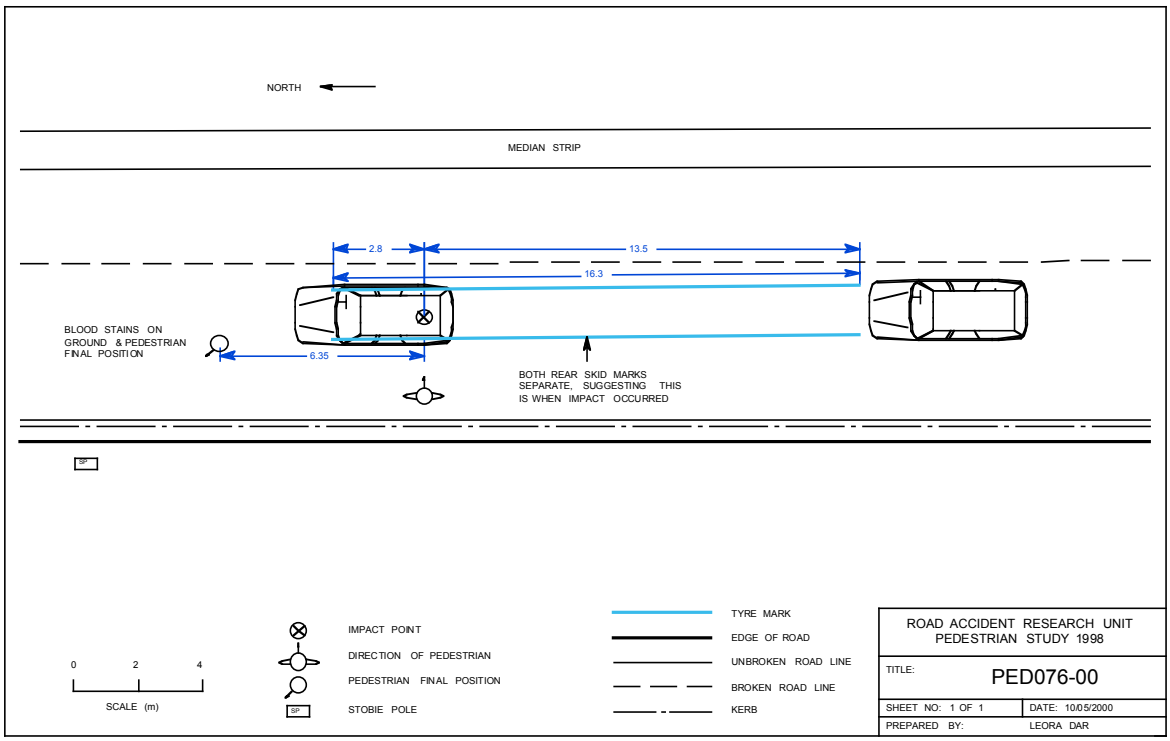

Figure 16-1 Site diagram of the collision in Case PED076-00.

16.2 PEDESTRIAN INJURIES

The pedestrian was transported by ambulance to hospital where she remained for five weeks following the accident. She briefly lost consciousness at the scene and had a degree of disorientation until she returned from surgery. Her other injuries included:

Bimaleolar fractures to the distal right tibia,

Fractured neck of her right humerus, and

Bruising to her face and back.

16.3 ACCIDENT RECONSTRUCTION

An impact point was estimated based on the position on the road where the front and rear skid marks started to diverge. Two impact speeds were calculated: one based on a projection/throw distance of 6.4 m, which gave a 29 km/h average, and an impact speed of 22 km/h based on the post-impact skid mark of 2.8 m.

There was a small dent on the bonnet that was identified as the point on the vehicle that the pedestrian's head struck. This dent measured 225 mm from the bonnet centre-line, and was located at a wrap around distance of 1820 mm. The vehicle was equipped with an original-equipment bullbar, and there was no evidence of the contact that broke the pedestrian's leg.

16.4 MADYMO SIMULATION

Five gait postures were used for the simulation investigation. The sixth gait position was not used in this case because the location of the fracture on the leg of the pedestrian suggested that at the moment of impact, the leg was not raised to the height of the leg in that gait position.

The simulation was based on the anthropometric and vehicle information listed in Table 16-1. The vehicle model and the initial position of the pedestrian model are illustrated in Figure 16-2 and Figure 16-3. To simulate the braking of the car, the vehicle model was lowered 100 mm and tilted from the front of the model by 5˚. The bull bar is modelled by a series of deep but narrow elliptical cylinders. The depth of these cylinders is designed to ensure that the interaction between the pedestrian and the bar is sound throughout the collision, and prevents the bar from penetrating too far into the ellipsoids that represent the body of the pedestrian.

The five postures were simulated using the two estimates of the vehicle impact speed and the results of the two sets of simulations are given in Table 16-2.

Table 16-1 Case details for reconstruction

Pedestrian details		
	Age, sex and height	79 year old female, 160 cm
	Orientation	Struck on right side
Vehicle details		
	Year, Make and model	1996 Ford EL Falcon with Bull bar
	Impact speed	22 - 29 km/h

16.5 PHYSICAL RECONSTRUCTION

The impact with the pedestrian's right leg was reconstructed using the Full Legform, and the head impact was reconstructed using the Adult Headform. Two Headform and two Full Legform tests were conducted. These were based on the two estimates of the striking speed of the vehicle.

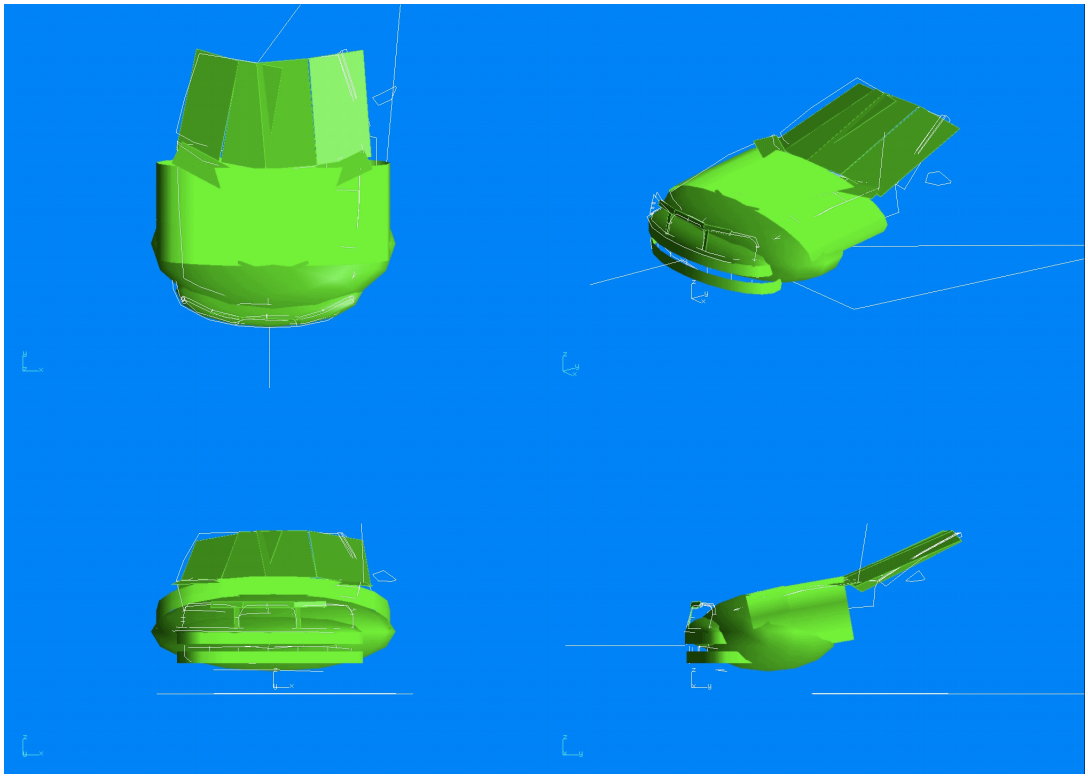

Figure 16-2 The approximation of the vehicle geometry for the simulation is shown by planes and ellipsoids illustrated.

16.5.1 Head impact reconstruction

The head impact velocity estimates in this case were relatively low, and the design of the launcher is such that it is not possible to fire the Headform at such low speeds, at the angle estimated for this case. This is because gravity would cause the Headform to interfere with the launcher before it exits. The only feasible alternative in this case was to drop the Headform vertically, from a height that would produce the required velocity. The set-up and results of both tests are shown in Table 16-3 (lower speed) and Table 16-4 (higher speed). The acceleration traces recorded in these test are shown in Figures 16-4 and 16-5 respectively. Figure 16-6 shows a comparison of the head impact dent on the case vehicle, and that created by the test at the lower speed. Both tests indicated an impact of a minor nature

16.5.2 Leg impact reconstruction

The reconstruction tests were conducted at each estimate of the vehicle impact speed. The exact location on the bumper bar of the leg impact could not be identified on the case car. A location was chosen that was in line with the head impact (i.e. 225 mm from centre-line) and tests at the lower and upper speed range were performed on the same location, as the first test caused no deformation of the steel bull bar whatsoever. The set-up and results of these tests are shown in Table 16-5 (lower speed) and Table 16-6 (higher speed). The acceleration of the tibia and the kinematics of the knee of the tests are plotted in Figures 16-7 to 16-12. Figure 16-13 shows that the tests did not create any damage to the bull-bar.

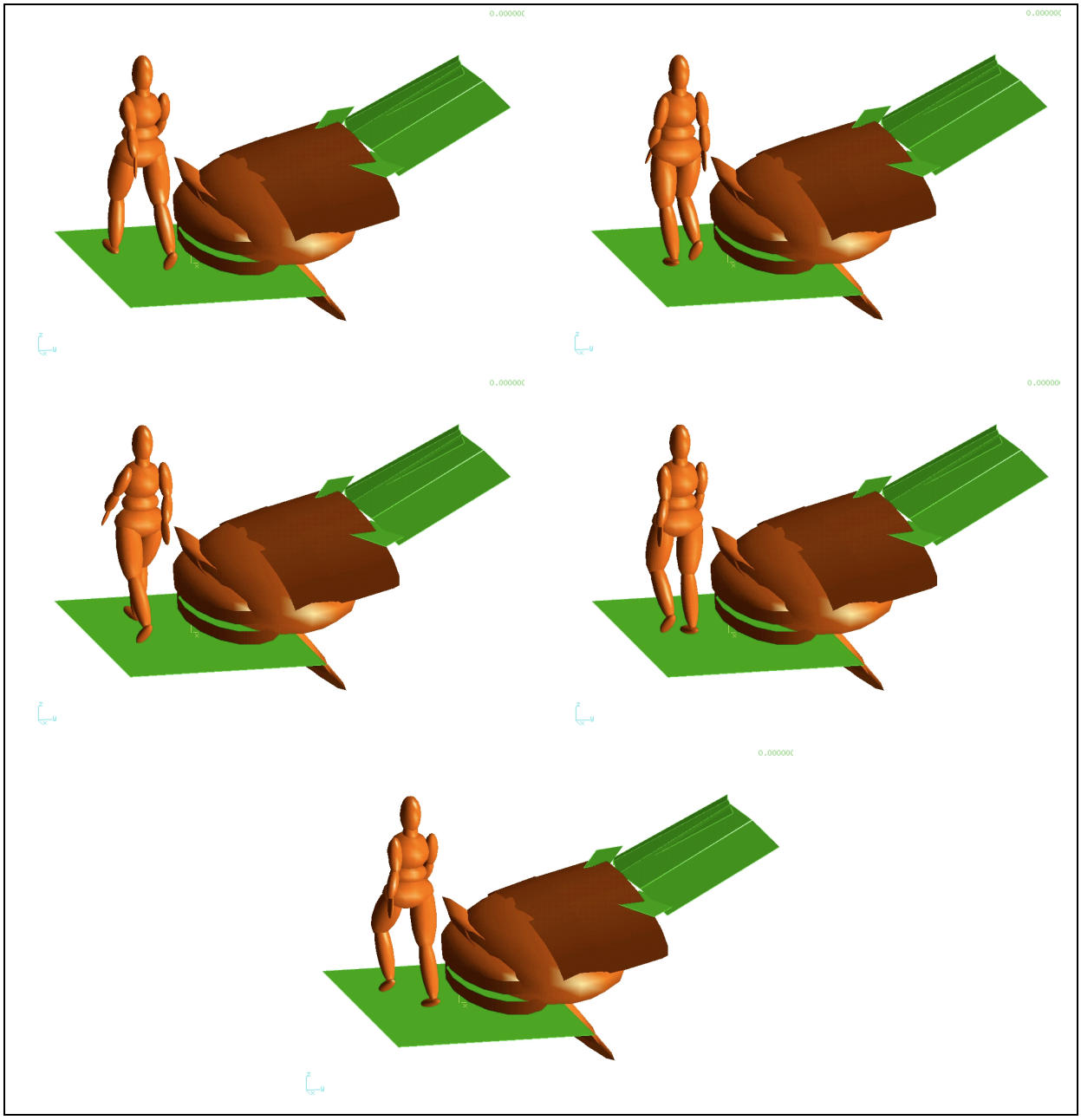

Figure 16-3 Initial position of the pedestrian and vehicle in the simulations PED076-g1 through PED076-g6 (*left to right and top to bottom*).

Table 16-2 Simulation results for PED076-00

Simulation number	Head Velocity	Impact angle
	(m/s)	(deg.)
ped076g1_29	4.69	65.78
ped076g2_29	3.85	54.80
ped076g3_29	-	-
ped076g4_29	3.52	56.63
ped076g5_29	4.95	58.54
ped076g6_29	5.05	66.76
Average	**4.41**	**60.50**
ped076g1	2.57	82.90
ped076g2	3.20	61.76
ped076g3	-	-
ped076g4	1.86	55.43
ped076g5	3.82	69.69
ped076g6	2.99	81.36
Average	**2.89**	**70.23**

Table 16-3 Physical reconstruction parameters and results (test no. 18060100)

	Parameter	Value
Test set-up	Launch Angle	Vertical, drop test
	Measured velocity	2.89 m/s
Results	Peak acceleration	28 g
	HIC value (interval)	46 (18.5 ms)

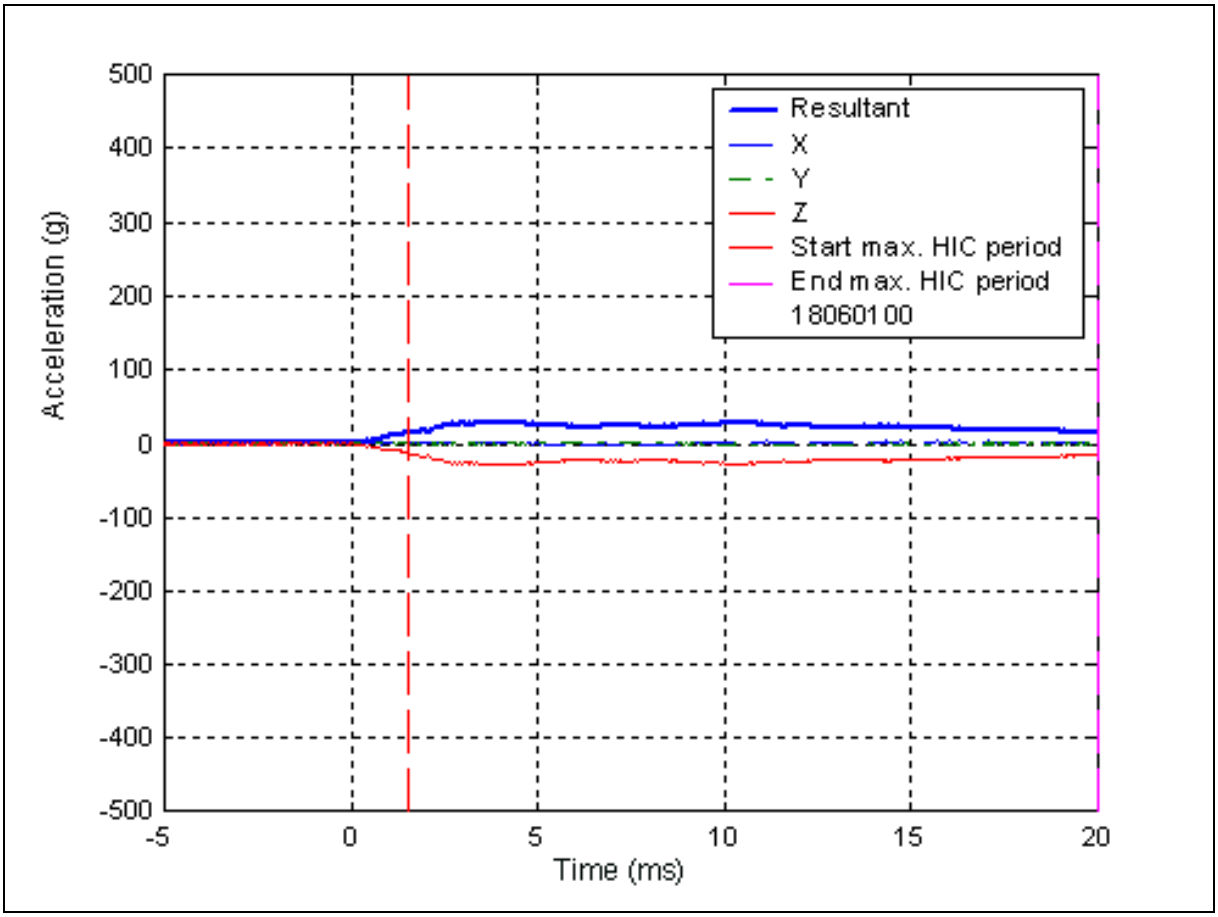

Figure 16-4 The acceleration recorded in the physical reconstruction of case PED076-00 for the lower speed range.

Table 16-4 Physical reconstruction parameters and results (test no. 19060100)

	Parameter	Value
Test set-up	Launch Angle	Vertical, drop test
	Measured velocity	4.41 m/s
Results	Peak acceleration	47 g
	HIC value (interval)	128 (16.4 ms)

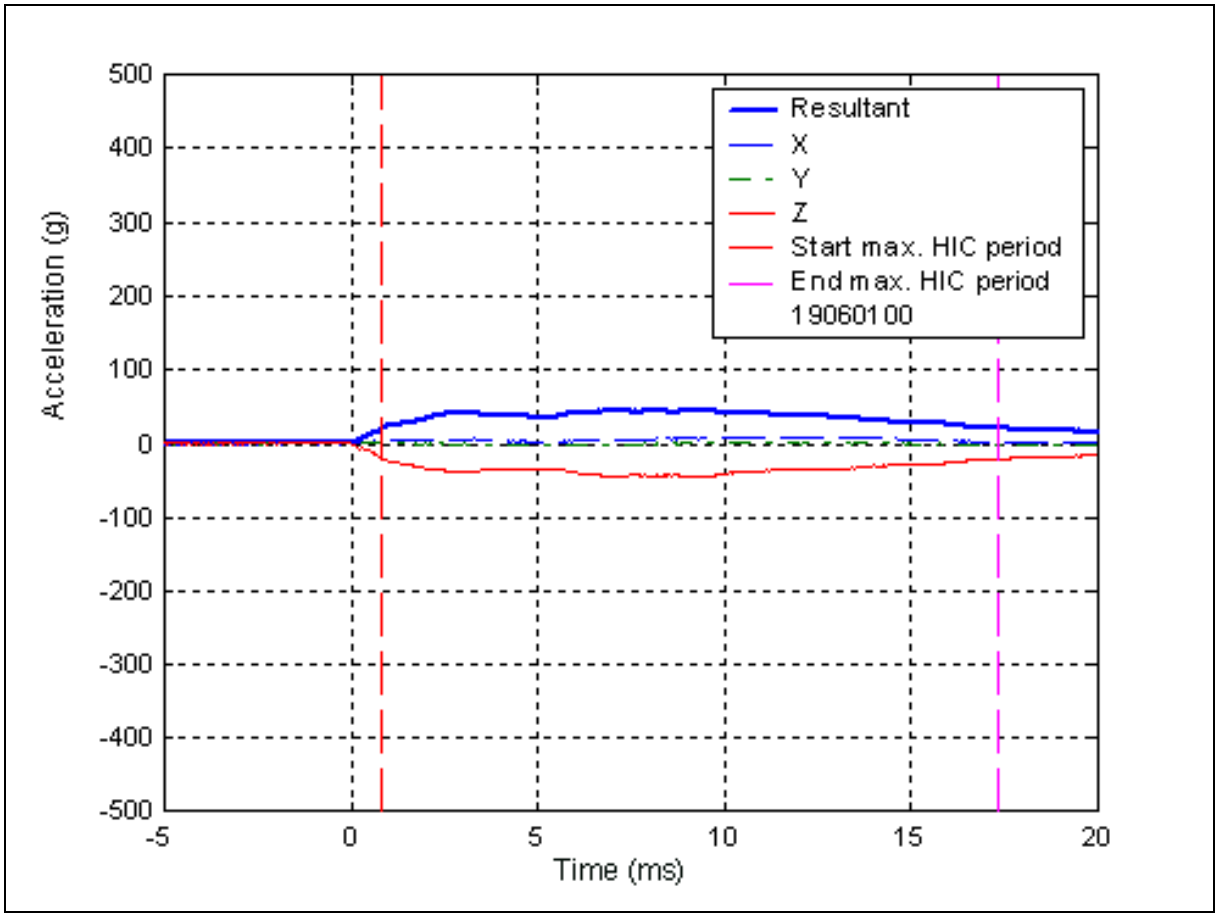

Figure 16-5 The acceleration recorded in the physical reconstruction of case PED076-00 for the higher speed range.

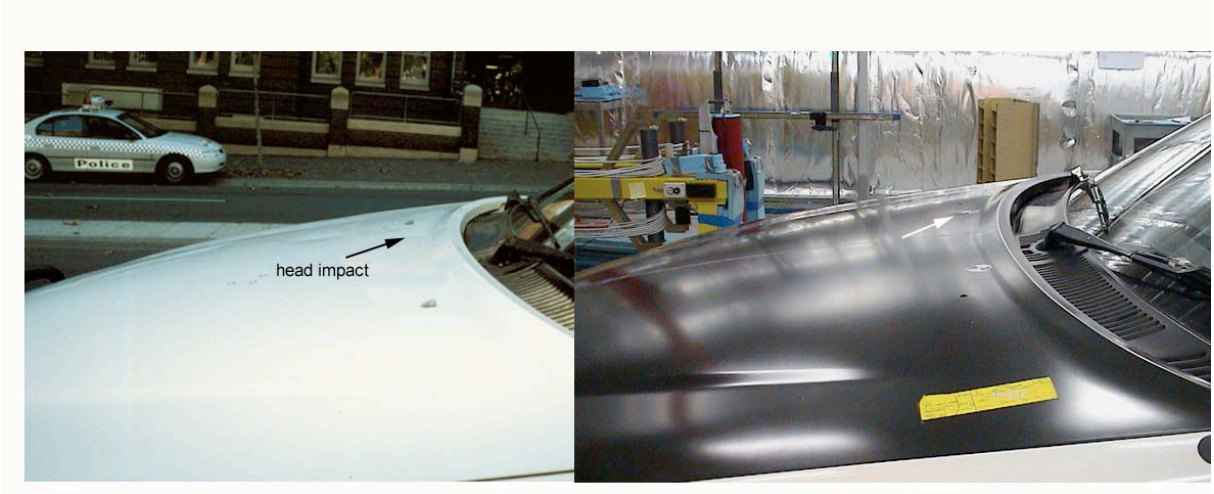

Figure 16-6 The accident damage (left) from impact with the pedestrians head compared to the damage produced by the reconstruction of case PED076-00 (test # 18060100)

Table 16-5 Physical reconstruction parameters and results for the Legform test (test no. 12060101)

	Parameter	Value
Test set-up	Measured velocity	6.08 m/s
Results	Tibia acceleration	233.7 g
	Knee bending angle	15.9°
	Knee shear displacement	3.4 mm

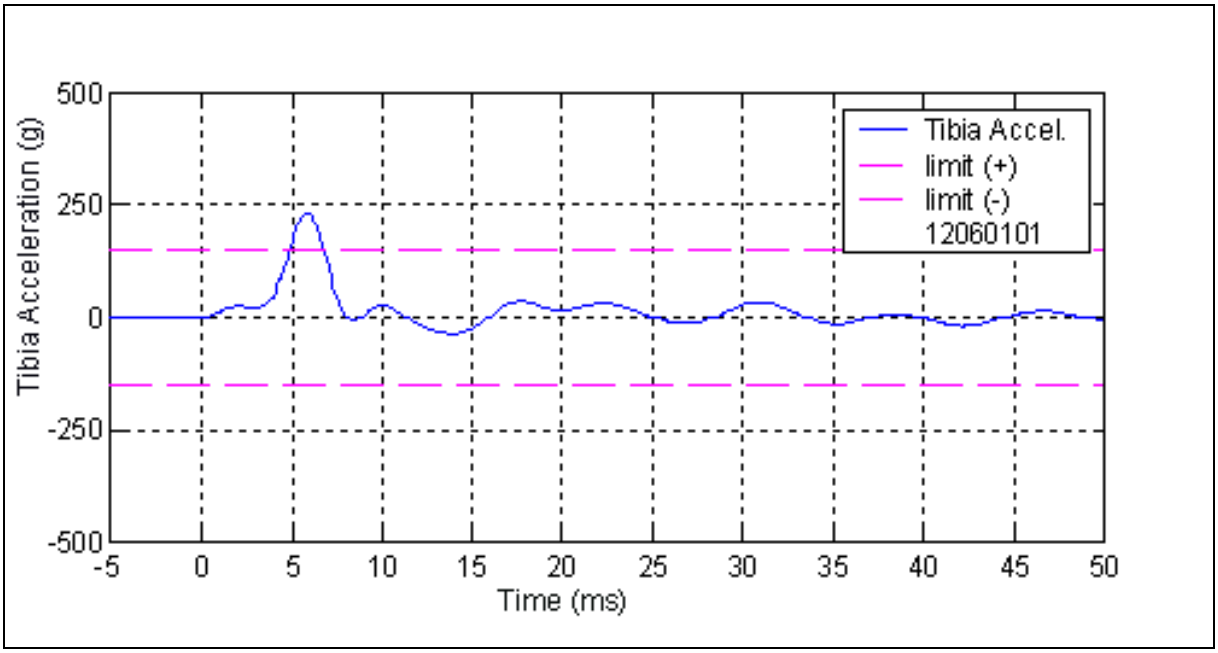

Figure 16-7 The acceleration recorded in the physical reconstruction of case PED076-00 for lower impact speed of the range.

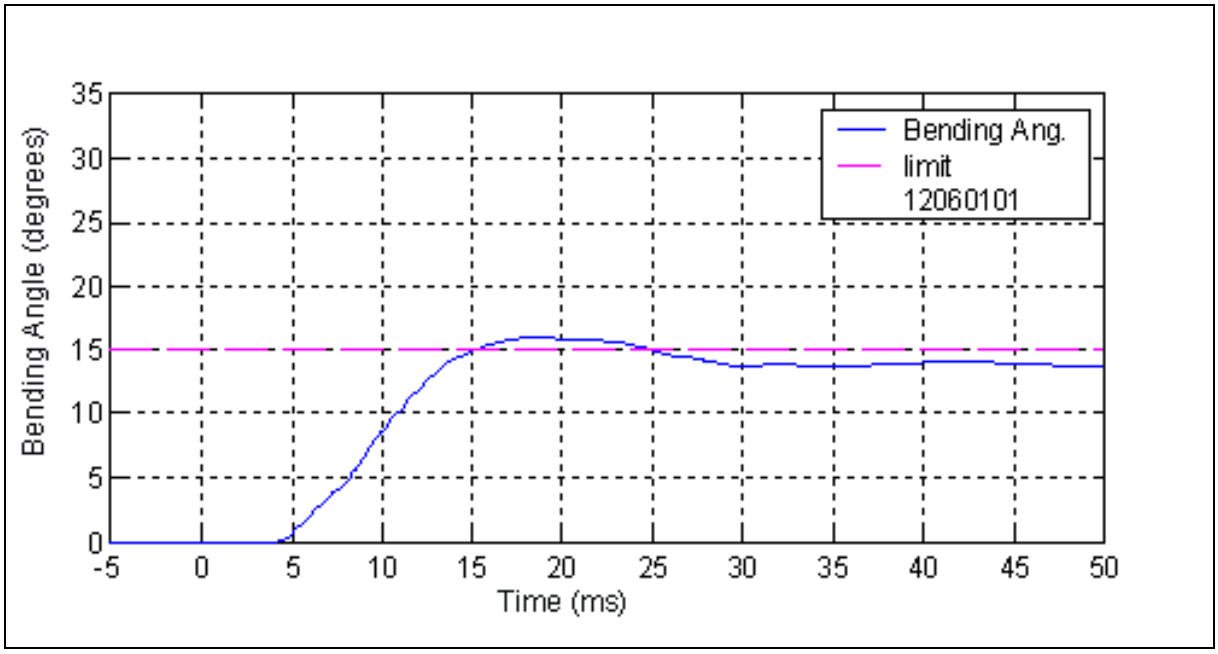

Figure 16-8 Knee bending angle recorded for the physical reconstruction of case PED076-00 for lower impact speed of the range.

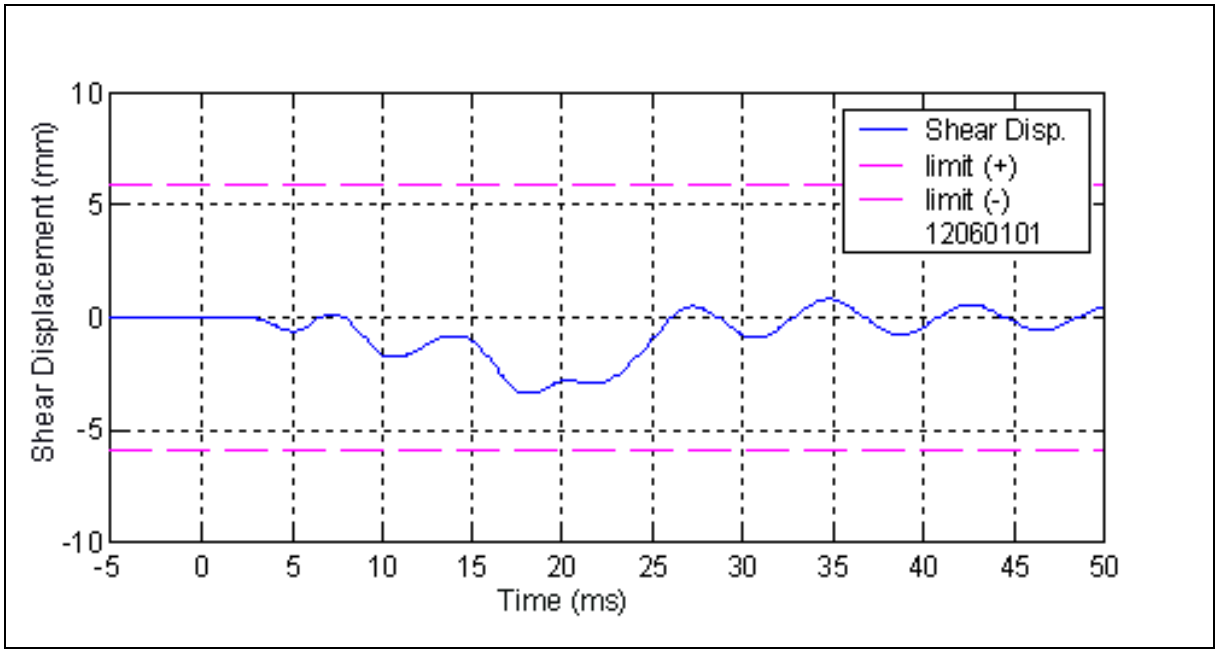

Figure 16-9 Knee shear displacement recorded for the physical reconstruction of case PED076-00 for lower impact speed of the range.

Table 16-6 Physical reconstruction parameters and results for the Legform test (test no. 14060101)

	Parameter	Value
Test set-up	Measured velocity	7.72 m/s
Results	Tibia acceleration	338.0 g
	Knee bending angle	21.7˚
	Knee shear displacement	3.7 mm

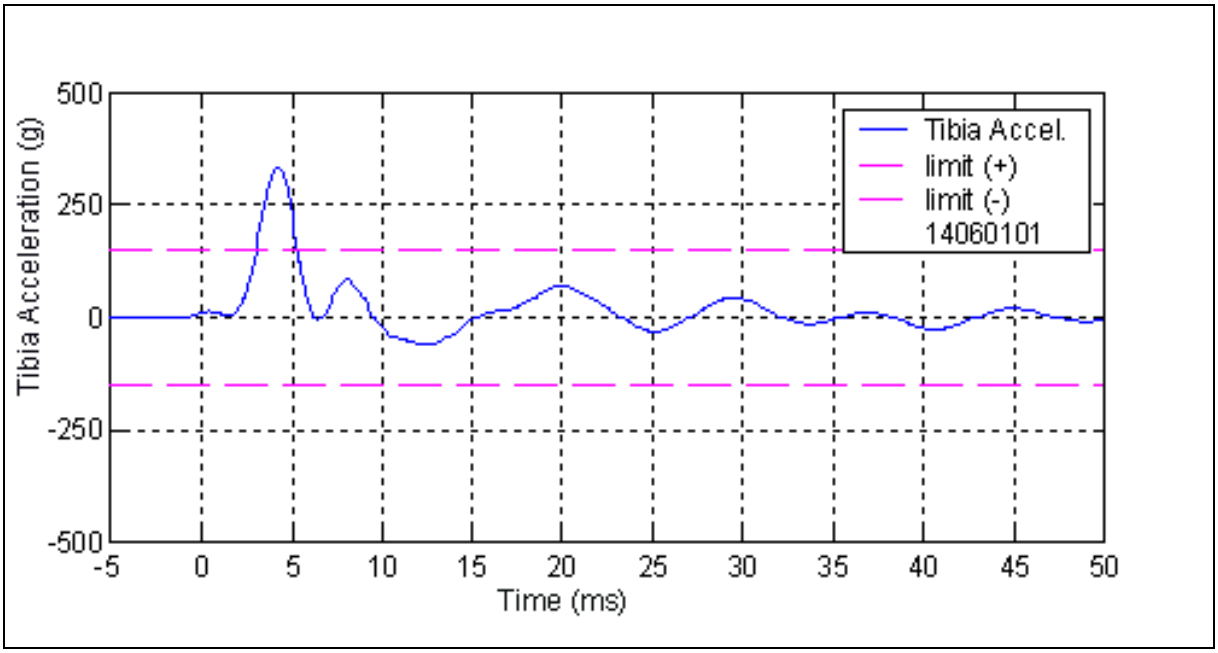

Figure 16-10 The acceleration recorded in the physical reconstruction of case PED76-00 for higher impact speed of the range.

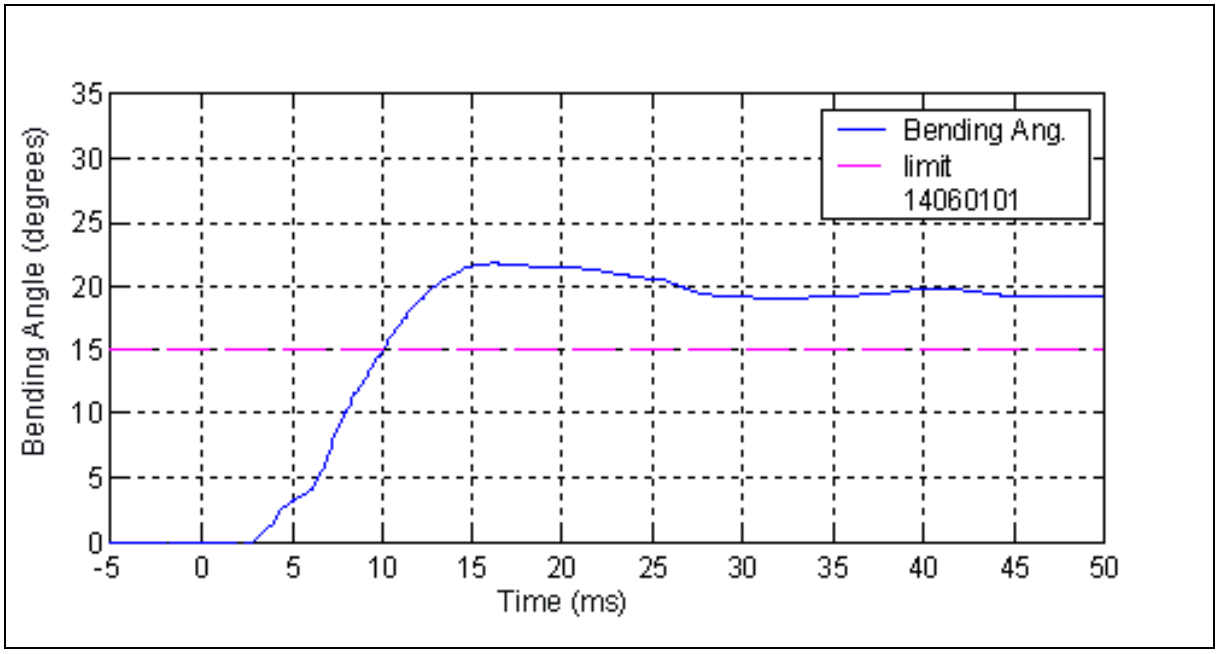

Figure 16-11 Knee bending angle recorded for the physical reconstruction of case PED076-00 for higher impact speed of the range.

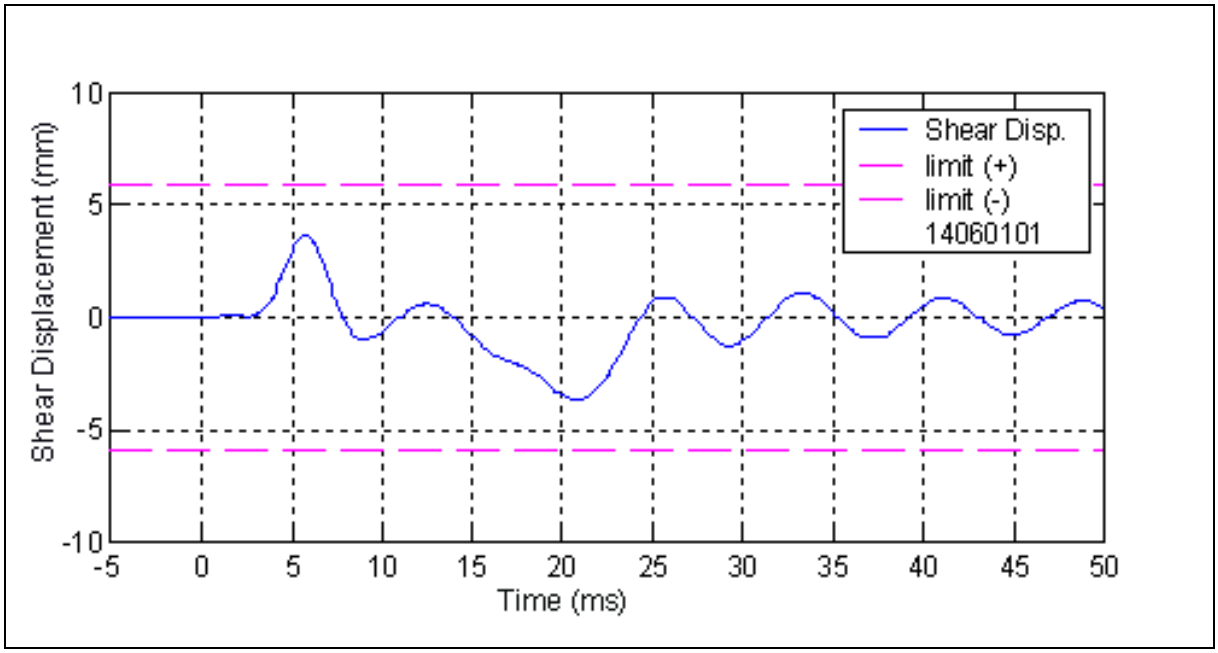

Figure 16-12 Knee shear displacement recorded for the physical reconstruction of case PED076-00 for higher impact speed of the range.

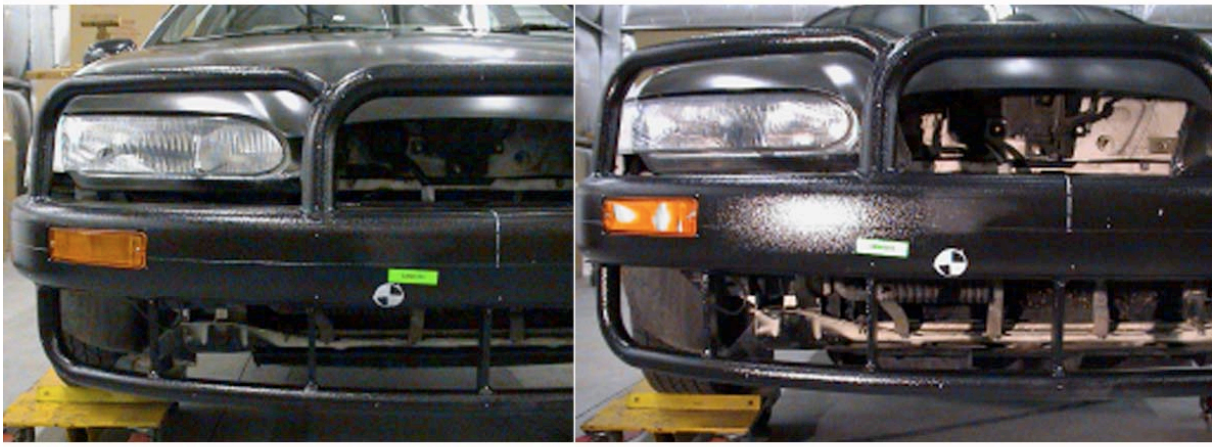

Figure 16-13 Close-up view of impact points of test # 12060101 (left) and test # 14060101 (right) there was no evidence of damage in either test.

16.6 SUMMARY OF RECONSTRUCTION RESULTS AND INJURY DIAGNOSIS

Table 16-7 summarises the results of the impact reconstructions and the related injuries suffered by the pedestrian in the collision. The bull-bar structure appears to have prevented excessive knee kinematics, although the tibia acceleration was very high. The fractures to the tibia were low on the bone, and were probably created by a concentrated load on the leg by a bull-bar member.

The head impact that was reconstructed was very mild, which is not necessarily consistent with the pedestrian's loss of consciousness. The bruising on the pedestrian's back could have been caused as she slid over the bull bar as she fell to the ground. The pedestrian's head may have struck the bar or the ground, as well as the bonnet of the car, and it is possible that the most significant head impact was not the impact that we reconstructed.

Table 16-7 Summary of test results and relevant injuries

Test	Measure	Result	Relevant Injury
Full leg	Tibia acceleration	233.7 g	Bimaleolar fractures to the distal right tibia
	Knee bending	15.9°	
	Knee shear	3.4 mm	
	Tibia acceleration	338.0 g	
	Knee bending	21.7°	
	Knee shear	3.7 mm	
Head	HIC	128	Brief loss of consciousness
	HIC	46	

Indicates a result which exceeds a safe limit according to EEVC WG10